



## Non-Inverting Heliostat Study

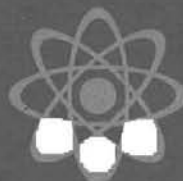
Prepared by Sandia Laboratories, Albuquerque, New Mexico 87115  
and Livermore, California 94550 for the United States Department  
of Energy under Contract DE-AC04-76DP00789.

Printed August 1979

***When printing a copy of any digitized SAND  
Report, you are required to update the  
markings to current standards.***



Sandia Laboratories  
energy report



Issued by Sandia Laboratories, operated for the United States Department of Energy by Sandia Corporation.

---

---

#### NOTICE

This report was prepared as an account of work sponsored by the United States Government. Neither the United States nor the United States Department of Energy, nor any of their employees, nor any of their contractors, subcontractors, or their employees, makes any warranty, express or implied, or assumes any legal liability or responsibility for the accuracy, completeness or usefulness of any information, apparatus, product or process disclosed, or represents that its use would not infringe privately owned rights.

Printed in the United States of America  
Available from  
National Technical Information Service  
U. S. Department of Commerce  
5285 Port Royal Road  
Springfield, VA 22161  
Price: Printed Copy \$6.00 ; Microfiche \$3.00



**NON-INVERTING HELIOSTAT STUDY**

JULY 1979

MDC G7876

PREPARED BY:

*J. B. Blackmon*

**J. B. BLACKMON**  
PRINCIPAL INVESTIGATOR

*D. W. Harvey*

**D. W. HARVEY**  
HAIL EFFECTS TASK LEADER

*R. H. McFee*

**R. H. McFEE**  
BEAM SAFETY TASK LEADER

APPROVED BY:

*H. H. Dixon*

**H. H. DIXON**  
DIRECTOR - PROGRAM ENGINEERING  
ENERGY PROGRAMS

**MCDONNELL DOUGLAS ASTRONAUTICS COMPANY-HUNTINGTON BEACH**

5301 Bolsa Avenue Huntington Beach, California 92647 (714) 896-3311

## PREFACE

This report was prepared under Sandia Laboratories Contract No. 18-7872 with technical monitoring by S. Peglow, Sandia Laboratories, Livermore, California. The test support assistance of James Pryor, Naval Weapons Center, China Lake, California, and Roscoe Champion and Dr. Richard Pettit, Sandia Laboratories, Albuquerque, N.M., is appreciated. The assistance of M. Curcija in data reduction and analysis is acknowledged. The assistance of B. F. Blanchard in preparing the report is greatly appreciated.

## NON-INVERTING HELIOSTAT STUDY

Implications of employing a non-inverting heliostat design with a lower capital cost relative to an inverting design are considered from three standpoints: (1) effects of dust buildup, corresponding cleaning frequencies, and resultant cleaning costs; (2) effects of hail impact; and (3) reflected beam safety issues. It is concluded that elimination of the inverting stow hardware and addition of reflector area in the slot required for inverting the reflector provides a direct subsystem cost savings. Since the non-inverting heliostat must be stowed face-up during high winds, reflectance degradation rates due to dust buildup are increased. The economic optimum cleaning frequency and allowed loss of reflectance due to dust buildup are determined so as to minimize the total system cost, and it is found that an overall cost savings of 12-13 percent results if the inverting capability is eliminated. Hail impact damage and probability of occurrence for the United States are determined within the accuracy of available data. Analysis indicates that the commercial heliostat laminate glass design considered will survive 1-1/2 inch hailstones and is suitable for installation over most of the U.S. with low to negligible risk from hail damage.

Reflected beam safety hazards are analyzed for the non-inverting design relative to the inverting design. No compelling reason is found to require an inverting stow capability, and therefore, a non-inverting stow heliostat is concluded to be a viable, cost-effective option.

## CONTENTS

Section 1	INTRODUCTION AND SUMMARY	1
Section 2	TASK I -- DUST BUILDUP EFFECTS	5
	2.1 Objective	5
	2.2 Approach	5
	2.3 Recommended Additional Effort	33
	2.4 Conclusions	34
Section 3	TASK II -- HAIL STUDY	37
	3.1 Objective	37
	3.2 Hail Statistics	37
	3.3 Recommended Work	62
	3.4 Heliostat Vulnerability	63
	3.5 Heliostat Cost and Vulnerability Conclusions	72
Section 4	TASK III -- SAFETY ISSUES	75
	4.1 Objective	75
	4.2 Technical Approach	76
Section 5	REFERENCES	91
Appendix A	HAIL IMPACT IMPULSE-MOMENTUM VULNERABILITY MODEL	95

## Section 1

### INTRODUCTION AND SUMMARY

This study was conducted to assess the implications of employing a non-inverting heliostat design for which vertical stow is normally used at night or during occasional periods of non-operation, and mirror-up stow is used to survive extreme winds. An inverting heliostat would normally also be stowed vertically, but would be stowed face-down to survive extreme winds. The effects of lack of capability to invert were investigated in three principal areas:

1. Dust buildup effects, cleaning frequency, and costs
2. Increased heliostat damage probabilities due to hail effects
3. Reflected beam safety issues.

The McDonnell Douglas heliostat design shown in Figure 1-1 and an equivalent non-inverting version were used as the heliostat models. The principal differences between the two designs are: (1) elimination of the additional linear actuator and associated hardware required to invert, and (2) addition of reflector area in the slot required for the inverting heliostat. These design changes decrease the cost of each heliostat and the number of heliostats required for a given generating plant total energy output. However, lack of an inverting stow position does increase the dust buildup rate, and therefore, maintenance cleaning costs are increased. These effects were considered for a commercial plant of approximately 18,000 heliostats.

Although total cleaning life cycle costs are strongly dependent on assumptions of cleaning frequencies, manpower levels, material costs, etc., the difference in dust buildup rates between the inverting and non-inverting scenarios is such that over a wide range of conceivable variations in washing cost parameters, it is still not economical to provide for an inverting capability with the existing design, in lieu of simply washing somewhat more frequently.

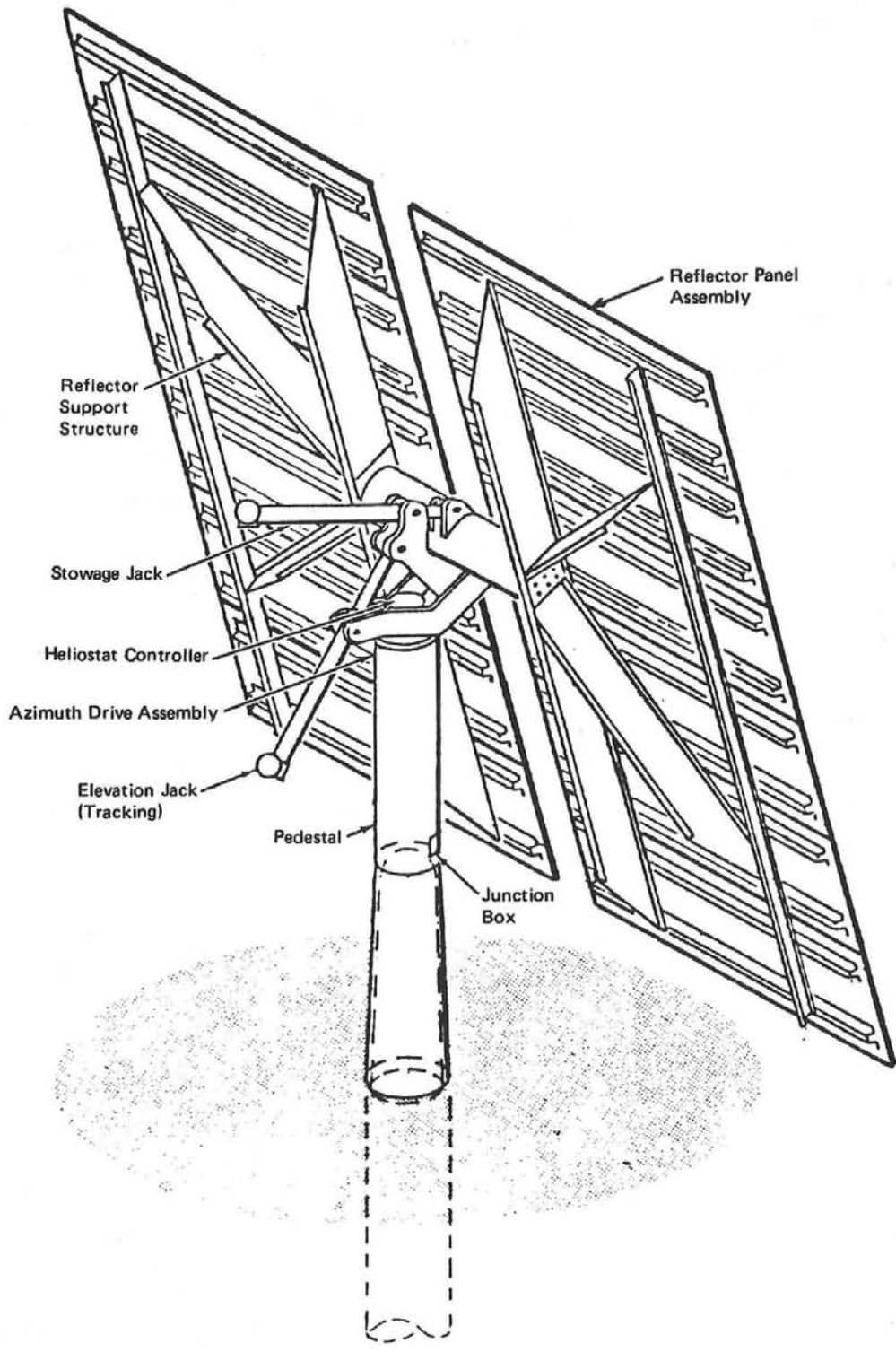


Figure 1-1. Inverting Heliostat Design

This conclusion holds over a wide range of assumptions of monetary inflation rates and discount rates over a 30-year power plant life. It is concluded that for the heliostat design used in the analysis, a non-inverting heliostat allows an overall cost savings of approximately 12-13 percent, even though the dust buildup rate and cleaning frequency required is higher than for an inverting heliostat.

Hail impact data for glass breakage were reviewed and a semi-empirical breakage model derived to determine glass thickness required to withstand hailstone impact. An analysis was conducted to determine the probability of hail impact as a function of hail size and geographical location. The breakage model and probability data were used to estimate required heliostat mirror thickness. It was found that the laminate glass reflector design (Reference 2-1) used for the commercial plant analysis would survive hail impact by stones up to 1.5 inch diameter without a design change. It was also found that hailstorms having stones  $\geq 1.5$  inch occur infrequently (less than once every 20-30 years) in most of the U.S. Southwest. It therefore appears that there is a negligible cost penalty associated with the non-inverting heliostat, insofar as design modifications are not required to provide the capability to withstand hailstones up to 1.5 inch. It was further found that increasing the glass thickness, so as to survive a 2-inch diameter hailstone impact increases the system cost of the heliostat by 7-8 percent, or \$163/heliostat. However, this cost would be incurred with either the inverting or non-inverting laminate glass design, since hailstorms frequently occur under conditions of high winds, necessitating horizontal stowage, and therefore, both the inverting and non-inverting laminate glass heliostats would be subjected to impact at a glass surface. Heliostats deployed in these areas would thus be designed to meet the more stringent hailstone impact requirements.

Since the existing design appears to have the intrinsic capability to meet a relatively conservative requirement of withstanding 1.5-inch diameter hailstones, and since this requirement will be sufficient for most of the U.S. Southwest, it is tentatively concluded, subject to additional hail test data, that the current commercial design is suitable without cost penalty. This heliostat design would therefore be deployable over U.S. land areas sufficiently large so as to not increase the heliostat costs by imposing overly conservative requirements on hail impact resistance.

However, there are areas in the midwest, principally parts of Colorado and Texas, which have severe hailstorms, and heliostats used in these areas may require the inverted stow capability, and additional protection for the reflector.

Hazards associated with non-inverting heliostat reflected beams were considered and compared with the hazards for an inverting heliostat design. In general, it was found that with both designs, certain hazards can exist in terms of excessive levels of irradiance, but that these hazards can be controlled by appropriate operating procedures and use of exclusion zones, and that no significant additional hazard is presented by the non-inverting design.

Based on the results of the cleaning and hardware cost analysis, the lack of any significant cost penalty associated with hail impact and the lack of any significant additional safety hazard, it is concluded that a non-inverting heliostat design is an appropriate cost effective option for commercial solar thermal plants and provides a potential collector subsystem total cost savings of the order to 12-13 percent.

In the following sections, each aspect of the non-inverting heliostat and inverting heliostat design comparison is discussed. Section 2 presents a summary of the results from the Interim Report, Reference 2-2, devoted to an analysis of the dust buildup rates, associated cleaning costs, and the overall system cost savings. Section 3 presents the hail impact statistical results and the hail impact damage model. Section 4 presents the redirected beam safety considerations.

Section 2  
TASK I -- DUST BUILDUP EFFECTS

2.1 OBJECTIVE

The objective of this task is to analyze readily available data from current and previous dust buildup studies and evaluate the dust buildup rates as a function of stowage positions (mirror down, mirror up, mirror vertical, etc.). Cleaning cycle frequencies and resultant cleaning cost effects are then determined. Overall cost savings with the non-inverting heliostat, considering both capital costs and operations and maintenance are then determined, relative to the inverting heliostat, over the 30-year life of the plant.

Hardware cost reductions are considered for a non-inverting design, and overall cost savings determined.

2.2 APPROACH

The approach for this study consists of a sequence of analyses. Starting with a review of readily available dust buildup data for specimens and heliostats, reflectivity degradation rates due to mirror soiling are determined for normal environmental conditions. Severe environmental effects are then considered. High winds require stowage of a non-inverting heliostat in a face up, horizontal orientation, and dust buildup therefore is greater than for inverted or vertical stow. Light rains and blowing sand and dust, which significantly increase the dust buildup, are considered. Next, natural cleaning effects are considered to determine a range of expected benefits in terms of decreased maintenance cleaning cycles and frequency of occurrence of natural cleaning. Environmental conditions are assessed.

Dust buildup rates are prescribed for operational heliostats and cleaning frequencies determined for a range of allowable reflectance losses from 3% to 14% below the clean reflectivity. A cost analysis for various cleaning scenarios is performed, and comparisons made with the costs of providing an

inverting stow capability. Overall subsystem cost savings associated with the non-inverting heliostat are then determined. Recommendations for additional tests and analyses are presented.

### 2.2.1 Dust Buildup Rate Correlations

Readily available data on the soiling of mirror specimens and full scale heliostats under desert conditions were reviewed. Three principal sources were used:

1. Data from References 2-2, -3, and -4 consist mainly of 1-2 year observations and reflectivity measurements for (a) sixty 5" x 5" mirror specimens of various types and orientation installed at the Naval Weapons Center (NWC), China Lake, California and at Sandia Laboratories, Albuquerque, New Mexico, and (b) full scale heliostats at NWC.
2. Data from Reference 2-5 consist of frequent reflectivity measurements of mirror specimens exposed at various locations at Sandia Laboratories, Albuquerque, New Mexico.
3. Preliminary data on reflectivity variations of specimens attached to heliostats at the Solar Thermal Test Facility, Sandia Laboratories, Albuquerque, New Mexico were also used.

These data were reviewed to determine an approximate nominal reflectivity degradation rate for relatively benign conditions of no rain, high winds, etc. Next, the data were reviewed to assess severe environmental effects, and to determine an approximate frequency of occurrence.

Dust buildup rates, as a function of stowage position, are briefly discussed below for benign and severe weather conditions and are presented in more detail in Reference 2-2.

#### 2.2.1.1 Degradation Rates - Benign Conditions

Tables 2-1 and 2-2 summarize data on full scale MDAC heliostats and 5" x 5" reflector specimens tested at the Naval Weapons Center. Table 2-1 gives the time averaged reflectivity degradation, and degradation rate for full scale heliostats as presented in References 2-2 to -4. The degradation rate is taken as the mean of the degradation rates occurring between measurements and is equal to the reflectivity difference divided by the number of days between measurements. The rates correspond to relatively benign conditions.

Table 2-1. Average Reflectance Variations

Heliostat no.	Exposure time (days)	Time averaged reflectivity (%)	Time averaged degradation (%)	Degradation rate, R (% per day), mean $\pm$ standard deviation
H1 (acrylic)	113	$\bar{\rho} = 75.46$	$\Delta\rho = 7.76$	$R = 0.4 \pm 0.4$
H2 (acrylic)	113	$\bar{\rho} = 68.37$	$\Delta\rho = 8.13$	$R = 0.45 \pm 0.32$
H3 (acrylic)	97	$\bar{\rho} = 80.47$	$\Delta\rho = 6.99$	$R = 0.28 \pm 0.18$
H4 (laminated glass)	121	$\bar{\rho} = 81.10$	$\Delta\rho = 6.55$	$R = 0.36 \pm 0.32$
IH1 (laminated glass)	121	$\bar{\rho} = 83.30$	$\Delta\rho = 3.19^*$	$R = 0.1 \pm 0.13$

0.37 $\pm$ 0.07 for four heliostats stowed face-up

\*Note: IH-1 was stowed in the face-down position for most of the test period ( $\approx 2/3$  of exposure time). Data above are for periods without rain or other significant natural cleaning conditions.

In order to assess dust buildup rates as a function of different stowage position, specimens were installed at NWC and Sandia Laboratories as described in References 2-2 to -4. Table 2-2 summarizes the degradation rates. These specimens were installed on five racks. Two racks kept the specimens permanently face up or face down. One rack turned the specimens face up during the day and face down at night or during overcast conditions, as detected by a sun sensor. The other two racks were controlled by an astronomical timer which turned the specimen face up at dawn and face down or near-vertical at sunset.

Data from References 2-2 to -4 on long term exposure effects on heliostats and specimens at NWC and specimens at Sandia Laboratories, Albuquerque, showed that reflection losses exceeding 25% could occur, and therefore some type of purposeful washing will be required.

Mirror specimens were mounted on heliostats at CRTF over a 33-week period and degradation rates determined by weekly laboratory measurements. These data

Table 2-2. Combined Ranking of Degradation Rates vs Stow Position (NWC Site)

Combined ranking for both glass and acrylic	Rate (% per day)	Average (% per day)
1. Permanent face-down, $R_{FD}$	0.03 to 0.06	0.045
2. Sensor face-up/face-down, $R_{FU/FD}$	0.12 to 0.23	0.175
3. Astronomical timer face-up/face-down, $R_{FU/FD}$	0.20 to 0.283	0.242
4. Astronomical timer face-up/near vertical stow, $R_{FUNV}$	0.315 to 0.32	0.318
5. Permanent face-up, $R_{FU}$	0.40 to 0.45	0.425

Note: Data for NWC specimens, November-December 1977, and June-August, 1977.

were made available by Sandia Laboratories in a preliminary form prior to publication in a report and are presented in Figure 2-1. The specimens were mounted so as to be permanently face-up, face-down, or vertical. Considering the portions of the reflectance curve which correspond to relatively benign weather conditions, the mean and standard deviation degradation rate is  $0.356 \pm 0.13\%/day$  for the permanent face up specimen, and is remarkably close to the degradation rates observed with MDAC heliostats tested at NWC.

Table 2-3 compares the preliminary CRTF specimen data with the NWC data. In general, the degradation rates for the relatively benign weather conditions are approximately the same.

2.2.1.2 Effects of Severe Environmental Conditions on Reflector Soiling  
Consideration has been given to effects of severe weather conditions on soiling rates and reflector degradation.

NWC meteorological data has been briefly reviewed to assess severe environmental effects (wind, rain, frost, snow) on dust buildup rates. Data from December 1976 to March 1978 was reviewed in detail, since this was the period of exposure of the specimens and heliostat, as reported in Reference 2-3. These data were then compared with the NWC climatological data summaries from 1946 through 1976. Results to date are summarized below. In addition, preliminary data from the Sandia, Albuquerque Solar Thermal Test Facility, and the Sandia Report (Reference 2-5) on outdoor exposure effects on mirrors was reviewed.

#### Winds Above Safe-Stow Initiation Speed

A field of non-inverting heliostats is assumed to be stowed in a vertical position at night or during occasional plant shutdowns during the day unless high winds occur or are forecast. It will be assumed that the non-inverting heliostats will normally, but not always, be placed into a face-up stow position when peak winds exceed 35 mph since gusts greater than the maximum permissible wind of 50-55 mph might occur and time must be allowed to achieve face-up stowage. However, high winds often accompany storm fronts bringing heavy rains, and under these conditions, the heliostats would not likely be soiled further, but would probably be cleaned. Conversely, high winds accompanied by light rains would significantly increase dust buildup due to rain

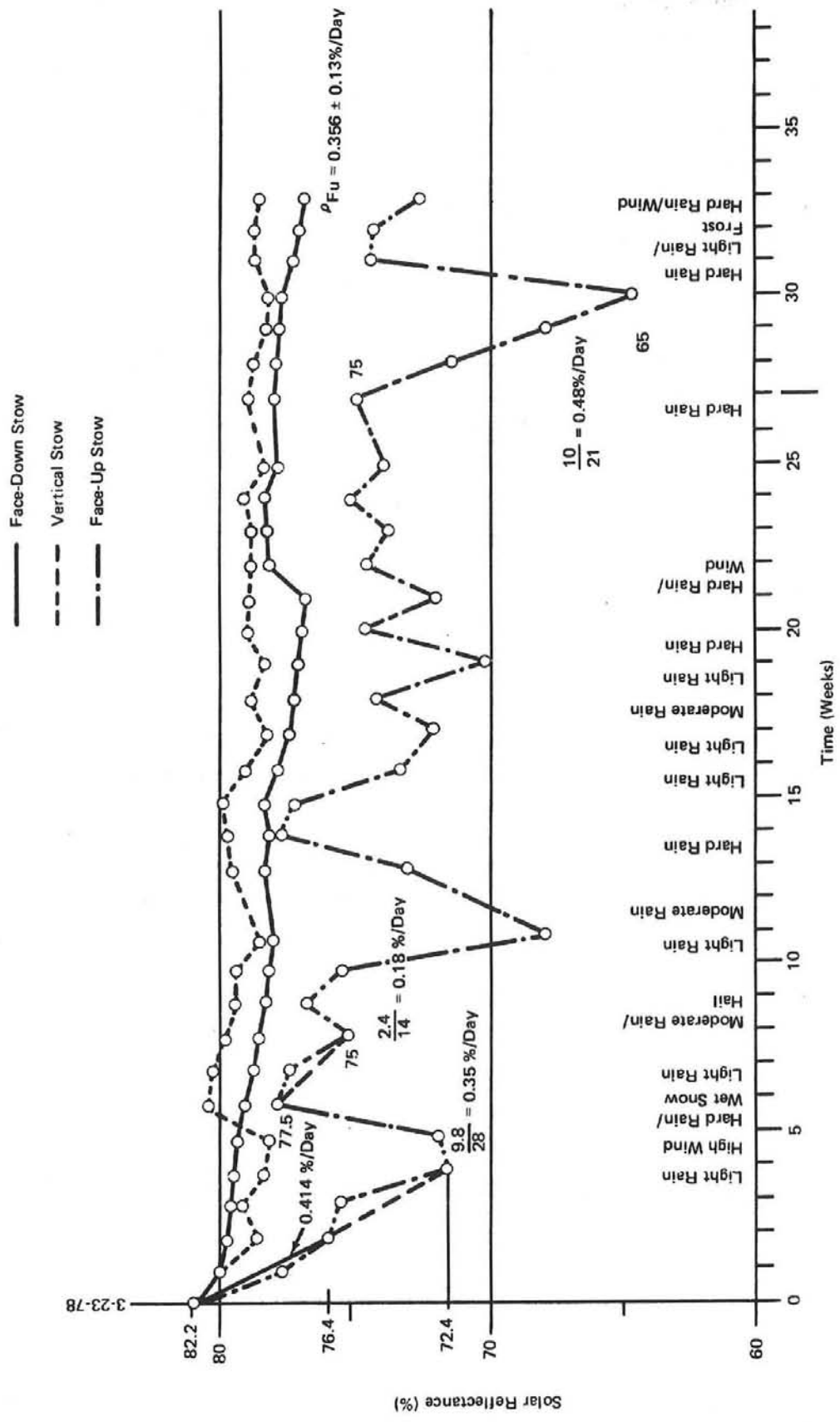


Figure 2-1. Reflectance vs Time for Different Storage Orientations in CRTF Heliostat Field (From D. King, Sandia Laboratories, Albuquerque, N. Mex.)

Table 2-3. Comparison of NWC Heliostat/Specimen and CRTF Heliostat-Mounted Specimen Degradation Rates

Heliostat position	Degradation rate (% per day), MDAC heliostat/specimens at NWC	Degradation rate (% per day), CRTF heliostat - mounted specimen
Permanent face-up	0.37±0.07 (heliostats H1, H2, H3, H4)	0.356±0.13
Permanent vertical	No data	0.02
Permanent face-down	0.04 (NWC specimens)	0.04

depositing airborne dust on the mirrors. It has been observed that light rains falling without high winds also can increase soiling, for heliostats stowed face-up, but will have little effect on inverted stow or vertical stow heliostats.\* Although these effects have been observed often, the range of variation in effect on reflectance degradation rate is too large to establish an accurate rate for light rains or combinations of rain and wind conditions. Therefore, approximations were made and a range of reasonably acceptable rates then used in assessing increased cleaning frequency due to storms.

Table 2-4 summarizes the additional reflectance degradation rates associated with the severe weather conditions compiled for minimum and maximum rates. These rates will be combined with the average daily degradation rate for benign conditions to give the range for the total degradation rate associated with the non-inverting heliostat.

\*It should be noted that wind rise rate for an approaching storm is an important consideration in sizing the heliostat drive unit. A non-inverting heliostat will normally achieve a face-up stow position in 3 to 6 minutes, and will, therefore, be subjected to lower wind loads than an inverting heliostat, which requires 9 to 12 minutes to move into a face-down position. The reduced wind load for this scenario with the non-inverting heliostat appears to be such that the slot area can be filled with reflector. However, a detailed point design of this option is required to determine the optimum area.

Table 2-4. Additional Reflectance Degradation Due to Severe Weather Conditions

Weather condition (heliostat face-up stow required)	Weather condition occurrence frequency per year (days)	Additional loss per occurrence (%/day)	Additional loss per year (%)	Additional daily averaged loss (%/day)	
				Minimum	Maximum
Wind gusts > 35 mph	23	0.37	8.6	0.0236	
Average wind < 40 mph	39	0.74	28.86		0.079
Light rain and high winds	2	2	4	0.011	
	3	10	30		0.082
Severe blowing sand and dust (average wind > 40 mph)	1	5	5	0.0137	
	2	5	10		0.0274
			Total	0.0483	0.1884

### Natural Cleaning by Frost, Rain and Snow

As discussed in References 2-2, -3, -4 and -5, certain severe weather conditions can be used to advantage to clean properly positioned heliostats. The number of days per month for which these conditions occur is therefore an indication as to the probability that natural cleaning can occur in such a way as to eliminate certain percentages of maintenance cleaning cycles. In general, heavy frost, rain, or snow can be used to clean heliostats quite effectively. The number of occurrences of these conditions at NWC for 16 months is summarized in Table 2-5. There are sufficient instances of heavy rain, snow, and frost during December, January, February, and March (5, 14, 8.5, and 6 days, average, respectively, for 1977-78) to provide the distinct possibility of eliminating essentially all requirements for washing during this period.

A set of assumptions on natural cleaning has resulted from a review of NWC weather data and heliostat reflectivity results (Reference 2-3) and from a review of Reference 2-5.

1. Frost can be a highly effective cleaner under certain conditions, i.e., heavy frost was formed for nighttime humidity >60 percent, and temperature <32°F.\* Thus, the number of days with these conditions for typical desert sites is an indication of the probability of natural cleaning, assuming heliostats are properly positioned and no windblown dust occurs during the frost period (see Reference 2-3).
2. Rains >0.25" can clean properly positioned heliostats to within 1-3 percent. Rains less than 0.25" (but with vertical stow permitted) accompanied by moderate winds do not substantially decrease reflectance, as shown by CRTF data of Figure 2-1.
3. Heliostats cleaned naturally at NWC were always positioned horizontally. More effective cleaning would result from tilting the surface during the rain, but even with horizontal stowage, heavy rains have cleaned the surface to within 1-2 percent of the initially cleaned value.
4. Snow ≥1/4 inch can clean properly positioned heliostats to within 1-2 percent (i.e., to within measurement error) (see Reference 2-2).

---

\*Note: Heavy frost followed by rapid temperature rise at dawn cleaned tilted heliostats at NWC due to frost layer sliding off glass surface. Light frost on heliostat at CRTF did not clean the surface, as noted by D. King.

Table 2-5. NWC Severe Weather Summary

Date	Heavy frost	Rainfall >0.5 in.	Snow	Possible natural cleaning days
Dec 76	4 days of H* >60%, T <32°F		--	4
Jan 77	16 days of H >60%, T <32°F	1	1	18
Feb 77	10 days of H >60%, T <32°F	--	--	10
Mar 77	8 days of H >60%, T <32°F	1	1	10
Apr 77	--	--	--	--
May 77	--	--	--	--
June 77	--	--	--	--
July 77	--	--	--	--
Aug 77	--	One 3-day storm	--	3
Sep 77	--	--	--	--
Oct 77	--	--	--	--
Nov 77	--	--	--	--
Dec 77	4 days of H >60%, T <32°F	2	--	6
Jan 78	7 days of H >60%, T <32°F	3	--	10
Feb 78	4 days of H >60%, T <32°F	3	--	7
Mar 78	--	2	--	2

\*H stands for relative humidity

A summary of weather conditions at NWC for 31 years is given in Reference 2-6. From this summary, the monthly average severe weather conditions were determined and are presented in Table 2-6. The summary does not provide a correlation of days of multiple weather occurrences, such as high winds followed by trace rains or heavy rains. Also, precipitation occurrences are based on measurable rain exceeding 0.01", whereas our data indicate a heavy rain of the order of  $\geq 0.25$ " is required to effectively clean heliostats. However, these

Table 2-6. Summary of Natural Cleaning and Severe Dust Buildup Weather Conditions\*

Mo	Temperature summary for 31-year period, 1946-1976		Relative humidity for 31-year period, 1946-1976		Average no. of days with low of 32° or less	Average no. of days with high of 100° or more	Average of daily maxima	Average humidity	Avg precipitation, 1946-1976 inclusive (in.)	Avg no. of days with 0.01 in. or more precipitation, 1946-1976 inclusive	Avg precip/day	No. of days with snow (mean ± standard deviation)
	Low-est	Date	High	Low								
Jan	0	13/63	57.6	30.7	22	0	74	51	0.51	2.06	0.248	0.677 ± 1.45
Feb	14	13/48 12/65	63.8	34.2	11	0	73	50	0.51	2.16	0.236	0.226 ± 0.56
Mar	17	2/71	69.0	39.7	5	0	65	40	0.25	1.48	0.169	0.161 ± 0.45
Apr	28	9/53 22/63	76.8	46.6	1	0	56	34	0.15	1.26	0.119	
May	34	1/67	86.2	55.2	0	1	47	29	0.04	0.677	0.059	
Jun	42	10/54	95.5	63.1	0	10	39	24	0.02	0.419	0.048	
Jul	52	5/64	102.3	70.0	0	23	37	23	0.16	0.903	0.177	
Aug	50	24,29/73 20/75	100.5	67.7	0	19	41	24	0.09	0.581	0.155	
Sep	39	26/70	94.0	60.3	0	7	44	27	0.22	1.032	0.213	
Oct	21	30/71	81.9	48.8	*	*	50	32	0.12	0.774	0.155	
Nov	18	20/64 30/75	68.0	37.0	8	0	63	42	0.47	1.710	0.275	0.032 ± 0.17
Dec	2	27/62	58.6	29.1	23	0	75	52	0.43	1.839	0.234	0.290 ± 0.46
Year	0	1,13/63	79.5	48.5	70	60	55	36	2.97			

\*Compiled from U.S. Naval Weapons Center climatological summaries for 1946 through 1976.

Data assembled by the NWC Meteorology Section, Code 6234.

Data from observations made at Armitage Field through November 1959; thereafter at the Instrumentation Laboratory, G-1 Range.

data summaries do support the indications of the 1977-78 weather data and reflectivity measurement that natural cleaning in the form of frost, rain, and snow may be effective from December through March. Further, April, September and November may also have a sufficient number of days of natural cleaning to be effective in eliminating a significant percentage of maintenance cleaning cycles.

It should be emphasized that the Naval Weapons Center has, as discussed in References 2-2 and -6, a relatively dry climate. As shown in Table 2-7, Albuquerque has a much higher frequency of occurrence of weather conditions which are potentially effective for natural cleaning. There is roughly an order of magnitude higher frequency of occurrence of thunderstorms, snow, sleet, and freezing rain compared to NWC, and roughly twice the frequency of rain/drizzle. It appears that estimates of natural cleaning effectiveness and frequency based on the NWC data may be conservative.

#### 2.2.2 Expected Dust Buildup Rates for Operational Heliostats

Since the CRTF data and MDAC heliostat and specimen data of Table 2-1 show agreement, the expected dust buildup rates can be determined with a reasonable degree of confidence for actual heliostat operational conditions for which there is no full-scale data at present. It is necessary to use accumulated data for various heliostat and specimen exposure and stowage positions and modify these data for the operational and stowage positions under consideration, and then estimate the additional dust buildup losses, and/or natural cleaning occurring as a result of severe weather conditions. Results are presented below for the expected nominal degradation rates of heliostats under actual operating conditions, using NWC heliostat and specimen data, followed by estimates of natural cleaning and severe dust buildup rate estimates.

Based on the results of References 2-2 to 2-5, the nominal dust buildup rate is approximately determined by exposure time at a given angle, with the rate decreasing linearly with the projected horizontal area of the surface. Assuming during daytime operation that the heliostats have an average elevation angle of 45°, the nominal face-up stow dust buildup rate is decreased by a

Table 2-7. Meteorological Summary

Station	Location	Elevation	Mean percentage of days per month for occurrence of various meteorological phenomena, from daily observations					
			Thunderstorms	Rain/drizzle	Snow/sleet/freezing rain	Fog	Dust/sand	Years of observation
Naval Weapons Center	Indian Wells Valley, CA	760 m	0.9	9.6	0.5	0.7	1.2	20
Edwards Air Force Base	Western Mojave Desert Near Mojave	770 m	1.2	9.6	0.9	1.9	1.6	19
George Air Force Base	Western Mojave Desert Near Victorville	960 m	1.7	10.1	1.4	2.3	1.0	18
Kirtland Air Force Base	Albuquerque, NM	1,780 m	10.2	22.9	6.9	2.7	1.2	26

Notes

Data compiled from Aerospace tapes.

Blowing dust/sand reported only when visibility is less than 1 km.

HelioStat Array Test Site located at Randsburg Wash, elevation 650 m.

factor of  $\sin 45^\circ$ . The nighttime vertical stow dust buildup rate is known for specimens as presented in Reference 2-5. The specimen and full-scale data are normalized to improve the accuracy. However, no effort is made to vary the degradation rate as a function of time of year or to determine time integrals of the degradation rate for different portions of the field, since these refinements would probably add little to the confidence in the resulting values, due to the variation in observed rates. Using the  $45^\circ$  assumption, the combined face-up/face-down and face-up/vertical stow rates are:

$$R_{FU/FD} = R_{FU/V} = \frac{\sin 45^\circ \times 0.425 + 0.045}{0.425} (0.37 \pm 0.07)$$

$$= 0.150 \pm 0.05\%/day$$

The above degradation rate holds for nominal conditions with heliostats operated during the day at a  $45^\circ$  angle, and stowed either face-down or vertical at night. It should be noted that the degradation rates for converted and vertical stow are assumed to be equal.

Adding the previously determined range of severe weather degradation rates to the above benign condition degradation rates gives the averaged total degradation rate. For the inverting heliostat, the reflector can be positioned vertical or inverted, depending on wind and rain conditions, with the vertical or near vertical position probably preferred whenever any natural cleaning occurs.

It should be noted that face-down stow is an assumed option, not necessarily a required stow position. The inverted stow capability may only be used under high wind conditions, and vertical stow used under nominal conditions. This stowage mode may decrease dust buildup on the back surface, which could be washed onto the mirror under conditions of inverted stow in a rainstorm accompanied by high winds. Although there are degradation effects with inverted stow under severe weather conditions, these possible additional losses have not been included to make the increased washing cost values for a noninverting heliostat even more conservative. The non-inverting heliostat would, of course, be stowed vertical whenever practical, and face-up under high wind conditions.

In summary, the total daily average degradation rates due to both nominal severe dust buildup conditions, assuming an average 45° angle during the day, and ignoring natural cleaning, is given in Table 2-8.

Table 2-8. Total Degradation Rate Summary

Inverting heliostat degradation rate	R = 0.150%/day
Non-inverting heliostat degradation rate	
Nominal degradation rate	0.150%/day
Additional average degradation rate due to severe weather	<u>0.0483</u> to <u>0.1884%/day</u>
Total degradation rate for vertical stow	0.198 to 0.338%/day

### 2.2.3 Washing Frequency Analysis

Using the previously generated reflectance degradation rates, the average number of cleaning cycles required per year to maintain reflectance above a prescribed value is determined. Two conditions are used. First, it is assumed that washing is only required eight months out of the year, since at least four months (December through March) and possibly August, September and November have sufficient rain, snow and/or frost, to maintain high reflectance values for properly positioned heliostats. It is next assumed that natural cleaning is not at all effective. Based on NWC results, and supported by CRTF data, it appears to be far more likely that at least four months, on the average, of natural cleaning can be utilized by properly positioning the heliostats. However, washing frequencies and associated costs assuming a full year of required maintenance cleaning will be more conservative when comparing the inverting stow and non-inverting stow economics. The minimum and maximum average degradation rates for the non-inverting heliostat are used.

The number of washing operations per year,  $N_W$ , is determined from:

$$N_W = \frac{365}{\Delta\rho/R}$$

where  $\Delta\rho = 3\%$ ,  $6\%$ ,  $9\%$ , or  $12\%$ . The degradation rates used for the inverting and non-inverting heliostat are:

- $R_{IH} = 0.15\%/day$  for the inverting stow heliostat
- $R_{NIN_{MIN}} = 0.20\%/day$  for the non-inverting stow heliostat, minimum rate.
- $R_{NIH_{MAX}} = 0.34\%/day$  for the non-inverting heliostat, maximum rate.

The results are summarized in Table 2-9, without consideration of the cost optimum allowed reflectance loss and hence the optimum number of cleaning operations required on an average yearly basis. These effects are considered in following sections.

### 2.2.3.1 Cleaning Materials Usage

The quantity of wash solution and deionized water assumed for this analysis is based on results of tests at NWC which are summarized in Table 2-10. For example, based on the results of washing heliostat H4 with minimum quantities of cleaning solution (1.25 gallons of CB120 and 5.75 gallons of deionized water) and achieving full recovery of the initial reflectivity, it is assumed that 1.5 gallons of cleaning solution and six gallons of deionized water will be effective.

### 2.2.3.2 Heliostat Cleaning Rate

The time required to clean a full scale heliostat ( $40-50M^2$ ) with one technician using a single hand held-spray wand has been shown to be of the order of three minutes (see Table 2-10). Use of multiple spray wands positioned on a truck will allow much more rapid cleaning. If a single wash truck is used to clean and rinse the heliostat, it can be assumed that the truck moves by each heliostat at a rate that allows 30 seconds for the wash application, followed by 30 seconds of dwell time and 30 seconds for rinsing. If the wash spray wands are positioned on a near vertical support and the width of the heliostat is 22 ft; then the truck can move at a steady rate of 0.5 mph. If the rinse spray wands are also positioned on a vertical support, then the dwell time for each incremental column of wash solution residing on the heliostat before rinsing will be 30 seconds. The separation distance between the wash and rinse wands would be 22 ft. If the distance between heliostats is assumed to be of the order of the width of the heliostat, the net transit time per heliostat would be one minute.

Table 2-9. Number of Washing Operations Per Year

Stow position assumptions and rate	Wash 8 months/year allowed loss				Wash 12 months/year allowed loss			
	Allowed loss:	<u>3%</u>	<u>6%</u>	<u>9%</u>	<u>12%</u>	<u>3%</u>	<u>6%</u>	<u>9%</u>
Inverting heliostat, face down stow R = 0.150%/day*	12.2	6.1	4.1	3.0	18.3	9.1	6.1	4.6
Non-inverting heliostat, vertical stow with 0.05%/day additional degradation due to winds and light rain and forced face-up stow R = 0.20%/day	16.2	8.1	5.4	4.1	24.3	12.2	8.1	6.1
Non-inverting heliostat, vertical stow with 0.19%/day additional degradation due to winds and light rain and forced face-up stow R = 0.34%/day	27.6	13.8	9.2	6.7	41.4**	20.7	13.8	10.3

\*The face down stow rate of 0.15%/day does not include the detrimental effect of accumulated dust on the bottom of heliostats being washed onto the mirror surface during heavy winds and rain with the heliostat inverted. This effect was observed at NWC.

\*\*The maximum predicted wash frequency corresponds to essentially continuous washing on a weekly basis, and is not economically viable.

Table 2-10. Washing Effectivity Results, 3/15/77

Helio- stat no.	Prewash reflectance, $\rho_{in}$ (%)	Postwash reflectance, $\rho_{final}$ (%)	Reflectance increase, $\Delta\rho$ (%)	Application time		Solution quantity		Solution type		Nozzle type	
				Wash (min)	Rinse (min)	Wash (gal)	Rinse (gal)	Wash	Rinse (water)	Wash (gpm)	Rinse (gpm)
H1	65.88	78.24	12.36	1.0	5.0	1.50	14.00	A69M	D.I.	1	5
H2	56.08	76.50	20.42	1.0	3.7	1.25	8.75	A69M	D.I.	1	5
H3	69.23	87.46	18.23	1.0	3.0	0.75	8.0	A69M	D.I.	1	5
H4	73.31	87.65	10.69	1.0	2.0	1.25	5.75	CB120	D.I.	1	5
IH1	76.80	86.5	8.30	1.4	2.8	1.60	7.75	CB120	D.I.	1	5
IH1'	72.16*	86.60	14.44								

Waiting period between wash and rinse = 1 minute. A69M and CB120 available from McGeon Chemical Company.

IH1' = 3/32 in. float glass (foam core)  
 IH1 = 1/4 in. float glass (laminated)  
 H4 = laminated glass

H1, H2, H3 = acrylic coating  
 \*Reflectivity of IH1' as received from  
 plant following fabrication.

To achieve shorter wash times with the flexibility of longer dwell times, two trucks may be used. The wash truck would precede the rinse truck by one minute, for example, and would move at a rate of one mph. The net transit time per heliostat could then be decreased to 30 seconds. An advantage of using two trucks is that dwell times can be varied as required by changing environmental conditions, without affecting the total wash time, simply by varying the distance between the two trucks. However, rates much faster than one heliostat per 30 seconds may not be practical for spray techniques because of the limitation of water runoff times. Esoteric wash techniques involving mechanical brushes, air jets, vacuums, etc., are not considered in this analysis.

The manpower required in both of the above cases may be the same because it is customary to use a "buddy" system and, therefore, the single wash/rinse truck could require a driver and technician, whereas the tandem trucks may use only one driver in each truck who could assist each other in the event of accident. The single truck may also require a driver and a technician to monitor the positions of the two spray wands.

#### 2.2.3.3 Equipment, Materials, and Manpower Levels

The equipment, materials, and manpower levels required to wash a field of heliostats was determined for a range of conditions. Two extreme wash conditions were considered with corresponding intermediate conditions. These conditions for a 100 MWe plant field are that provisions are made for:

1. Sufficient equipment to wash 18,000 heliostats in five days, eight hour shifts with 30 seconds per heliostat, and tandem trucks, with two drivers,
2. Sufficient equipment to wash 18,000 heliostats in ten days, 8 hour shifts, with 30 seconds per heliostat, and tandem trucks, with two drivers.
3. Sufficient equipment to wash 18,000 heliostats in five days, 8 hour shift with one minute per heliostat, and a single truck, with a driver and technician.
4. Sufficient equipment to wash 18,000 heliostats in ten days, 8 hour shifts, with one minute per heliostat, and a single truck, with a driver and technician.

#### 2.2.4 Cost Analysis

Cost analyses are presented in the following which consider labor, capital equipment, materials usage, and cleaning frequency cost implications from four standpoints. First, the cost of providing an inverted stow capability are determined. Second, the costs in constant 1978 dollars of cleaning a field of heliostats is determined for a range of reasonable values of manhours and quantity usage. Third, the effects of inflation and monetary discount rates are considered. Fourth, allowable degradation is determined based on a minimum total cost associated with both cleaning and adding heliostats to the field to make up for the lost energy due to additional allowed degradation. The cost optimized degradation values and associated cleaning frequencies are then compared on a total cost basis to determine the relative costs of the inverting and non-inverting designs. It is shown that the non-inverting design results in a substantial net cost savings compared to the inverting design.

##### 2.2.4.1 Inverted Stow Costs

###### Cost of Providing Inverting Stow Capability

The costs of providing an inverting stow capability to be used predominately during periods of high winds has been determined as part of the Prototype Heliostat study (Reference 2-1). Elimination of this capability gives a potential cost savings of approximately \$552 per heliostat, as shown in Table 2-11. Thus, any non-inverting annualized additional washing cost (for a 30-year life) less than this amount would indicate that from a cleaning standpoint, it is cheaper to eliminate the capability to invert. The details of the cost breakdown for inverting are summarized below.

The cost of being able to invert the heliostat is associated with three aspects of the design: (1) added azimuth weight, (2) additional elevation drive parts, and (3) lost mirror area, due to the slot required to clear the pedestal. These costs are shown in Table 2-11 (from Reference 2-2) and are based on the costs as factored for the production rate of 25,000 heliostats per year. For the inverting heliostat, an additional 5.2 square meters of mirror is lost due to the slot required to invert, and therefore, more heliostats are required for a field of a given total energy capacity. The

Table 2-11. Approximate Heliostat Costs Associated With a 100 MWe Stand-Alone Electric Generating Plant\* (Not Including Respective Washing Costs)

Inverting		Noninverting	
Cost:	$\$72/m^2R$	Cost:	$\$3,249$ less hardware costs associated with inverting, plus cost of additional reflector area.
Area:	$49.05 m^2$		
Reflectivity, R =	0.92	Hardware savings:	
Number of heliostats:	18,000	Azimuth housing weight	0.90
Total cost = $\$72 \times 49.05 \times 0.92$		Elevation drive	
= $\$3,249/\text{heliostat}$		Drag link	$\$ 22.56$
= $\$58,483,296/\text{field}$		Bushing	0.50
		Pin	1.50
		Inverting hinge point	6.00
		Stowage jack	224.58
		Motor	49.25
		Electronics	10.00
		Total	$\$315.29$

Additional reflector area cost:  $\$49.46 (5.2 m^2)$

Net savings =  $\$265.83$

Total cost/heliostat =  $\$2,983.17/\text{heliostat}$

Number of heliostats = 16,275

Total cost per field =  $\$48,551,091$

Cost savings =  $\$9,932,205$  per field for reduced hardware and increased heliostat area if inverting stow capability is eliminated.

Cost savings =  $\$552/\text{heliostat}$  (based on 18,000 heliostats)

\*From Solar Central Receiver Prototype Heliostat. Final Technical Report. August 1978. McDonnell Douglas Astronautics Co., Huntington Beach, CA. DOE Contract EG-77-C-03-1605.

cost of the mirror includes both the added square footage of the mirror module and added stringer length, both of which are costed on a dollar per area basis. The overall hardware costs are determined for a 100 MWe field of 18,000 inverting heliostats, and 16,275 non-inverting heliostats. The net hardware savings, and the savings associated with increasing the reflector area are approximately equal.

There are additional possible savings associated with elimination of the inverted stow capability and use of face-up stow in high winds. For example, the motor torque and horsepower ratings, drive ratio, and maximum loads are determined in part by the requirement to achieve an inverted stow position during a period of increasing wind due to an approaching storm front. Achieving a face-up stow position can be accomplished more rapidly, and therefore the loads, torque, horsepower, etc., would be less. It is this particular aspect which allows the area of a non-inverting heliostat to be greater than that of an inverting heliostat, while using the same drive unit. Also, the reflector may be positioned in a more optimum manner if the inverting requirement is eliminated, possibly reducing wind and gravity loads, and hence weight and cost. The heliostats may be located closer to the tower; thereby reducing tower height, tower and receiver costs, atmospheric attenuation and spillage. With fewer heliostats for a given application, operations and maintenance costs will also be reduced. These additional considerations have not been included in this study, but will lead to significant additional cost savings.

#### 2.2.4.2 Cleaning Costs

The costs associated with cleaning a field of 18,000 heliostats are summarized in Tables 2-12 and -13, along with key assumptions as to amount of equipment and material required, washing technique, manpower levels, etc. It is seen that the cost of washing a heliostat is of the order of \$0.77 to \$1.32 per heliostat, per cleaning, where a range of cost assumptions generate the maximum and minimum washing costs.

#### 2.2.4.3 Monetary Effects

Since monetary parameters can have a substantial effect on total cleaning costs, and since it is necessary to compare the effective 30-year cleaning costs with the additional capital cost of providing an inverting capability, it is necessary to reduce the 30-year cleaning costs to a "present value," based on inflation and monetary discount rates. The "present worth factor" (PWF) is used, where

Table 2-12. Washing Cost Factors Using Spray-Soak Washers on a Single Truck for an 18,000 Heliostat Field (1 Minute per Heliostat Wash Period with Sufficient Equipment to Wash Entire Field in 5 Working Days, 8 Hour Night Shift Operation)

<u>Assumptions</u>					
1.	One minute wash per heliostat				
2.	Wash truck sized for 480 heliostats				
3.	Two man crew per truck				
4.	Cleaning solutions: 5%				
5.	1.5 gal cleaning solution per heliostat				
6.	6 gal DI rinse water per heliostat				
7.	Diesel fuel consumption 12 gal/hour				
8.	0.5 hours per truck reload				
9.	Equipment depreciates to zero value in 10 years				
10.	Approximately 12 cleanings/year				
	<u>Calculations</u>	<u>Equipment/req'd materials/wash</u>	<u>Man-hours/wash</u>	<u>Unit cost</u>	<u>Cost/wash</u>
	$\frac{18,000}{60 \text{ min}} = 300 \text{ hours for field}$				
	$\frac{18,000}{480} = 37.5 \text{ reloads for field}$				
	$37.5 \times 0.5 \text{ hr} = 18.75 \text{ hrs. reload}$				
	$300 + 18.75 = 320 \text{ hrs. total wash time for entire field}$				
	Trucks required: $\frac{320}{40} =$	8 trucks		\$50K	\$ 3,333.0
	Manhours required:				
	8 vehicles x 2 <sup>men</sup> vehicles x 40 hrs =		640	\$15.0	\$ 9,600.0
	Vehicle maintenance:				
	8 vehicles x 40 hrs x 10%		32	\$30.0	\$ 960.0
	Fuel required:				
	40 hrs. x 12 gal/hr x 8 vehicles =	3,840 gal.		\$ 0.56	\$ 2,150.0
	DI water required:				
	$18,000 \times 6 + (18,000 \times 95\%) =$	133,650 gal.		\$ 0.025	\$ 3,341.0
	Cleaning solution required:				
	$18,000 \times 1.5 \times 5\% =$	1,350 gal.		\$ 3.25	\$ 4,387.0
				Total:	\$23,771.0
					or \$1.32/heliostat/wash

Note: Softened water, at  $\leq 1\text{¢}/\text{gal.}$ , rather than deionized water, at  $2.5\text{¢}/\text{gal.}$ , may be used for rinsing. Rinse water costs would then be \$1,336.50, for a savings of \$2,005 per wash. Cleaning solution costs may be as low as \$2.90/gal., for a cost per wash of \$3,915, and a savings of \$472. The total cost per wash would then be \$21,294 or \$1.18/wash/heliostat.

Table 2-13. Washing Cost Factors Alternate Spray Soak Method, Using Two Trucks on an 18,000 Heliostat Field (30 Second Wash Period With Sufficient Equipment to Wash Entire Field in 10 Working Days, 8 Hour Night Shift Operation)

Assumptions

- |  |   |
|--|---|
| 1. 0.5 min wash per heliostat                | 6. 1.5 gal cleaning solution per heliostat            |
| 2. Both wash trucks sized for 480 heliostats | 7. 6 gal DI rinse per heliostat                       |
| 3. One man crew per truck                    | 8. Fuel consumption 12 gal/hr.                        |
| 4. Two trucks in tandem                      | 9. 0.5 hour to reload both trucks                     |
| 5. Cleaning solution 5%                      | 10. Equipment depreciates to zero value over 30 years |

<u>Calculations</u>	<u>Equipment req'd materials/wash</u>	<u>Manhours/wash</u>	<u>Unit cost</u>	<u>Cost/wash</u>
$\frac{18,000}{120 \text{ min.}} = 150$ hours for field				
$\frac{18,000}{480} = 37.5$ reloads for field				
$37.5 \times 0.5 \text{ hr.} = 18.75$ hours reload				
$150 + 18.75 = 170$ hours for field				
Trucks required $\frac{170}{80} \times 2 =$	4 trucks		\$50K	\$ 1,555.0
Manhours required $170 \times 2 =$		340	\$15.0	\$ 5,100.0
Vehicle maintenance $4 \times 80 \times 10\% =$		32	\$30.0	\$ 960.0
Fuel required $80 \times 12 \times 4 =$	3,840 gal.		\$0.56	\$ 2,150.0
DI water required $6 \times 18,000 + (1.5 \times 18,000 \times 95\%) =$	133,650 gal.		\$0.025	\$ 3,341.0
Cleaning solution required $1.5 \times 18,000 \times 5\% =$	1,350 gal.		\$3.25	\$ 4,387.0
				\$16,493.0/wash or \$0.92/heliostat/wash

Note: Softened water, at 1¢/gal., rather than deionized water at 2.5¢/gal., may be used for rinsing. Rinse water costs would then be \$1,336.50 for a savings of \$2,005 per wash. Cleaning solution costs may be as low as \$2.90/gal., for a cost per wash of \$3,915 and a savings of \$472. The total cost per wash would then be \$14,016 or \$0.77/wash/heliostat.

$$PWF = \frac{1}{1+i} \left[ \frac{1-x^n}{1-x} \right] \quad (3)$$

and

$i$  = Discount rate (return on investment, % per year)

$r$  = Inflation rate (% per year)

$n$  = Number of years

$$x = \frac{1+r}{1+i}$$

It should be noted that for  $x = 1$ , it is necessary to use L'Hospital's rule, and equation (3) reduces to  $PWF = n/1+i$ . Normally,  $i \leq r$ , and, therefore,  $x \leq 1$ , and the present worth is less than  $n/1+i$ .

#### 2.2.4.4 Cost Optimum Cleaning Frequency and Allowed Degradation

In a simplified manner, the minimum cost of delivering a given amount of power can be determined as a function of the allowed degradation rate. For a given solar plant yearly output, more heliostats are required as the allowed degradation value is increased. In Reference 2-2, the minimum total cost equation is derived, which gives the allowed degradation,  $\Delta \rho$ , in terms of heliostat costs  $C_H$ , cleaning costs per wash,  $C_W$ , degradation rate,  $R_D$ , and monetary parameters (inflation,  $r$ , and discount rate,  $i$ ).

From Reference 2-2, the total cost of the collector field, including (1) costs for the heliostats (18,000 for inverting, 16,275 for non-inverting), (2) additional heliostat costs to account for the decrease in operational reflectivity, and (3) present worth of the 30-year cleaning costs, is given by

$$\text{Total Cost} = D \left\{ A \left[ \frac{B}{C-\Delta\rho} \right]^1 + C_H \left[ \frac{B}{C-\Delta\rho} - 1 \right] \right\}$$

where,

$$A = 365 C_W R_D \left[ \frac{1}{1+i} \left( \frac{1-x^n}{1-x} \right) \right]$$

$$B = 181$$

$$C = 2\rho_{\text{initial}} = 184$$

$$D = 18,000 \text{ for inverting, and } 16,275 \text{ for non-inverting}$$

The minimum total cost corresponds to an allowed decrease in reflectivity,  $\Delta\rho$ , given by

$$\Delta\rho = \frac{-A + \sqrt{A^2 + C_H AC}}{C_H}$$

It is assumed that cleaning occurs when the initial reflectivity is decreased by  $\Delta\rho$ .

Figure 2-2 shows the dependence of total collector field costs on washing cost per heliostat, heliostat stowage configuration, heliostat cost, and reflectance degradation. It should be noted that the relatively shallow curves indicate that the cost minimum is relatively insensitive to the  $\Delta\rho$  selected. However, once the  $\Delta\rho$  is selected, the number of additional heliostats, as well as the stowage configuration, is set for that field, and the  $\Delta\rho$  allowed before cleaning is initiated is then set for that field. Figure 2-2 does not indicate that plant operators can allow  $\Delta\rho$  to vary widely without incurring changes in total cost due to lost energy, or additional maintenance cleaning.

Table 2-14 summarizes the major results of this task. Using reasonably practical values for inflation rate,  $r = 8\%$ , and monetary discount rate,  $i = 10.2\%$ , the total potential cost savings achievable by eliminating the inverted stow capability is found to be 12.07 to 13.28%, and is not sensitive to the cost of washing a heliostat. For a commercial 100 MWe field, the net cost savings achieved by eliminating the inverted stow capability is approximately \$8 million.

The number of times the field of heliostats would be washed per year ranges from 9 to 12, depending on cleaning costs per heliostat, assuming natural cleaning does not occur. The number of cleanings may be reduced to 6 to 8 per year if natural cleaning occurs roughly four months out of the year.

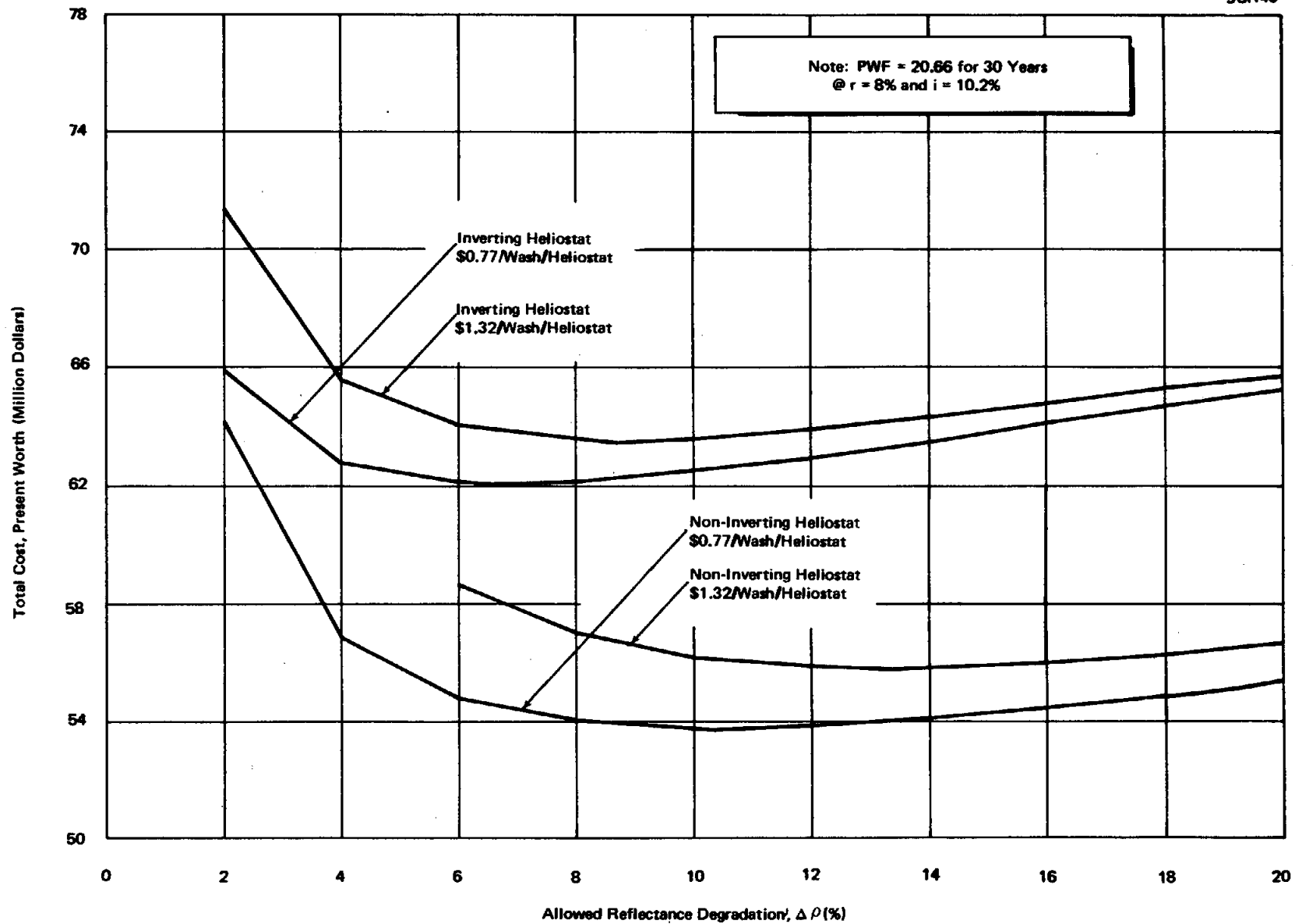


Figure 2-2. Total Commercial Field Cost Dependence on Degradation/Cleaning Parameter

Table 2-14. Total Cost Comparison of Inverting and Non-Inverting Heliostats

Inverting heliostats conditions			Non-inverting heliostats conditions		
	\$0.77/wash/heliostat	\$1.32/wash/heliostat		\$0.77/wash/heliostat	\$1.32/wash/heliostat
	$\Delta\rho = 6.75\%$	$\Delta\rho = 8.74\%$		$\Delta\rho = 10.36\%$	$\Delta\rho = 13.35\%$
	$N_W = 8.11$	$N_W = 6.26$		$N_W = 11.97$	$N_W = 9.29$
	$N_H = 18,382$	$N_H = 18,591$		$N_H = 16,968$	$N_H = 17,263$
Item	Cost	Cost	Item	Cost	Cost
Present worth washing cost	\$2,367,296	\$3,145,924	Present worth washing cost	\$3,227,159	\$4,376,365
Additional heliostats at \$3,249	\$1,241,118	\$1,920,159	Additional heliostats at \$2,983.17	\$2,067,219	\$2,947,496
Subtotal	\$3,608,414	\$5,096,082	Subtotal	\$5,294,378	\$7,356,381
Cost of 18,000 inverting heliostats at \$3,249/heliostat	\$58,482,000	\$58,482,000	Cost of 16,275 non-inverting heliostats at \$2,983.17	\$48,548,325	\$48,548,325
Total	\$62,090,414	\$63,578,082	Total	\$53,842,703	\$55,904,706

Results

Net cost savings =  $\frac{\$62,090,414 - \$53,842,703}{\$62,090,414} \times 100\% = 13.28\%$  for \$0.77/wash/heliostat case

Net cost savings =  $\frac{\$63,578,482 - \$55,904,706}{\$63,578,082} \times 100\% = 12.07\%$  for \$1.32/wash/heliostat case

- (1) Conditions shown are for minimum total cost based on optimum  $\Delta\rho$ .  
 (2) Present worth factor is 20.66 for a 30 year life generating plant. Assumes inflation rate  $r = 8\%$ ,  $i = 10.2\%$ , and monetary factor  $x = \frac{1+r}{1+i} = 0.980$ .

The approach presented above is adequate for estimating a first order cost savings for the non-inverting heliostat design including the effects of additional cleaning. However, this approach does not give the overall minimum cost of delivered power as a function of cleaning frequency since it assumes that the inverting and non-inverting fields are compared on the basis of equal total energy delivered. To obtain the minimum cost of delivered energy as a function of cleaning frequency, it is necessary to compare the incremental cost of additional cleaning with the incremental value of additional energy. This technique has been used recently by Eason (Reference 2-7). The optimum cleaning frequencies found are somewhat higher than those predicted above, assuming the same degradation rate.

### 2.3 RECOMMENDED ADDITIONAL EFFORT

Additional studies which would be beneficial in assessing cleaning cost and operational implications of inverting and non-inverting heliostats are listed below.

1. Continual monitoring of existing specimens and heliostats will provide useful information on reflectance losses and gains associated with severe weather conditions. In particular, the effect of seasonally heavy rains on specimens and heliostats exposed for over two to three years at NWC could be determined to assess long term natural cleaning and degradation.

2. Heliostats at Sandia Laboratories and possibly NWC or other desert sites should be monitored while being operated and stowed in various ways which simulate actual plant operation. To date, this has not been practical.

3. Heliostat dust build-up patterns on surfaces due to wind and rain, condensation patterns, etc., can cause wide variations in reflectance degradation. Overall reflectance losses for the entire heliostat are therefore preferred and require techniques more practical than isolated point measurements or laboratory measurements of small specimens.

4. Analyses such as those herein can be refined by additional effort and improvements made for field average degradation rates, cost optimums, etc. In particular, field optimization computer programs, or derived results from these programs, should be used to determine the number of additional heliostats required to maintain the same output energy load as the allowed degradation is increased. More accurate cost projections can then be made including cost increments for tower height, atmospheric attenuation, maintenance, heliostat power requirements, optimum stowage angles, etc.

5. The operational modes required to take full advantage of potential natural cleaning deserve further investigation. For example, since heavy frost formation can be used to clean heliostats, heliostats may be stowed face up at night to accumulate frost and then positioned facing the sun in the morning to allow the frost to slide off. These conditions have been observed, but are not well understood. Similarly, it is not clear what the best orientation sequence is for heavy rainfall.

6. Operational algorithms can be developed which allow plant operators to properly position the heliostats as a function of actual or forecasted weather conditions.

7. Data is required from other sites, including such considerations as air pollution effects on soiling rates. In particular, hybrid and repowering solar plants will be located in the vicinity of coal or oil burning power plants, and the stack gas emissions, cooling tower effluent, and in the case of coal, delivery and handling system for the fuel, can have significant effects on mirror soiling rates compared to the relatively clean conditions in the desert. These rates would be required before a final recommendation could be made regarding stowage conditions.

8. Vertical stow of heliostats under desert conditions (without pavement as at CRTF) has not been investigated. The possibility of additional dust buildup near the bottom of the reflector exists and deserves consideration.

9. Full scale washing tests of heliostats are required to determine actual costs in terms of manpower, quantity usage, and rates. Use of softened rinse water should be considered in view of potential savings of 20 percent of the total cleaning cost.

10. The effects of scattering of the reflected beam due to various levels of dust buildup deserve consideration, especially in terms of spillage on the receiver and irradiation of adjacent receiver structural support areas.

11. Design and cost estimates for a non-inverting heliostat are justified at this time, and would provide the basis for a subsequent fabrication and test program.

## 2.4 CONCLUSIONS

1. For a 100 MWe Commercial Central Receiver Solar Thermal Power System, a cost savings of approximately  $\$7.7 \times 10^6$  to  $\$8.25 \times 10^6$  per field, or 12.07 to 13.28%, is achievable by eliminating the inverted stow capability, even though additional cleaning cycles are required.

2. Monetary parameters have a significant effect on the cleaning costs.
3. For the optimum total cost condition of a non-inverting heliostat, with an 8% inflation rate and 10% discount rate, the number of cleaning operations ranges from 6 to 8 per year with natural cleaning, to 9 to 12 per year without natural cleaning (assuming constant annual energy delivered).
4. The range of cleaning costs is \$0.77 to \$1.32/wash/heliostat, depending on cleaning technique and use of softened or deionized water.
5. Cost savings associated with eliminating the inverting capability are based on prototype heliostat costs in mass production. The necessarily higher heliostat costs associated with near term, low production rate demonstration projects accentuate the potential savings if the inverting stow capability is eliminated. Further consideration of an inverting stow requirement for near term projects is therefore in order.



Section 3  
TASK II - HAIL STUDY

3.1 OBJECTIVE

The objective of this task is to review and summarize the historical weather data for the eight southwestern states, including the size of hailstone, frequency of occurrence and associated wind velocity. Storm correlations with location, season of year, meteorological conditions, and ability to predict hailstorms in time to orient the heliostats (if such maneuvering is effective in protecting the heliostats), is an additional objective. Maximum use is made of existing national weather data, other studies, and previous hail test results. Advantageous additional hail testing is proposed. A further objective is to utilize available hail test data to construct an analytical vulnerability model for heliostat glass mirror breakage.

One of the major objectives of this task is to assess the cost implications of hail impact on a non-inverting heliostat. Because of the probable correlation between severe hail storms and high winds, it is assumed that the non-inverting heliostats would be stowed face-up. It is therefore necessary to determine: (1) what conditions of hail impact will cause breakage for various candidate glass reflectors, and (2) the probable hailstone diameters to be encountered by the field throughout its life, for various regions of the U.S.. Each of these aspects is presented below, and the cost implications of the non-inverting heliostat compared with the inverting heliostat.

3.2 HAIL STATISTICS

3.2.1 Approach

Hail, as a spectacular and damaging meteorological manifestation, has been the subject of considerable interest for many years. Early work did not yield much quantitatively useful information of the sort needed for the present study. Changnon gives a brief survey of this work in Reference 3-1. Changnon

has also listed the data available as of June 1977 by type of source (U.S. Weather Service, hail insurance industry data, and relatively small scale ("meso-network") hail data).<sup>3-1</sup> Because of the availability of this authoritative survey, the present report will emphasize areas where additional information is available (or in some cases, where additional work should be done).

To anticipate, in what follows it will be clear that insufficient data exist to thoroughly characterize the hail environment of the eight southwestern states. However, hail density and fall speeds under gravity are well known. Point frequencies of hail ("point" ranging in meaning from a hail detection device of about one square foot to the field of view of an observer at a weather station or on a farm) are reasonably well known, as is the general pattern of causality and intensity throughout the country. Some information is available on hailstone sizes and size distributions, and on hailstone shapes. Some information also exists on the ratios of area-to-point hail frequencies, but these may vary from place to place and perhaps are controlled by the care of observation. Finally, not much information is available on the correlation of wind speed with hailstone size.

In addition to the above data, another source of information exists: records of crop and property damage caused by hail. These are discussed, and property damage is chosen as the more useful data. The available information is shown; it is more directly applicable but less well supported than hail characteristics data. The property damage data are generally in agreement with the point frequency and intensity data, with one exception of importance to this study: in Utah, northern Arizona and northern New Mexico, point frequencies are high, and intensity is listed as moderate, but the property damage potential (as a fraction of local property value) is quite low.

### 3.2.2 Available Meteorological Data

#### 3.2.2.1 Point Frequency and Intensity

Point frequency of hail is generally taken to mean the average annual number of days in which hail is observed at a given location. Observation can be by an observer, or by impact on a detector. Some discussion of instrumentation

will appear in succeeding sections; here it may suffice to note that the type of observation can affect the results, as a human observer is not likely to miss seeing a large hailstone that barely misses him, while a near miss of a detector might as well be in another state. However, hail data are almost always subject to this sort of uncertainty, and their use must be with reservations.

The best available information on point frequency of hail was based on data from 1285 stations in 17 states.<sup>3-2</sup> This information is shown in Figure 3-1, in which "first-order stations" refers to U.S. Weather Service stations manned by trained observers. It is not clear whether the small-scale structure in Figure 3-1 is entirely valid; for example, the drop from nine to four days and the following rise to seven days on a straight line some 200 miles long from the southeast corner of Wyoming to almost directly south to eastern central Colorado is suspect. Nevertheless, the general pattern is believed to be reliable.

Point frequencies, together with the primary cause of hail, peak hail season, and intensity, were used to define 14 hail regions in the contiguous U.S.<sup>3-1</sup> These are shown in Figure 3-2. In view of the causal input and the absence of small-scale structure, the information of Figure 3-2 may well be more appropriate for predictions than that of Figure 3-1.

#### 3.2.2.2 Effect of Target Area on Frequency of Hail Impact

In attempting to predict hail damage, it is not sufficient to know the rate of occurrence of hail at a "point." The area of the target will clearly affect its probability of being hit, and this must be accounted for.

#### Area-to-Point Frequency Ratios

One method of determining impact vulnerability for an object is by establishing a ratio of area hail-day frequencies to point hail-day frequencies. This ratio would be expected to be a function of the area for which the hail frequency was sought, and of the size of the "point." The results of some attempts at correlating this ratio are shown in Figure 3-3 (see also References 3-1, 3-3, 3-4, and 3-5).

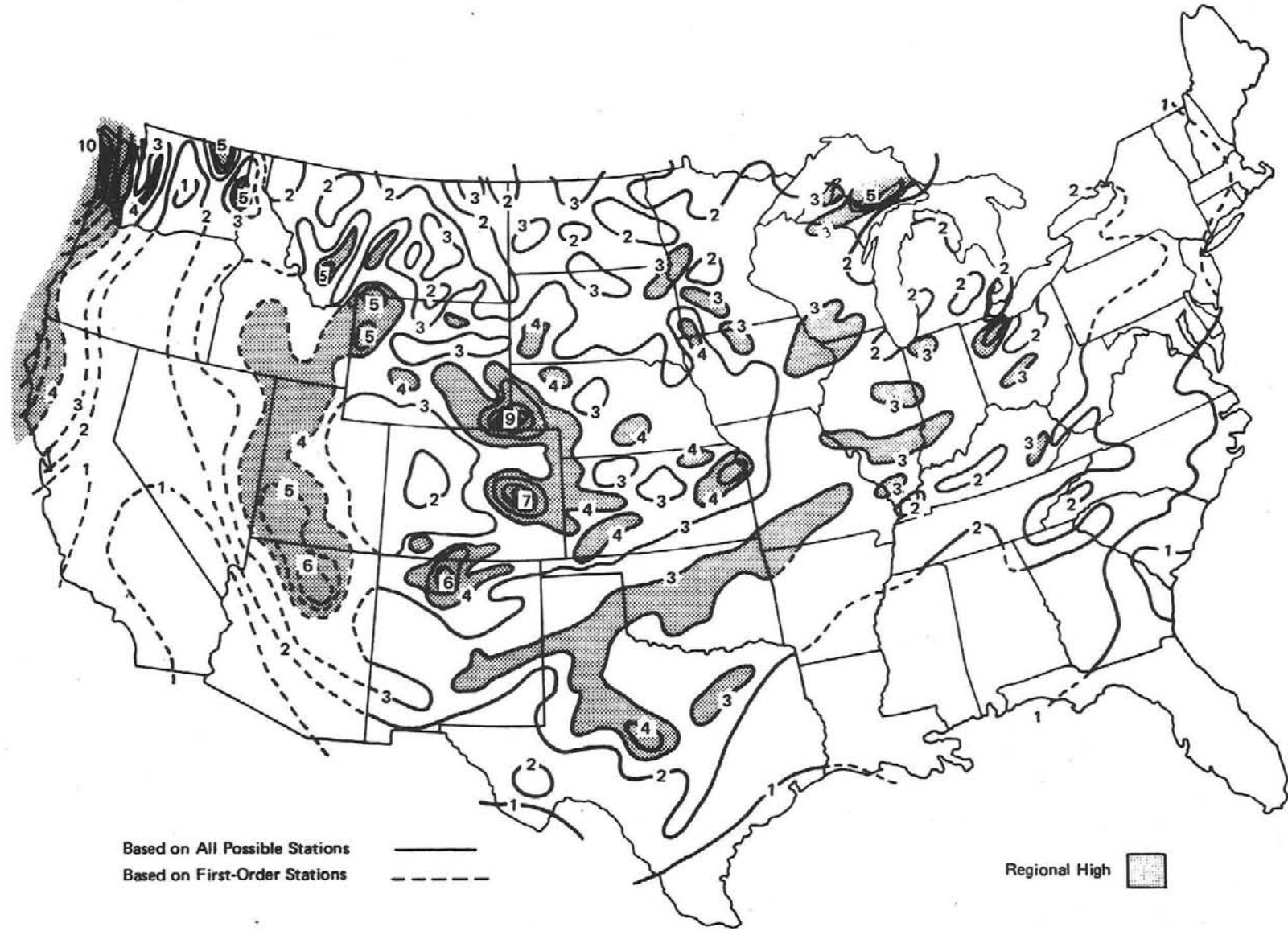
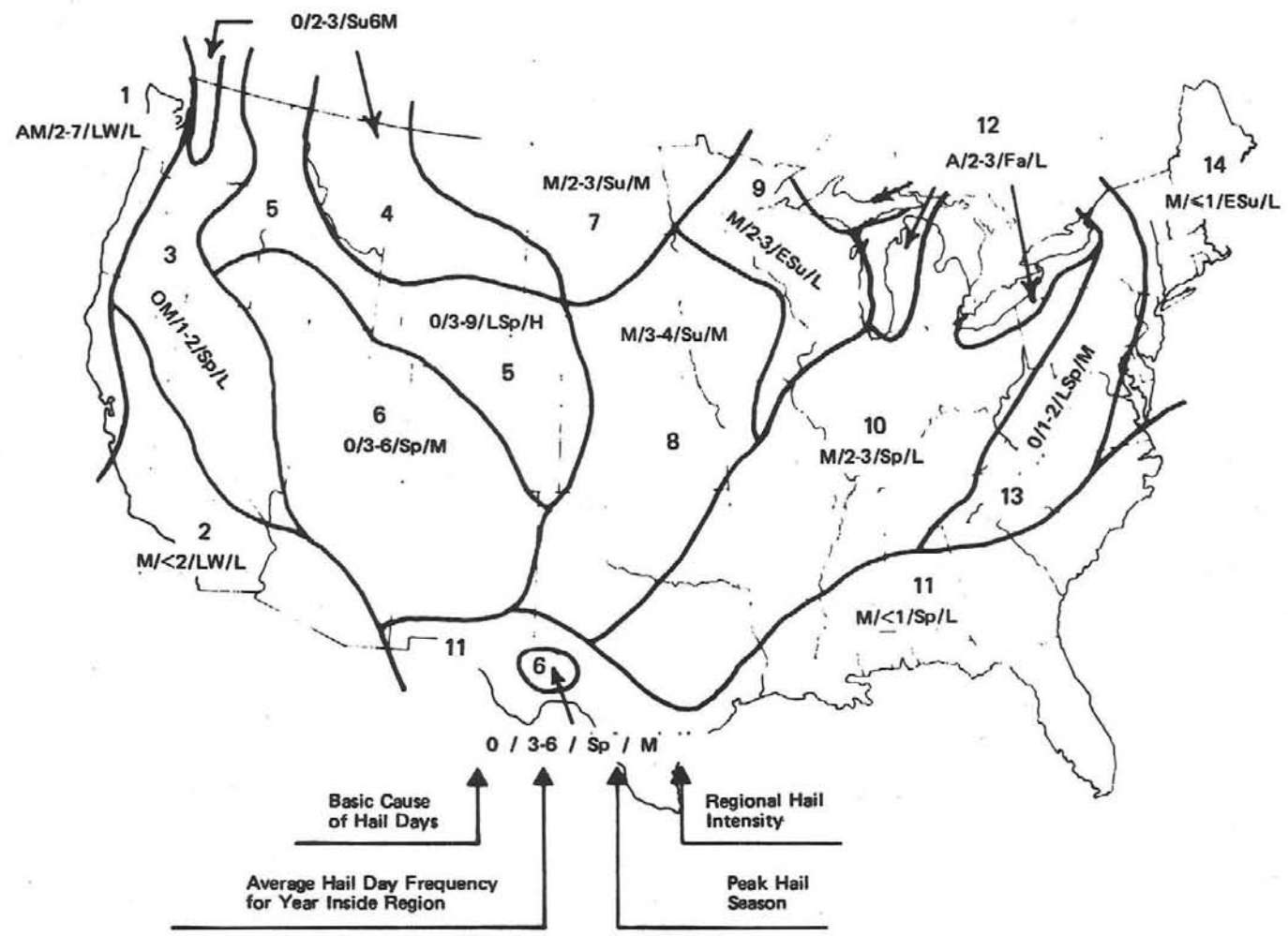
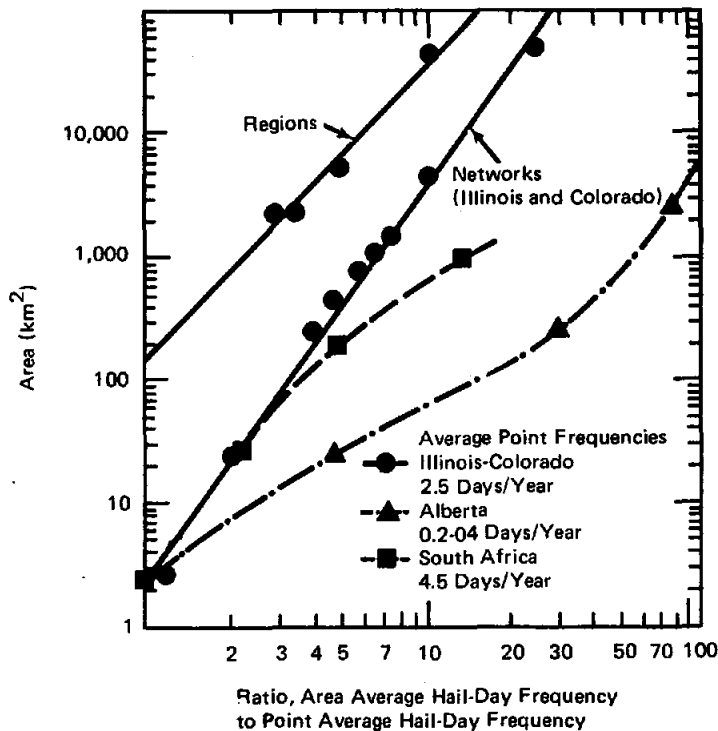


Figure 3-1. Average Number of Hail Days per Year Based on Point Frequencies (After Changnon<sup>3-1</sup>)



41

Figure 3-2. Hail Regions of the United States (After Changnon 3-1)



**Figure 3-3. Area-Point Hail-Day Ratios as a Function of Area Size**

Some of these results seem to correlate well, but some questions arise. One is of self-consistency, which seems to require that the area-to-point frequency ratio is one at a target area equal to the "point" area. This cannot be checked from the work leading to Figure 3-3, as "point" areas are not given.

Hints of consistency appear in Figure 3-3, as it implies that the curve for states involved data from U.S. Weather Service stations with human observers, while the Illinois and Colorado networks used detectors; the latter cover much less area, consistent with the intercept of the respective curves with the area axis. These conclusions are not firm, but can in principle be made so, by examining the relevant information. This should be done before the results of Figure 3-3 are used.

A second question is whether the curves shown in Figure 3-3 can be expected to change as they cross a characteristic hailstorm length dimension (it is not clear what the proper dimension is; the width of a hailstorm path (a hail swath) is some 10 Km, while the width of one of the discrete deposition areas

(hailstreaks) of which it is composed is about  $2 \text{ Km}^{3-1}$ ). This expectation arises because for scales much larger than the characteristic dimension the area-to-point frequency ratio refers to the scale and spacing of hailstorms, while for scales much smaller than this, the ratio involves the scales and spacing of regions of varying intensity within individual storms. There seems no reason to expect these relationships to be the same. It thus is not clear that curves such as those of Figure 3-3 can be used with point frequencies of hail to get the frequency of hail impact on areas of dimensions of several meters (such as heliostats). Further, since for areas of the order of  $2-4 \text{ Km}^2$ , corresponding to a field of heliostats, the area to point average hail day frequency is approximately 1, the probability of occurrence for a field can be estimated by either method, but it will not be known if all heliostats and/or all panels will be impacted by stones sufficiently large and frequent to cause breakage.

#### Areal Density of Hailstones

Another, and more direct, means of finding the effect of target size on the probability of impact is to use the average number of hailstones or the average number of hailstones in a given size range striking the ground or a suitable detector, per unit area. Relatively few data of this sort are available (primarily because the volunteer observer networks were not asked to report this information). Some such data<sup>3-6</sup> are quoted in a study of hail risk to solar collectors<sup>3-7</sup>; this study will be treated in some depth in later sections. Other such data are available.<sup>3-8</sup> The same problem noted in the discussion of area-to-point frequency ratios, that of the possibility of changing behavior upon crossing the characteristic single-storm length scale, can be expected to occur here too; but in this case, the data are all taken at smaller scale lengths. It is conjectured more study of these two kinds of data, taken at such widely differing scales, would clarify some features of hail behavior, and would allow predictions to be made of hailstone size distribution frequency for given areas (e.g., the area of a heliostat or individual reflector panels).

### 3.2.2.3 Hailstone Sizes

#### Size Distributions

A great deal of information has been collected and published on hailstone sizes. Partial surveys of the literature exist.<sup>3-1,3-2,3-7,3-8</sup> The main emphasis in the present work has been given to finding correlation data rather than raw data.

The most widely used correlation for hail size distributions is the exponential,

$$N(D) = N_0 e^{-\lambda D} \quad (1)$$

where  $N(D)$  and  $N_0$  have units  $m^{-3} \text{ cm}^{-1}$ ,  $D$  is in  $\text{cm}$ , and  $\lambda$  in  $\text{cm}^{-1}$ . In equation (1)  $\lambda$  is of the character of an inverse diameter, and governs the width of the distribution. If  $\lambda$  is small there are many large hailstones, and the reverse is also true, while  $N_0/\lambda$  is equal to the total number of hailstones per cubic meter. The alternative expression

$$N(D) = N_0' e^{-\lambda(D-D_{\min})} \quad (2)$$

is sometimes used; for  $D \geq D_{\min}$ , (1) and (2) are clearly equivalent, for

$$N_0 = N_0' e^{\lambda D_{\min}}$$

It should be noted that (1) is not the best distribution function available. There is clear evidence that the lognormal distribution

$$N(D) = \frac{a}{D} e^{-b(\ln D - c)^2} \quad (3)$$

better represents physical reality<sup>3-16</sup>. The improvement appears as one goes to decreasing sizes: the lognormal distribution reaches a peak and then begins to decrease rapidly as  $\ln D$  begins to assume increasingly negative values, while the exponential distribution continues to increase (unless provided with

a cutoff, as in (2), which seems equally unphysical). In the middle and upper size ranges the lognormal follows the exponential quite closely, however, and since these are the ranges we are concerned with, the exponential suffices here.

Both distributions fit the data reasonably well from diameters of about 0.5 cm to some upper value between 1.5 and 3 cm. Parameters of the fit are shown in Table 3-1. Above this upper value, the number of hailstones per cm diameter interval often drops much more sharply than the exponential (or lognormal) function. This is what is referred to in Table 3-1 as a truncated distribution. In no case have more large hailstones been observed than would be predicted by the exponential distribution.

#### Size by Location

Some limited evidence exists that hailstone sizes vary by location<sup>3-1</sup>. This is not unreasonable as the causes of hail also vary (Figure 3-2). Some dis-

Table 3-1. Experimentally Determined Parameters in the Exponential Hail Distribution  $N(D) = N_0 e^{-\lambda D}$

Reference	Distribution	$N_0$ ( $m^{-3} cm^{-1}$ )	$\lambda$ ( $cm^{-1}$ )	Remarks
9, 10	Hail collected from ground	10	3.1	Many individual distributions were truncated
11			2.2	
13			3.8	
14		About 10 to 1,000; mean = 121	3.3 to 6.6; mean = 4.2	
15	Data taken aloft by armored aircraft		3.9	Average of 16 distributions
16	Not seeded	8	2.75	Distributions truncated, especially at large sizes
	Seeded	7	2.67	

tributions from Reference 3-1 are shown in Figure 3-4 from that reference, in which Changnon states, "...the greatest frequency of larger stones is found in the lee-of-the-mountain locales (Alberta and Colorado) with smaller stones dominating the distributions in Illinois, New England and Arizona (a mountain-top area)." While insufficient data seem to exist to correlate these variations, they should be kept in mind.

Maximum Sizes

This subject is not always directly useful, but it is always interesting. Outside of anecdotal and single-instance examples, there appear to be few correlations of maximum sizes. One such appears in Reference 3-12, in which  $\lambda$  (equation (1)) was plotted against  $D_{max}$  for data of several investigations (References 3-9, 3-10, 3-11, 3-13, 3-14). A curve of the form  $D_{max} \lambda^n = k$  was fit to the data; the best fit was approximately

$$D_{max} \lambda = 8 \tag{6}$$

9CR45

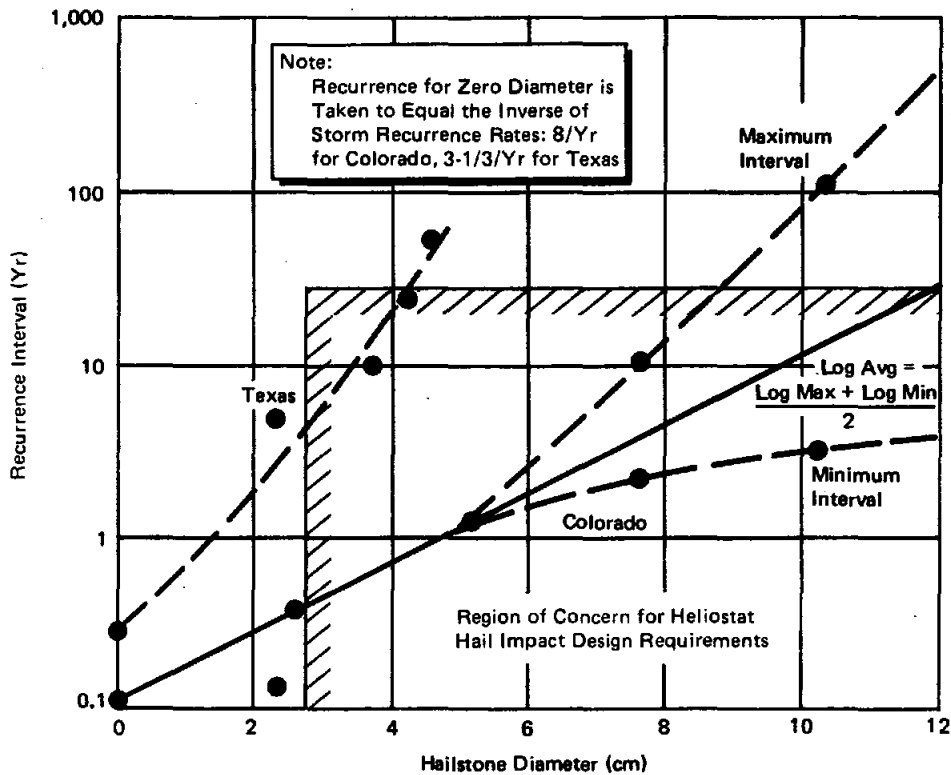


Figure 3-4. Hailstone Recurrence

This is an interesting result, but the present author views it with some skepticism. This is because the data on which it is based scatter rather widely. For example, for  $\lambda = 3 \text{ cm}^{-1}$  (a not unreasonable value, see Table 3-1), Equation (6) predicts  $D_{\text{max}} \approx 3 \text{ cm}$  while a data result is shown at  $D_{\text{max}} \approx 6 \text{ cm}$ .

Nevertheless, the idea of a correlation between  $\lambda$  and  $D_{\text{max}}$  is interesting, and is not inconsistent with the fact that for rain, which also obeys the exponential distribution,  $\lambda$  decreases as the rate of precipitation and thus the storm intensity, and perhaps  $D_{\text{max}}$  increases<sup>3-17</sup>. One problem with plotting and using data on  $D_{\text{max}}$  is that since there is by definition only one hailstone of that size, it may be missed. It seems at least as justifiable to say that the stones found are all less than or (at most) equal to  $D_{\text{max}}$ , and to draw a curve on that basis. When this is done to the data considered in Reference 3-12, the result is

$$D_{\text{max}} \lambda^{1.34} = 30. \quad (7)$$

A consistency test can be applied by comparing the largest reliably recorded  $D_{\text{max}}$  with the observed range of  $\lambda$  (Table 3-1). The largest hailstone in the U.S. fell at Coffeyville, Kansas in September, 1970<sup>3-18</sup>. It weighed 766 gms and, using  $\rho_{\text{ice}} = 0.915 \text{ gm/cm}^3$ , was equivalent to a sphere of 11.7 cm diameter. For this  $D_{\text{max}}$ , (7) predicts  $\lambda = 2.0$ , a result not too far at variance with the results shown in Table 3-1, and probably in the right direction. We conclude here that if there is a correlation between  $\lambda$  and  $D_{\text{max}}$ , it is probably more accurately represented by (7) than by (6), but the absolute accuracy of either is not known.

#### Sizes and Recurrence Times

Direct data on recurrence intervals for hailstones of various sizes was obtained for northeast Colorado<sup>3-19</sup> and for the "Texas south plains" near Lubbock<sup>3-20</sup>. Results are shown in Table 3-2 and are plotted in Figure 3-4. It is clear that substantial differences exist between Texas and Colorado. For example, in Texas 1-inch diameter hailstones recur every three years, while in Colorado, the figure is more like three times a year. Note too that the data for hailstone recurrence and storm recurrence seem reasonably consistent.

Table 3-2. Hailstone Recurrence Intervals

Hailstone diameter (cm)	Recurrence Intervals (Yrs)	
	NE Colo <sup>19</sup> (max/avg/min)	Texas South Plains <sup>20</sup>
2.3		5
2.5	0.3	
3.7		10
4.2		25
4.6		50
5.1	1.3	
7.6	10.6/4.0/2.2	
10.2	125/12.9/3.2	
12.7	1000/56,2/4,0	

A region is shown on Figure 3-4 which delineates hailstones larger than 2.5 cm (1 inch) and occurrence frequency greater than about once every 30 years, since these limits correspond to current design and life requirements for heliostats. Clearly, hailstones of 2.5 to 4 cm occur frequently enough to be of concern in Texas and Colorado, and much larger stones occur in parts of Colorado.

#### 3.2.2.4 Hailstone Terminal Velocities

Considerable work has been done on this subject. The equation of motion for a spherical particle with a constant drag coefficient yields an equation of the form

$$V_T = k D^{1/2} \quad (4)$$

where  $V_T$  is terminal velocity in m/sec,  $D$  is diameter in cm, and  $k$  is a constant, given by<sup>3-21</sup>

$$k = \sqrt{\frac{4}{3} \frac{\rho}{\rho_g} \frac{g}{C_D}} \quad (5)$$

For spheres of ice density and 1 to 10 cm in diameter, the Reynolds number at terminal velocity is in the laminar range, and a drag coefficient  $C_D = 0.47$  is appropriate<sup>3-17</sup>. The resulting value of  $k$  is 14.6.

However, hail is often neither round (some data show the average ratio of minimum to maximum diameter to be about 0.8<sup>3-22</sup>), nor smooth. Roughness, in particular, can have a very large effect on drag if it promotes transition to turbulence; hailstones, like golf balls, are in the right Reynolds number range for this to happen. When transition occurs, drag is greatly reduced,  $C_D$  can drop to about 0.1, and much higher fall speeds will occur. Successive transitions to turbulence and then back to laminar have been observed, the latter occurring when the hailstone was smoothed by melting. Interaction with gusts may also have been implicated<sup>3-22,3-23</sup>.

Considering these uncertainties, one is probably best advised to consult the literature for data, while remaining skeptical as to the accuracy of any given value of  $k$ . Some results are given in Table 3-3.

### 3.2.2.5 Wind Speeds with Hail

If wind occurs with hail, its damage-causing potential can be greatly magnified. Only recently has instrumentation capable of detecting lateral motion

Table 3-3. Parameters in the Hailstone Terminal Velocity Expression  $V_T = kD^n$

Reference	$k$ ( $\text{msec}^{-1} \text{cm}^{-n}$ )	$n$	Remarks
21	14.6	1/2	Analytical ( $C_D = 0.47$ )
24	15.0	1/2	
25	16.2	1/2	
26	15.9	1/2	$P_\infty = 900 \text{ mbar}$
	17.5		700
	20.0		500
	22.0		400

of windblown hail been introduced. This is the "hailcube," essentially a cube with aluminum foil-covered styrofoam pads on the four vertical sides and the top. From the impact impressions formed by hail, several important parameters of the hailfall, including lateral velocity induced by wind, can be inferred<sup>3-27</sup>.

Data have been found for individual storms. Kinetic energy contributed by the wind exceeded that due to terminal velocity alone for some 33 percent of 524 observations made in the Po valley of Italy, and for most of the 88 measurements made in the two Nebraska hailstorms<sup>3-27,3-28,3-29</sup>. In the Nebraska storms, wind speeds of up to 40 meters/second, or 90 mph, were reported, as well as increases of factors from 2 to 4 in peak total kinetic energy over peak vertical kinetic energy.

Simultaneous data are, however, usually not available. Some work has been found relating daily maximum wind with the occurrence of thunderstorms and hail<sup>3-30</sup>. Typical results are shown in Figure 3-5, which shows that higher winds occur on hail than on nonhail days. Note, though, that there is no

9CR45

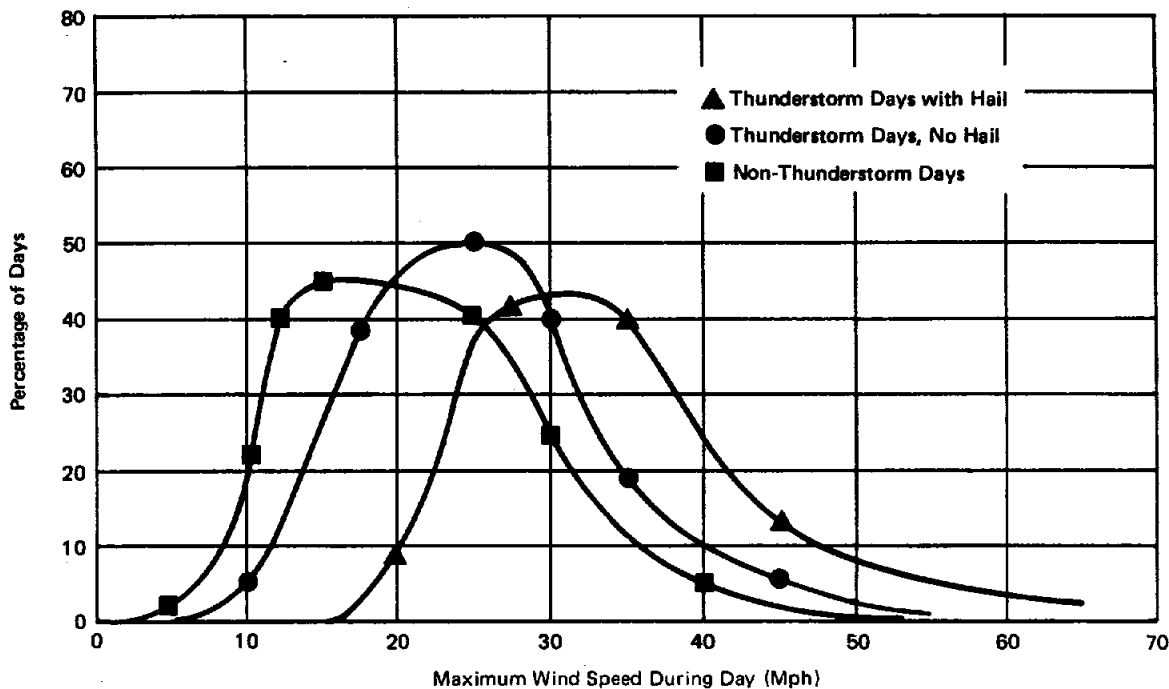


Figure 3-5. Relation Between Daily Maximum Wind, Thunderstorms, and Hail

conclusive indication that the wind and the hail occur together; they may or may not do so, but it seems clear that it is at least possible that high winds generally occur with hail, and probably increase its potential for damage.

It is also possible that the coexistence of wind with hail can be put to good use. Reductions of damage downwind of obstacles, to some 10 times the obstacle height, has been observed under circumstances that rule out direct interception of the hail by the obstacle<sup>3-31</sup>. However, this would not provide a means for preventing hail damage to heliostats even when wind direction is reasonably constant, as seems to be the case<sup>3-31</sup>. Potential benefits of supposed decreased hail damage resulting from orienting heliostats vertical, and parallel to the prevailing wind, must be weighed against the risks of major structural and drive unit damage resulting from major shifts in wind direction, local funneling and redirection of the wind due to interactions with the heliostats, and the uncertainty and potential for rapid change of any prevailing wind during a severe storm. Without supporting data to show that vertical stowage during a storm is practical, it is considered prudent to require that heliostats will be stowed horizontally, and the reflector designed to withstand impact by the maximum hailstone diameter which can reasonably be expected to fall in a recurrence interval of the order of 30 years. It should also be noted that since high winds (>35 mph) will occur with at least some fraction of the severe hailstorms, heliostats will be stowed horizontally (face-up, for a non-inverting heliostat) but the additional kinetic energy provided by horizontal winds will not increase the kinetic energy on impact normal to the surface. Wind gusts can cause additional vertical kinetic energy, as can transitions from laminar to turbulent flow of the hailstone. The obvious implication of the potential for increased kinetic energy is that in a given storm, with hailstones equal in nominal diameter and velocity to the verified design capability of the heliostats, some heliostats may suffer damage. Unfortunately, there is insufficient data and understanding of these variations to determine a cost optimum set of design requirements, and therefore, either an element of risk is introduced, by designing for expected nominal conditions, or perhaps unnecessary cost penalties will be imposed by designing for overly conservative impact conditions. These uncertainties are in addition to the uncertainties of occurrence frequency, areal density, and maximum

stone diameters for a given location, especially in regions where data is sparse. It should also be noted that hail impact with high winds is potentially more damaging to collector subsystem designs having regions of exposed reflector normal to the hail impact velocity. Various configurations of concentrating collector designs (e.g., parabolic trough, dish, and fixed mirror-moving receiver, etc.) may therefore require more conservative design requirements on hail impact, or provide for reflector surface protection.

### 3.2.3 Prediction of Hail Impact

The interest in hail statistics demonstrated in the present report and in many of those referenced is based on the potential of damage to objects on the ground, including crops and, more recently, heliostats, solar cells, and other solar collectors. In order to evaluate damage potential, it is desirable to calculate impact probabilities for various hailstone sizes as a function of target size and location. Only two such analyses are known (References 3-7 and 3-32). This section gives a brief critique of these analyses, together with suggested improvements.

#### 3.2.3.1 Reference 3-7

Gonzalez estimated the probability of impact by hailstones of various sizes. He developed the concept, and estimated the value of the mean time between hits (a concept based on the idea of mean time between failures in reliability analysis). His calculations are based on the following data:

- A. The average annual number of hail days at a given location (the point frequency of hail);
- B. The hailstone size distribution; and
- C. The areal densities of hailstones as observed on the ground.

The last item is used to relate point frequency to frequency for finite areas.

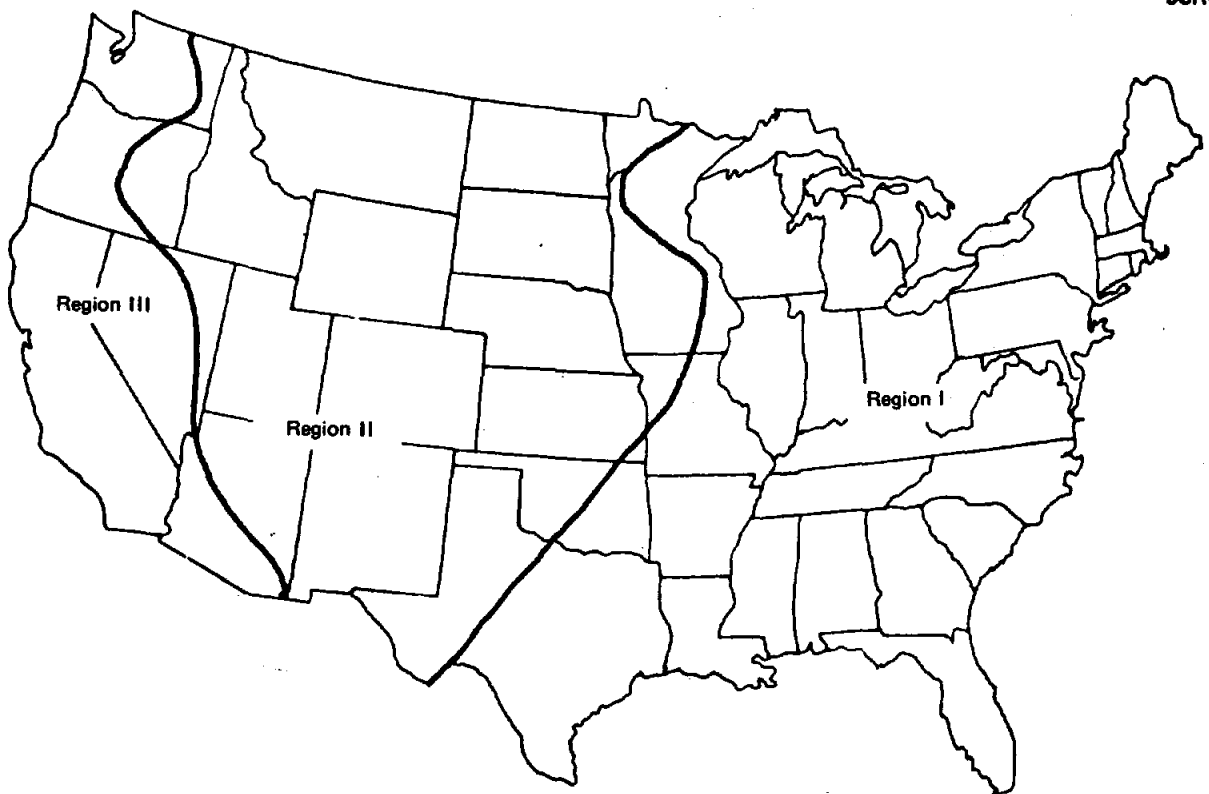
The approach used by Gonzalez thus accounts for the important factors. However, due to a shortage of data, he is forced to make several important simplifications and extrapolations.

### Choice of Areas

Because of insufficient data, Gonzalez divides the contiguous U.S. into three regions as shown in Figure 3-6. Such a simplification is subject to question if it is attempted to use the results right up to the boundary. On the other hand, central receiver deployment is envisioned for Regions II and III (and possibly the Southern part of Region I), and no climatic evidence is known for anticipating any marked fall-off in hail intensity on approaching the II-III border from the east, say through New Mexico and Arizona (see Figure 3-2). It appears that, given the data, the approximation represented by Figure 3-6 is as good as can be made, and that information about boundary regions will have to be sought in other types of data.

### Hail Diameter Distributions

Having obtained point frequency estimates for Regions I-III, the next step is to find hailstone size distributions. The division into three regions facilitates this task. In each region, the available distributions were plotted. In each there was a size above which no data were available. In



9CR45

Figure 3-6. Hail Regions (From Gonzalez<sup>3-7</sup>)

Region I, this was 1-2 inches, in Region II, 2-4 inches, and in Region III, 1 inch. Sizes larger than the minimum required some extrapolation. Maximum and minimum size envelopes were drawn and were used in making predictions and sensitivity calculations.

Two factors are of interest in terms of determining these envelopes. First, the extrapolations were made using "engineering judgment." Exponential curves were used, for which  $\lambda = 1.19 \text{ cm}^{-1}$  (see Equation (1)). This value can be compared with  $2 < \lambda < 4 \text{ cm}^{-1}$ , the experimental range shown in Table 3-1.

If Gonzalez had used a larger value of  $\lambda$  in his extrapolations, however, it would not have made much difference by itself to his prediction of 6-8 years between hits by 1.5-inch or larger hailstones on a 4 x 4 foot solar array in Region II. This is because the distribution of sizes up to 2 inches is covered by data, not extrapolations, and in fact, his extrapolations seem more consistent with his data than higher- $\lambda$  extrapolations would be. This brings up the second point of interest, which is the fact that the data used by Gonzalez are self-consistent, but appear inconsistent (at  $\lambda \leq 1.19 \text{ cm}^{-1}$ ) with the data of Table 3-1 above, for which  $2 < \lambda < 4 \text{ cm}^{-1}$ . In fact, the discrepancy is even more substantial than it appears, because in some of the references shown in Table 3-1, truncated distributions are observed, so that at some diameter between 1.5 and 3 cm the experimental number of hailstones drops off much more sharply than the exponential fit.

How does this discrepancy arise, and what does it imply? Gonzalez tended towards the use of uncorrelated size data, while the present work has made a special effort to find correlations. Each body of data involves several investigators. The data were put by Gonzalez in the form  $P(D \geq D_0)$  vs  $D_0$ , where  $P(D \geq D_0)$  is the probability of obtaining hailstones of diameters greater than or equal to  $D_0$ . Values of  $\lambda$  were found as follows: assume

$$P(D \geq D_0) = \frac{N(D \geq D_0)}{N_0} \quad (8)$$

From (1),

$$\frac{N(D \geq D_0)}{N_0} = \int_{D_0}^{\infty} e^{-\lambda D} dD = \frac{1}{\lambda} e^{-\lambda D_0} \quad (9)$$

so

$$P(D \geq D_0) = \frac{1}{\lambda} e^{-\lambda D_0} \quad (10)$$

Absolute values of  $P(D \geq D_0)$  as given by Gonzalez are also much higher than those given by (10) with  $\lambda$  from Table 3-1, but this may be due to the substantial lack of information on  $N_0$  shown in that Table.

To sum up: the somewhat cursory examination described in this section has shown considerable inconsistency between the data quoted by Gonzalez (Reference 3-7) and the data quoted in the present report (Table 3-1). This inconsistency may arise from the way the data were obtained, where they were obtained, or from some factor not yet identified. Work in this area is needed.

#### Areal Densities of Hailstones

The same phenomenon is visible in more extreme form in the data used by Gonzalez for the areal densities of hailstones. It is believed that his choice of data by which to relate point to areal frequencies was appropriate, as these data are on the correct side of the probable scale change (see Section 3.2.2.2 above for discussion). However, data of the type he uses are very sparse, and he was able to find only one set, from Illinois (Reference 3-6). These data cover sizes one-half to one inch; extrapolation above one inch is necessary, subject to consistency with the smaller-size data and to check by the given fraction of stones above one inch. The extrapolation used by Gonzalez is shown together with the data in Figure 3-7. This extrapolation also approximately satisfies the data for  $D > 1$  inch. Figure 3-7 also shows the result of extrapolation using  $\lambda = 3 \text{ cm}^{-1}$  (Table 3-1). The results show a decrease of about an order of magnitude in the number of

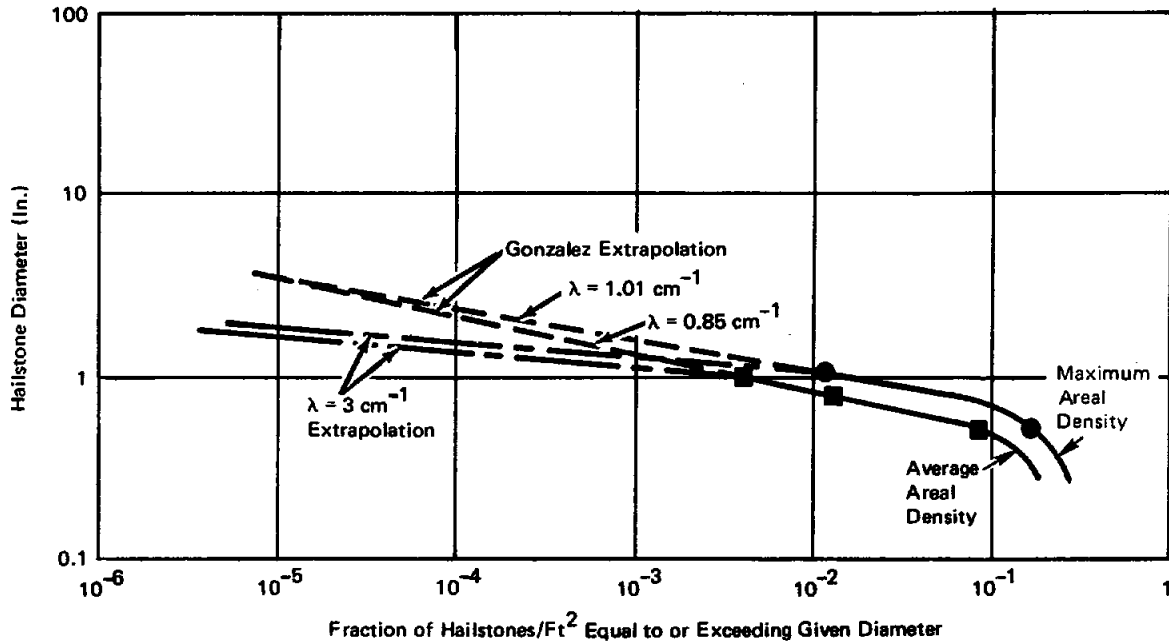


Figure 3-7. Areal Density of Heliostats, Illustrating Extrapolation

stones equal to or greater than 1-1/2 inch in diameter; note, however, that this extrapolation neither satisfies the data for  $D > 1$  inch nor as reasonably fits the data. On the other hand, it is better supported by the totality of data, and the actual number of larger stones may fall off even faster (see the discussion of truncation in connection with Table 3-1, and Reference 3-16).

We conclude that Gonzalez' pioneering effort (Reference 3-7) is directly applicable, but that more study is needed to determine internal consistency among the data that go into it. Evidence exists that hailstones of 1.5 inch diameter, or larger, may occur with areal densities an order of magnitude smaller than the values used in Reference 3-7. The implication of this possibility is that, in principle for a given storm, the area density of large stones might be small enough to allow less stringent design requirements to be used for the heliostats, since the potential cost savings for all of the heliostat could possibly affect the cost penalty associated with damage to a few heliostats. This possibility is examined in Section 3.4.

### 3.2.3.2 Reference 3-32

Friedman (Reference 3-32) calculates  $N_t$ , the annual number of hail days in "a city or county of given size" from the expression

$$N_t = a n p \quad (11)$$

where  $a$  is the area-to-point frequency ratio,  $n$  is the point frequency, and  $p$  is the probability that a day with hail will produce hailstones of sufficient size to cause property damage. This analysis is similar to that of Gonzalez (Reference 3-7). It treats scales larger than the storm scale, rather than smaller, as Gonzalez does. The area-to-point frequency ratio  $a$  is found from Figure 3-8, which resembles Figure 3-3, but includes consideration of the sampling area for which the area-to-point frequency ratio is one, thus avoiding the objection mentioned above. The probability of damaging hail,  $p$ , is found from Figure 3-9:

Results are reasonably good; predictions are compared with actual values in Figure 3-10. Figures 3-9 and 3-10 imply that portions of Texas have a probability of severe hailstorm occurrence more frequently than once every 30 years. For example, in 30 years, for areas having an average of four days of hail per year, or 120 hail days over the life of the plant, approximately six days of hail could have maximum hailstone sizes greater than 3 inches diameter. This does not necessarily indicate that such storms will occur in the vicinity of the central receiver, but it does indicate that in Region II especially, a location having an average of approximately four hail days per year is a potentially poor site for a collector field.

### 3.2.4 Data on Damage Due to Hail

An alternative to predicting the occurrence of hailstorms from meteorological data consists of finding direct information about hail-caused damage. Two primary types of damage are produced by hail: damage to crops, and damage to property. The latter is more appropriate for consideration in the present study, for two reasons:

1. Crops are damaged by hail as small as 1/2-inch, and such small hailstones cause most of the damage (because they occur much more frequently than larger stones), while the threshold value for hail damage (glass and clay tile

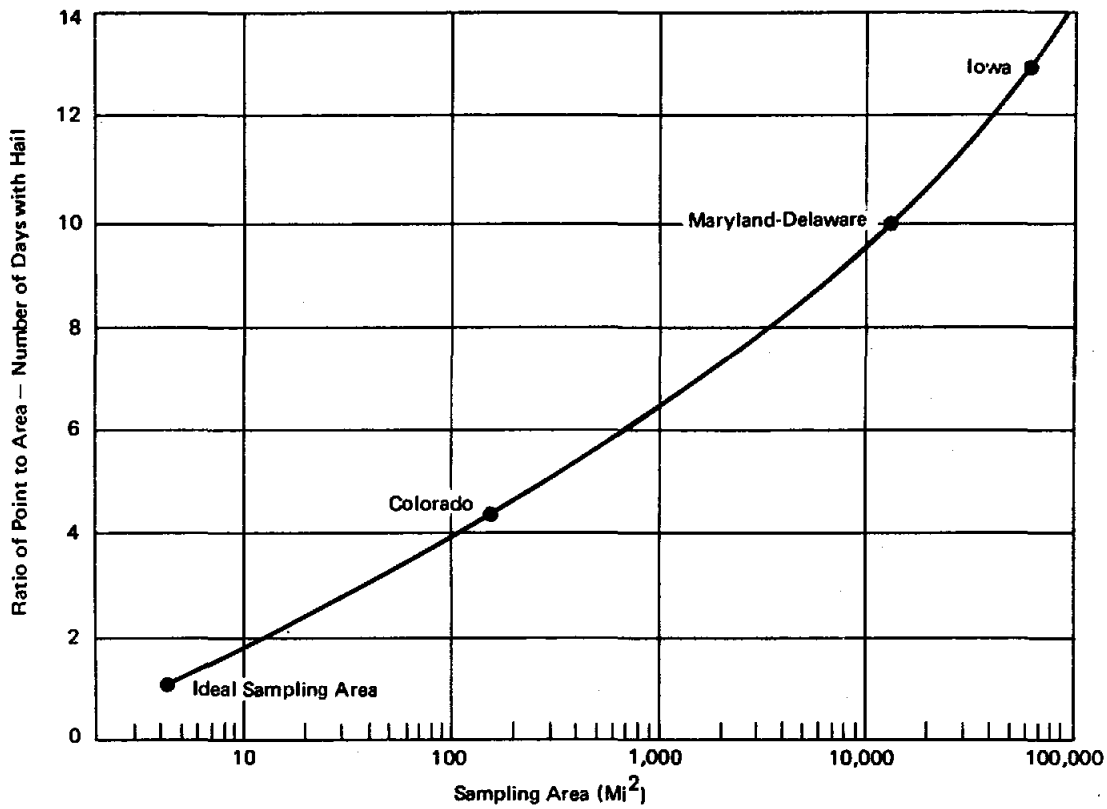


Figure 3-8. Relationship Between the Number of Hailstorms Observed at a Single Observation Location and the Number to be Expected in a Surrounding Area of Given Size (This Curve Used to Determine Value of  $\underline{a}$  in Equation 11) (After Friedman<sup>3-32</sup>)

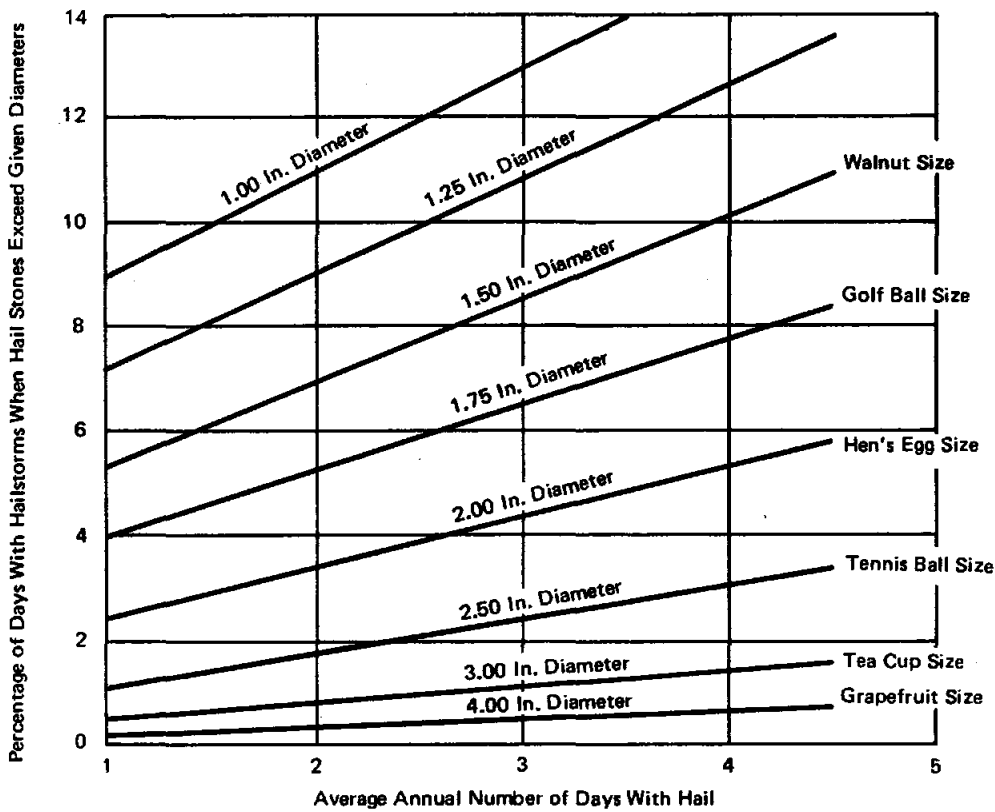


Figure 3-9. Assumed Relationship Between Frequency and Severity of Hailstorms in the Middlewest (This Graph Used to Obtain  $\underline{p}$  in Equation 11) (After Friedman<sup>3-32</sup>)

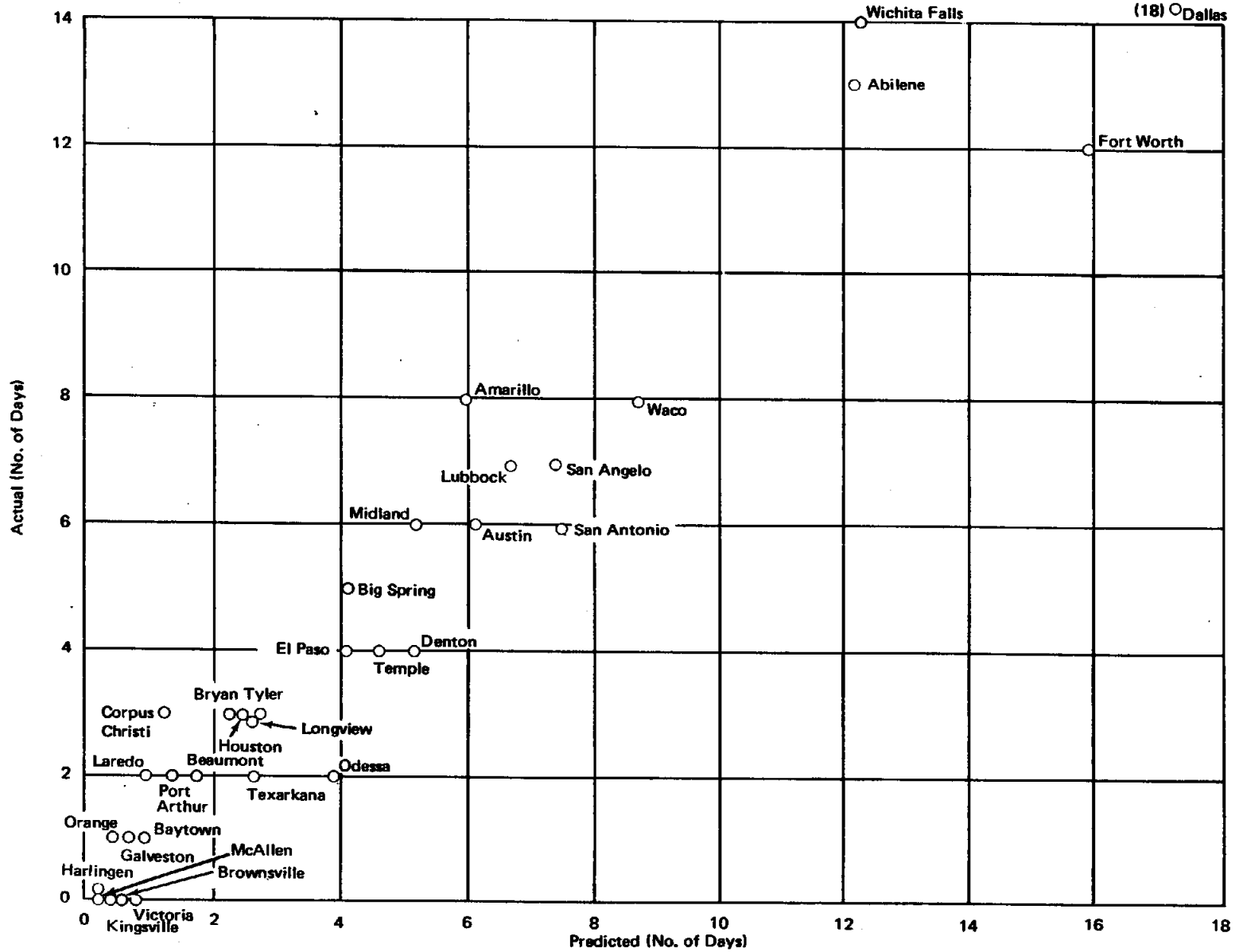


Figure 3-10. Relationship Between the Actual and Predicted (Based on Equation 11) Number of Days With Damaging Hail During a 15-Year Period at 33 Texas Cities (After Friedman 3-32)

breakage) is about 3 to 4 ft-lbs of kinetic energy, which corresponds to the fall of one inch hailstones with no wind.

2. Fixed property is susceptible to hail damage year-round, while crops are susceptible only during the growing season (References 3-32 and 3-33).

Unfortunately, little information seems to be available on property damage by hail. This is despite the fact that such damage is apparently substantial. For example, it is estimated that in the period 1948-1975, the average annual U.S. property losses due to "weather catastrophes" (winds, hurricanes and tropical storms, tornadoes and hail) was \$340.1 million, and that 12 percent, or \$40.0 million per year, was due to hail (Reference 3-34). Work is presently underway in the insurance industry in regard to developing costs and criteria for insuring solar heating units. Rather surprisingly, little attention is paid to possible wind and hail damage (Reference 3-35).

One exception to this general conclusion, and an important one, is the work of Collins and Howe (Reference 3-33), which resulted in an estimate of the annual potential damage to property, as a fraction of the local residential property value. The use of this index eliminates an objection common to crop damage data. The crop data, being generally in absolute amounts, does not distinguish between places where there is little damage because of little hail, and places where there are few crops.

The results of Collins and Howe (Reference 3-33) are summarized in Figure 3-11. This is interesting, especially in comparison to Figures 3-1 and 3-2, where they show moderate to high severity of hail in northern Arizona and southwestern Utah. Figure 3-11 shows a minimum there. As these are areas with substantial likelihood of potential heliostat installation, these results are interesting and encouraging.

It is also interesting to conjecture as to the implications of Figure 3-11 in an assessment of heliostat damage. There is at most a factor of 50 difference between the areas of least damage and maximum damage. If the value of a heliostat is placed at approximately \$3500, and if the life requirement is 30 years, then with 0.001 to 0.050 percent of property value per year over 30 years, the heliostat potential cost penalty due to hail damage ranges from

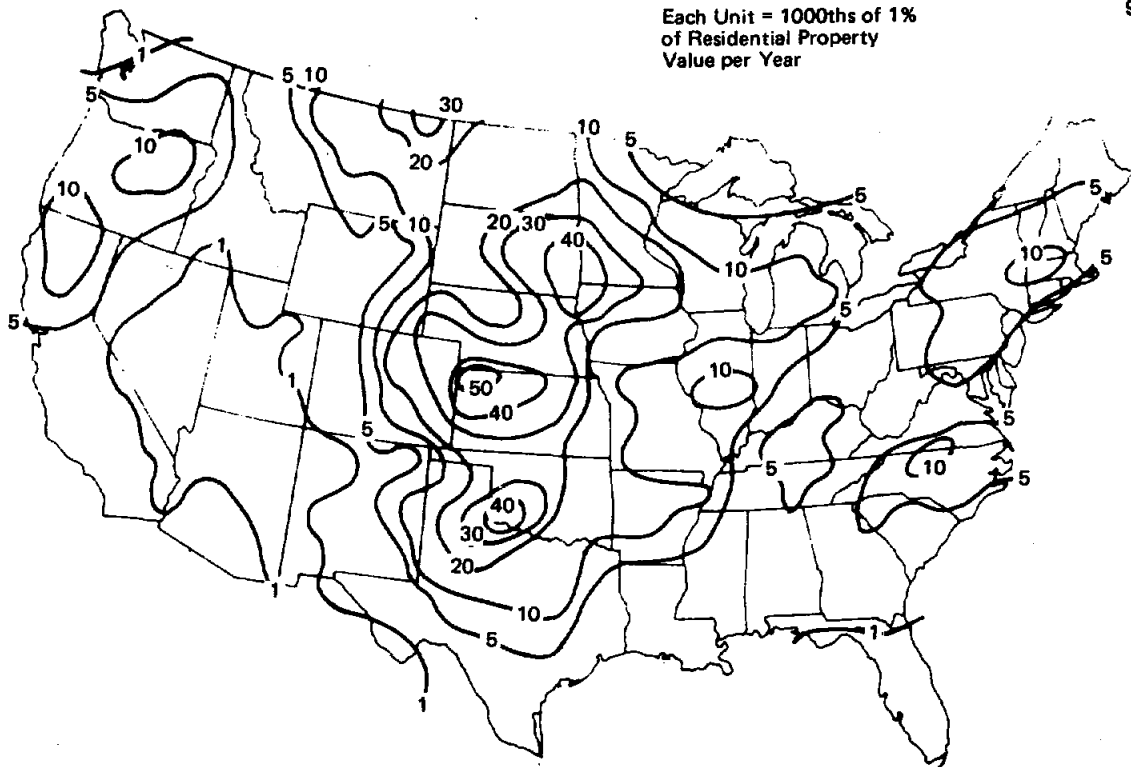


Figure 3-11. Index of Potential Hail Damage to Property (Quoted by Changnon<sup>3-1</sup> from Collins and Howe, *Weather and Extended Coverage*, Travelers Research Center Report, Hartford, Conn. 3-33)

\$0.04 to \$0.20. However, this figure may be misleading since a great deal of property is essentially insensitive to hail impact. For example, major buildings, industrial complexes, roof tops, etc., are rarely damaged by hail, whereas automobile roofs, wind shields, carports, thin glass windows and skylights, etc., are frequently damaged by severe hailstorms, but constitute a small percentage of total insured property value. Therefore, there may be substantial justification, upon further study, in increasing the effective index of potential hail damage by one or more orders of magnitude. In this case, potential heliostat damage, on a per heliostat basis, could climb to \$2 to \$200 over the life of the plant.

Figure 3-11 is also of interest, however, for making a rough assessment as to the regions available for installation of central receivers with little risk due to hailstorms. All of Southern California, Nevada, Arizona, New Mexico, and much of Texas and Utah are regions of relatively low potential damage. Colorado, and North-Central Texas are regions of high potential damage. However, the high damage potential areas are relatively small compared to the area

of the Southwestern states, and this indicates, along with the rarity of occurrence of stones larger than 1.5-inch diameter in the western region of the U.S., that substantial area is potentially available for central receiver installations with low risk from hail damage.

### 3.3 RECOMMENDED WORK

In view of the extremely poor present predictability of hail occurrence, both analytical and experimental work are needed.

#### 3.3.1 Analysis of Hail Statistics

It is clear from preceding paragraphs that the type of predictions made by Gonzalez (Reference 3-7) and Friedman (Reference 3-32) are good in methodology, but require the use of more data. These data are available, but are in disparate forms (e.g., area-to-point frequency ratios at different length scales, and size distributions treated different ways). The data need to be brought together into common forms. There is much information available and it should all be used, as at present it is not.

Some effort should follow on refinement of present analytical methods (References 3-7 and 3-32). Detailed evaluation of these methods was beyond the scope of the present work. Though the methods of References 3-7 and 3-32 are generally endorsed here, this does not mean that improvements are not possible or perhaps necessary. The use of the complete present data base should aid in this process.

#### 3.3.2 Hail Measurements

Even after all present data are in use, much is lacking. No data exist at all for many areas of interest (e.g., much of Arizona). These data are vital and can only be obtained in real time. No simulation is possible. Therefore, these experiments should be commenced immediately.

The experiments needed involve three steps.

A. Decide on the level of effort and, based on this, determine the number and location of measurement stations.

B. Emplace instrumentation, which will be simple hailcubes (Reference 3-27) yielding hail size distribution, energy distribution (including wind components and direction).

C. Collect the hailcube surfaces at appropriate intervals and reduce the data.

### 3.4 HELIOSTAT VULNERABILITY

#### 3.4.1 Introduction

Heliostat vulnerability to hail impact was investigated and results are presented in the following. A review of the available test data, correlations against a plausible model, and estimates of cost implications are given. Briefly, it is tentatively concluded that: (a) the Reference 2-1 baseline prototype laminate glass reflector (0.2475 inch total thickness with a 0.060 inch lite bonded to 0.1875 inch) will probably survive impact by a 1.5-inch diameter hailstone at terminal velocity, (b) the 1/8 inch foam core mirror may not survive impact by a hailstone  $\geq$  one inch diameter, (c) currently available breakage data for glass is correlated by the model to within  $\pm 20$  percent without use of a correction factor, (d) the model correlates currently available breakage data (Reference 3-36) for glass on a substrate to within  $\pm 15$  percent, but requires a correction factor (roughly a factor of 2), due to the strengthening of the glass by the substrate; (e) if a two-inch hailstone diameter requirement for non-inverted stow is imposed, the total glass thickness required is estimated to be 0.34 inch. This can be achieved with the laminate design by use of 0.090 inch on 0.25 inch glass. The additional reflectance loss will be approximately one percent, and the glass weight will be increased from the baseline (0.2475 inch total) by 37 percent. The glass cost for the baseline design is \$357. Increasing the amount of glass by 37 percent will increase the cost and will therefore be of the order of  $\$357 \times 0.37 = \$131$ . The cost penalty of an additional one percent reflectance loss is \$32 for a total penalty of \$163. Since the net savings for the heliostat without an inverted stow capability is approximately \$412, there is a net potential savings of \$249, even for a highly conservative hail impact design requirement and assuming that the penalties are associated with the non-inverting design alone. However, the cost penalty for a design requirement of a two-inch diameter stone should not be assessed against the non-inverting heliostat alone, since breakage could occur in the inverted position as easily as with the face-up position. Thus, hail impact requirements for two-inch diameter stones appear to pose a cost penalty on the laminate reflector, and the absolute cost penalty is less than five percent, assuming a

49 m<sup>2</sup> heliostat has a cost of approximately \$65/m<sup>2</sup>. This penalty would be assessed against the heliostat irrespective of its stowage capability.

### 3.4.2 Approach

Appendix 1 presents a quasi-static or "quick-static" loading model for a hailstone or ice ball striking a glass panel at its center. It is assumed that the ice ball crushes on impact and undergoes a uniform deceleration. Given the mass, diameter, and velocity, the impact force is determined. This force is then assumed to be exerted uniformly over a diameter equal to that of the ice ball. From Roark (Reference 3-37) an equation is selected which gives the maximum bending stress for a circular plate with a uniformly distributed load at the center. A minimum glass fracture stress of 3000 psi is assumed for glass. The equation is solved for the critical glass thickness (above which breakage does not occur) as a function of the ice ball size and velocity.

The equation is:

$$t_p = v r_o \left\{ \frac{\rho_{ice}}{2 m s_r} \left[ m + (m+1) \log_e \frac{a_p}{r_o} - (m-1) \frac{r_o^2}{4a^2} \right] \right\}^{1/2} \quad (12)$$

where

$$m = \frac{1}{\nu} = 4 = \text{reciprocal of Poisson's ratio}$$

$$s_r = s_t = 3000 \text{ psi}$$

$$a_p = \text{equivalent radius of panel}$$

$$r_o = \text{radius of hailstone}$$

$$v = \text{impact velocity (see Section 3.2.2.4 and Table 3-3)}$$

It should be noted that in all cases for which there is data, the glass panels are square or rectangular, and therefore the ratio of impact radius to panel radius is based on the shortest distance from the center of the panel to the nearest edge. However, examining the sensitivity of the term  $(4 + 5 \ln a/r)^{1/2}$  shows that it makes very little difference on the predicted critical thickness what the ratio is.

There is a great deal of uncertainty as to what the appropriate tensile strength of glass should be, partly because of the probabilistic nature of glass failure and partly due to the overly simplified quasi-static model. Originally, 3000 psi was used and was found to correlate the data for glass to within  $\pm 20\%$ , with a ratio of the actual to the predicted thickness of 0.943. From Eqn. 1, the glass thickness is inversely proportional to the square root of the glass tensile strength. Since the actual thickness is somewhat less than that predicted, it follows that the glass tensile strength used could be somewhat low, by the ratio of  $1/(0.943)^2$ , which gives a value of 3373 psi that more closely correlates the data. However, there are far more important oversimplifications in the model, such as the quasi-static assumption, distribution of the load over the diameter of the stone, and centered impact. Therefore, it is more meaningful to investigate the variation in breakage thickness, which is  $\pm 0.175$  for the ratio of actual to predicted. This ratio accounts for variations in critical bending stress in the glass, noncentered impact, and variations in the minimum tensile stress. Assuming as a worst case that all of the impacts were centered, and all other test conditions except for critical strength of the glass are equal, it is seen that the minimum strength of the glass varies from a low of  $3000/1.118^2 = 2400$  psi to a high of  $3000/(0.768)^2 = 5086$  psi.

It is highly doubtful that all of the test conditions can be held uniform, and impacts occurred near the edge, as well as the center. Further, there are relatively large discontinuities in the impact forces and glass thickness because of the limited data available. With all of these variations in conditions, it is likely that the actual spread in minimum tensile strength of the glass is less than 2400 to 5086 psi. A value of 3000 psi is reasonable both in terms of the expected values from the literature and test data correlated by the above equation.

The characteristic times associated with the load have been estimated to determine if it is reasonable to use a static bending stress equation for correlating impact induced breakages. One apparent difference between the impact of an ice ball on glass and that of, say, a steel ball is that the hailstone is observed to crush, and damage observed for typical, practical glass thicknesses is always "back-fracture." With steel balls, etc., cracking at the

first surface is common, due to the much lower impulse time, and higher stresses due to the more concentrated load for an essentially non-deforming body. In impacts with rocks, etc., Hertzian impact failures are expected as well as bending failures.

Assuming hail crushes with a uniform acceleration over a distance  $2r_0$ , then with  $a = v^2/4r_0$  and  $s = 2r_0 = 1/2 at^2$ , the characteristic impulse time is given by:

$$t = \left(\frac{4r_0}{a}\right)^{1/2} = \left(\frac{4^2 r_0^2}{v^2}\right)^{1/2}$$

$$t = \frac{4r_0}{v} = \frac{2D}{v}$$

For example, the impact time of a one inch diameter hailstone traveling at 100 ft/sec is

$$t = \frac{2 \times 1/12}{100 \text{ ft/sec}} = 1.67 \times 10^{-3} \text{ seconds.}$$

From Shand (Handbook of Glass Engineering) if the velocity of a crack exceeds the critical velocity of 4000 to 5000 ft/sec, then multiple cracks occur. Assuming the thickness is 0.1 inch, then the time for a critical velocity crack moving at 5000 ft/sec to pass through the glass is  $\Delta t$ , where

$$\Delta t = \frac{0.1'' \ 1/12}{5000 \text{ ft/sec}} = 1.67 \times 10^{-6} \text{ sec.}$$

Thus, the characteristic time of a crack (or a pressure wave) is roughly three orders of magnitude less than that associated with the crushing of the hailstone. Also, for a distance of 10 to 100 times greater, corresponding to the panel width, the characteristic time is still one to two orders of magnitude less, assuming that the load is applied quasi-statically.

However, it is not clear that the shape or deformation of the glass is the same as for a perfectly static load, since the dynamics of the plate subjected to

the impact force have not been considered. It appears from the data comparisons that the plate kinetic energy is small compared to the strain energy. Therefore, a quasi-static "quick static" load model may be adequate, but may not correspond to the actual shape of the deformed plate at the instant of maximum imposed stress. The fundamental square plate vibration frequency can be used to assess the applicability of a "quick static" approach. The frequency,  $f$ , is

$$f = \left(\frac{\pi}{a^2}\right) \sqrt{\frac{gD}{gH}}$$

where

$a$  = length of side = 12 inches

$h$  = thickness = 0.1 inch

$d$  = density (glass)

$$D = \frac{Eh^3}{12(1-\nu^2)}$$

$E = 10 \times 10^6$  psi

$\nu = 1/4$

The frequency is 134 cps, with a half-period of  $3.5 \times 10^{-3}$  seconds. Since this period is slightly longer than the time required for the hailstone impact, the plate response will not be complete. Further analysis of the hailstone impact and vulnerability may be required, including dynamic effects, in order to improve the reflector design for impact resistance, but the quick-static model correlates the available data sufficiently well to allow estimates of required thickness vs hailstone diameter to be made.

### 3.4.3 Data Summary

Data from Texas Tech tests reported in Reference 3-36 were reviewed, as well as MDAC data reported in Reference 2-1. Calculations and comparisons have been made for glass and for glass on various substrates. No suitable bending stress equation was found for glass mounted on substrates, and therefore, the same equation as for glass without substrate was used. Results are presented in Tables 3-4 to 3-6, and summarized in Figure 3-12.

Table 3-4. Correlation of Actual and Predicted Hail Impact Damage of Glass Specimens

Case no.	Source	Hail stone diameter (in.)	Terminal velocity* (ft/sec)	Minimum actual breakage velocity (ft/sec)	Predicted thickness (in.)	Actual thickness (in.)	Actual/predicted	Remarks
1	MDAC	1	78.5	75	0.120 ( $a_p=13$ in.)	0.125	1.04	1/8 in. mirror, corrugated Failed at corner
2	MDAC	1	78.5	75	0.120 ( $a_p=13$ in.)	0.125	1.04	1/8 in. mirror, hat sections. Failed on edge and corner
3	MDAC	1	78.5	75	0.120	0.24	(2.0)	1/8 in. mirror bonded to 1/8 in. mirror. No breakage
4	Texas Tech	1.5	96	45.5	0.112 ( $a_p=24$ in.)	0.125	1.116	Min breakage velocity
5	Texas Tech	2	111.0	85 (31 mph)	0.269 ( $a_p=24$ in.)	0.1875	0.696	Min breakage velocity
6	Texas Tech	1.5	96	96.4	0.227 ( $a_p=24$ in.)	0.1875	0.825	Min breakage velocity

Ratio =  $0.943 \pm 0.176$

Note: Texas Tech results show wide spread between minimum and maximum velocities, e.g., 31 to 83 mph, 63 to 135 mph and 58 to 89 mph, for glass of 1/8, 3/16 and 3/8 in., respectively, and 1-1/2, 1-1/2, and 2 in. hailstone diameter, respectively. These results imply that there are large variations in  $S_p$  of glass; only minimum velocity data is used, and  $S_p$  for glass is assumed to be a minimum of 3,000 psi.

\*Terminal velocity (mph) =  $53.5 d^{1/2}$ , where d is in inches.

Table 3-5. Correlation of Actual and Predicted Hail Impact of Glass Specimens  
(Substrate Supported Materials – Texas Tech)

Case no.	Source	Hail stone diameter (in.)	Terminal velocity (ft/sec)	Minimum actual breakage velocity (ft/sec)	Predicted thickness (in.)	Actual thickness (in.)	Actual/predicted	Remarks
1	Texas Tech	1	78.5	60.4 (41.2 mph)	0.096 ( $a_p=12$ in.)	0.04	0.417	Reported as average velocity
2	Texas Tech	1-1/2	96	76.3 (52.0 mph)	0.1717 ( $a_p=12$ in.)	0.09375	0.5460	
3	Texas Tech	1-1/2	96	111.0 (75.7 mph)	0.25 ( $a_p=12$ in.)	0.125	0.500	
4	Texas Tech	2	110	112.9 (77 mph)	0.325 ( $a_p=12$ in.)	0.125	0.385	Reported as average velocity
							0.462 ±0.07	

Note: Correlation equation predicted thickness is high by a factor of 1/0.462 or 2.16. This implies that use of glass on a soft substrate is not as effective as increasing the thickness of the glass, but does increase the resistance to hail impact. The use of a foam substrate has effectively doubled the resistance of a given thickness of glass to damage by hail.

Table 3-6. Hail Impact Damage of Laminate Glass and Various Substrate Materials (Sandia Laboratories and MDAC Data)

Case no.	Source	Hailstone diameter (in.)	Terminal velocity (ft/sec)	Measured velocity (ft/sec)	Predicted thickness (in.)	Actual thickness (in.)	Actual/predicted	Remarks
1	Sandia Labs Albuquerque	0.75	65	45 ± 6 (free fall from 52 ft)	(0.0597) (Note: model does not apply for this case. Predicted thickness based on edge supported plate) ( $a_p = 24$ in.)	0.236	(3.95)	4 ft x 4 ft x 6 mm (3 mm sheet on 1/8 in. float) lying on concrete impacted by 200/ft <sup>2</sup> ice balls. No damage.
2	Sandia Labs Albuquerque	1.00	78.5	63 ± 1	0.105 ( $a_p = 18$ in.)	0.217	(2.067)	4 ft x 4 ft x 5.5 mm (2.5 mm sheet on 1/8 in. float) laminate. Stressed as if on CRTF heliostat. No damage.
3	Sandia Labs Albuquerque	1.50	96	52.6 ± 2.4	0.124 ( $a_p = 18$ in.)	0.217	1.75	4 ft x 4 ft x 5.5 mm (2.5 mm sheet on 1/8 in. float) laminate. Stressed as if on CRTF heliostat. Severe damage to front and back glass.
4	Sandia Labs Albuquerque	1.50	96	52.6 ± 2.4	0.124 ( $a_p = 18$ in.)	0.236	1.9	4 ft x 4 ft x 6.0 mm (3 mm sheet on 1/8 in. float) laminate. Stressed as if on CRTF heliostat. Some damage to front and back glass.
5	Sandia Labs Albuquerque	1	78.5	80	0.135 (Note: model does not apply for steel balls)	0.125	(0.92)	1/8 in. float glass on foam core. 50% failure, mostly near edge. Steel balls.
6	Sandia Labs Livermore	0.75	65	65	0.073 ( $a_p = 6$ in.)	0.060	(0.82)	60 mil fusion glass on foam core. Extensive damage.
7	Sandia Labs Livermore	0.75	65	80	0.098 ( $a_p = 12$ in.)	0.125	1.275	1/8 in. on foam core 4 ft x 4 ft. Breakage occurred.
8	Sandia Labs (Mid-Temperature Test Facility)  Hail storm damage (Aug 1978)	0.75 (approximate)  Hailstones collected in culvert were collected 1 or 2 days after storm. Maximum diameter unknown.	65	75 (Assumed velocity is $\frac{65}{\cos \theta}$ where $\theta = 30$ deg. Indentations were observed on vertical sheet metal cylinders indicating high lateral velocities.	0.0596 ( $a_p = 1$ in.)	0.060 (Corning)	1.007	2 in. wide 0.060 glass bonded to concrete. Broken on edges, and possibly at voids between glass and concrete where not completely bonded. Gulf Atomic design.
9	Sandia Labs (MTTF) hail storm damage (Aug 1978)	0.75 (approximate)	65	75	0.066	0.090	1.36	3 in. wide by 24 in. long 0.90 glass supported on long edges by galvanized strips. No substrate. Fewer fractures than with 0.060 glass on concrete.
10	MDAC (Ref 3-38)	1	78.5	75	0.118	0.09375	0.795	3/32 in. float glass on foam core sandwich.
11	MDAC (Ref 3-38)	1	78.5	75	0.118	0.09375	0.795	3/32 in. ASG sheet glass, foam core sandwich.

Actual/predicted foam core data = 0.92 ± 0.24

It should be noted that the Texas Tech data show a range of impact velocities resulting in breakage for a given size ice ball. The minimum velocity data are used because these results are more conservative. It is expected that some glass specimens will be relatively free of flaws, voids, stress-risers, etc., and will therefore have maximum tensile strength values substantially higher than normal. However, it is also expected that repeated impacts, as with occasional hailstorms, will decrease the maximum tensile strength of the glass to a value of the order of 3,000 psi, and therefore, this value and the minimum impact velocity conditions are correlated.

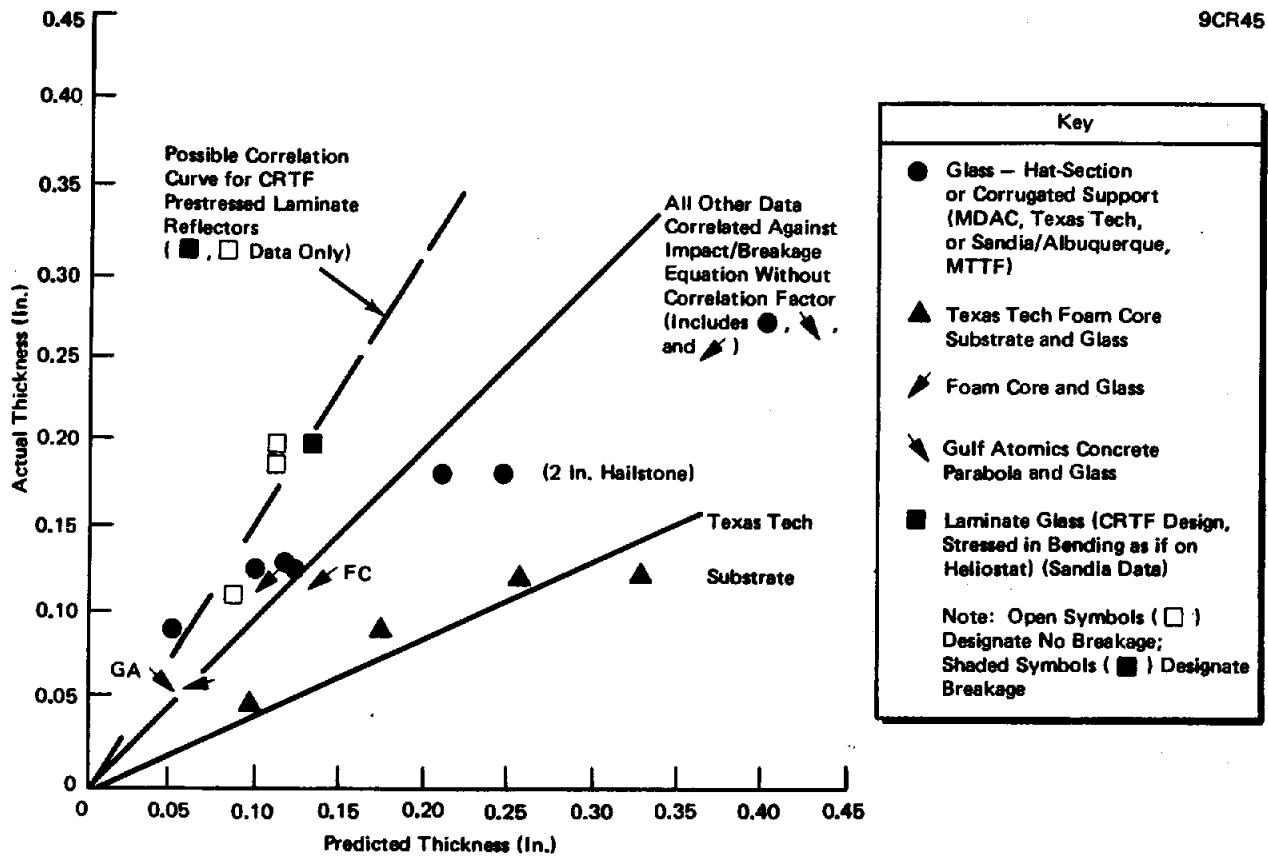


Figure 3-12. Comparison of Actual and Predicted Glass Breakage

Laminate Glass CRTF Design, Stressed in Bending as if on Heliostat) (Sandia Data)

The results of Table 3-4 show reasonable agreement between the predicted and actual breakage thicknesses as a function of ice ball diameter and velocity. Table 3-5 shows that the substrate effectively decreases the bending stress exerted in the glass by the ice ball because of the additional support. In effect, the substrate allows the glass thickness to be halved for the same impact condition. The data also are in good agreement with the model.

Table 3-6 summarizes data obtained from Sandia Laboratories. These data substantially support the model correlation with a few exceptions which are noted below. Cases 2, 3, and 4 indicate that for the CRTF stressed laminate, a glass thickness greater than about two times the predicted thickness is required for survival. This apparent degradation in breakage resistance may be due, at least in part, to (1) the laminate glass strength being less than for a single piece of glass of the same thickness, and (2) to the additional stress imposed on the glass to curve it. Case 6 data is in line with the model because extensive damage is seen with glass thinner than that required to resist impact. Case 7

data, however, indicates damage for a thickness greater than the predicted minimum thickness of unsupported glass, but the thickness discrepancy is approximately 28 percent, which is within expected repeatability for tests of this type. However, Case 7 is for a foam core backing, and it would be expected that the effective resistance to breakage would be increased, as is seen in Table 3-4.

### 3.5 HELIOSTAT COST AND VULNERABILITY CONCLUSIONS

Based on the summary of Table 3-7, it appears that the baseline laminate glass with 0.060 inch fusion on 0.1875 float will survive a 1.5 inch stone at terminal velocity, but will probably not survive a 2-inch stone. However, 0.090 inch fusion glass on a 0.25 inch float probably will survive impact of a 2-inch stone, although the reflectivity may be reduced by roughly one percent, and the amount of glass required will be greater. Assuming  $\$65/\text{m}^2$  and  $49.05 \text{ m}^2$  gives a cost per reflectance unit of  $\$31.88$ . The cost of the additional glass is given in Table 3-8, using data from Reference 2-1. Even if thicker glass is used to survive a 2-inch hailstone, the non-inverting heliostat has a net cost savings. However, impact of a 2-inch stone on the 0.060 inch + 0.1875 laminate will probably cause failure whether the heliostat is stowed face-up or face-down, for the existing laminate design, and therefore this penalty should not be assessed against the non-inverting design.

The granularity of available data, differences in design, and discrepancies between Sandia and MDAC tests of the foam core mirror all point to the need for additional tests of hail impact. These tests must be conducted so as to account for statistical variations in glass strength and allow for specific designs and variations.

If the hail impact design requirement is set at a hailstone value substantially greater than 2-inch diameter, then increasing the glass thickness may not be the appropriate approach, and a combination of inverted stow and a protective cover material for the backside of the reflector may be more cost effective. For example, the foam core design, with suitable modifications to the back sheet of galvanized sheet metal, used on an inverting heliostat may be the most cost effective solution for regions having potential for hailstones of the order of 2.5-inch diameter or greater. Also, protective material could be added to the inverted stow laminate glass reflector, on the backside. Either of these approaches should provide an inverting heliostat having a net cost penalty, relative to the non-inverting design, of somewhat over 12 to 13 percent, due to the inverting capability and cost of protective covers.

Table 3-7. Predicted Glass Thickness

Conditions/thickness	Remarks
1 in. diameter hailstone 42 in. wide mirror 78.5 ft/sec terminal velocity $t_p = 0.133$ in.	Compares with breakage observed in Sandia (but not MDAC) tests of 0.125 in. glass on a styrofoam substrate. No cost impact expected with face-up stow, laminate glass design. Foam core design does not meet criteria on thickness for face-up stow with >1 in. diameter hail impact.
1.5 in. diameter hailstone 42 in. wide mirror 96 ft/sec terminal velocity $t_p = 0.232$	Compares with 0.060 in. + 0.1875 in. or 0.2475 in. glass laminate. No cost impact expected with face-up stow, laminate glass design.
2 in. diameter hailstone 42 in. wide mirror 110 ft/sec terminal velocity $t_p = 0.342$ in.	Velocity compares with 0.060 in. + 0.25 in = 0.340 in. glass laminate. Some cost impact results since thickness increased.

Table 3-8. Cost Comparison for Design Requirement of 2-Inch-Diameter Hailstone

Glass type	Thickness (in.)	Cost (\$/ft <sup>2</sup> )	Cost (\$)
Fusion	0.060	0.32	168
Float	0.1875	0.36	189
			Total <u>\$357</u>
Fusion	0.090	0.45	236
Float	0.250	0.48	252
			Total <u>\$488</u>

Cost penalty for use of thicker laminate = \$131

Cost penalty assuming loss of 1% in reflectivity = \$ 32

Total cost penalty = \$163

Note: The approximate cost savings for elimination of inverted stow capability is \$412. Therefore, a net cost savings of \$249 accrues even if a conservative hail impact requirement is used. However, this requirement will cause thicker glass to be used even if inverted stow is required, and therefore should not be assessed as a penalty against the non-inverting design.



Section 4  
TASK III — SAFETY ISSUES

4.1 OBJECTIVE

The objective of this task is to assess the potential redirected solar radiation hazards associated with a non-inverting heliostat design, relative to the potential hazards of an inverting heliostat design.

Under conditions of nominal operation of the central receiver system, with reflected beams all focused at the receiver, there is little likelihood of exposure of personnel to redirected solar radiation. Although high levels of solar radiation occur in the immediate vicinity of the receiver, there is little hazard to personnel since this region is an exclusion zone during operation, and personnel would not be allowed in the vicinity of the receiver. However, during periods when the heliostats are in positions of noninverted stow, or at some intermediate position between stow and tracking on the receiver (focus), there is a real possibility of the occurrence of regions where the solar irradiation level exceeds one sun, either in the air space above the collector field, or at ground level. It should be emphasized, however, that these conditions are rare. Normally, heliostats would be stowed either vertically, or inverted, and could be brought to anticipatory positions at or before dawn, and would be stowed during or after sunset. Hazardous conditions would exist primarily during periods of high winds, when the heliostats would be brought to a stow condition (face-up for the noninverting heliostat, and normally face-down for the inverting stow heliostat). Potentially hazardous conditions also exist if all heliostats are focused at a standby point in space near the receiver, but this condition is identical for both the inverting and noninverting designs.

Eye hazards can exist for personnel flying over the collector area, or on the ground. Brumleve (Ref. 4-1) has made an analysis of eye hazard potential for the 5 Mwt Solar Thermal Test Facility at Sandia Laboratories, Albuquerque, New Mexico, using approximations of the heliostat geometry and field

arrangement. The objective of the present study is to refine some of the irradiation level estimates for a real heliostat configuration under conditions obtaining for a commercial-size central receiver system and to evaluate the relative hazard potential for the noninverting heliostat as compared to the inverting stow heliostat. Computer simulations of representative conditions, including heliostat panel canting and curvature, surface waviness, and pointing error, as well as collector field layout, have been carried out by means of the MDAC CONCEN central receiver irradiation code (Refs. 4-2 and 4-3). In general, it is found that the noninverting heliostat does not pose a greater hazard, overall, than the inverting stow heliostat.

#### 4.2 TECHNICAL APPROACH

The CONCEN program and variations of this program were the principal tools in the analysis. CONCEN computes flux density values at a reference surface (such as a receiver surface or any other definable surface in space) by compounding the elemental disk images of the sun from 480 elements of the surface of the heliostat. The location and irradiance of each image is determined from the geometry of the heliostat, reference surface, and intermediate space.

CONCEN was used to evaluate irradiance levels corresponding to operation of commercial field noninverting heliostats under two principal conditions: (1) conditions for which irradiation occurs in the air space above the field, and (2) conditions for which irradiation occurs at ground level. Baseline beam safety criteria were supplied by Sandia, based on the results of Reference 4-1, especially in terms of potential eye damage. Although there may be detailed physiological and optical conditions which can affect the range of safe retinal exposure levels, the results of Reference 4-1 are assumed to be satisfactory for this comparative evaluation of inverting and non-inverting stow heliostats. Results and hazards implications are discussed below.

##### 4.2.1 Airspace Irradiation Levels

Three conditions were investigated related to the irradiation levels to be expected in the airspace above a commercial-size collector field: (1) the stow condition where all heliostats are oriented face-up during daytime,

(2) the standby condition, when the collector field is focused near, but not on the receiver, and (3) the period when the heliostats are being slewed from focus direction to the face-up stow condition.

#### 4.2.1.1 Face-Up Stow Conditions

With the noninverting heliostat, face-up stow conditions result whenever wind gusts exceed a certain level, in order to guard against excessive wind loads. Although high winds usually accompany storm fronts with heavy overcast, face-up stow with direct solar insolation on the field can occur, and the hazard potential of the resulting reflection from the heliostats must be evaluated. However, face-up stow may also be required under certain circumstances (i.e., extremely rapid wind rise rates or during heavy rains to achieve natural cleaning) for the inverting stow heliostat. Therefore, face-up stow during daytime with direct insolation may occur more frequently than with the inverting stow heliostat, but this condition is not unique to the noninverting heliostat.

Two approaches were employed to simulate the face-up oriented field of heliostats, both using variations of the CONCEN code. A worst-case simulation was devised by assuming a close-packed field of nineteen heliostats, all face-up. The number was selected as being sufficient to simulate an indefinitely large array. Figure 4-1 shows the heliostat layout. By considering the field to be a series of individual heliostats horizontally displaced the computation can be made with an adaptation of the CONCENS code, which is designed to handle single heliostat irradiation.

The flux density distribution pattern from a single face-up heliostat is repeated 19 times, displaced each time to represent the 19 locations in the array, then summed to obtain the composite flux density pattern. Pointing errors are simulated by randomly applying to each heliostat a normal distribution of angular errors to each component of the reflected beam angles. Representative values of heliostat mirror parameters including size, panel cant angles, reflectance, and surface waviness are included.

The flux density distribution over a plane normal to the beam from the center heliostat in the array of 19 shows peak values when observed at different altitudes above ground as shown in Figure 4-2. No pointing errors were

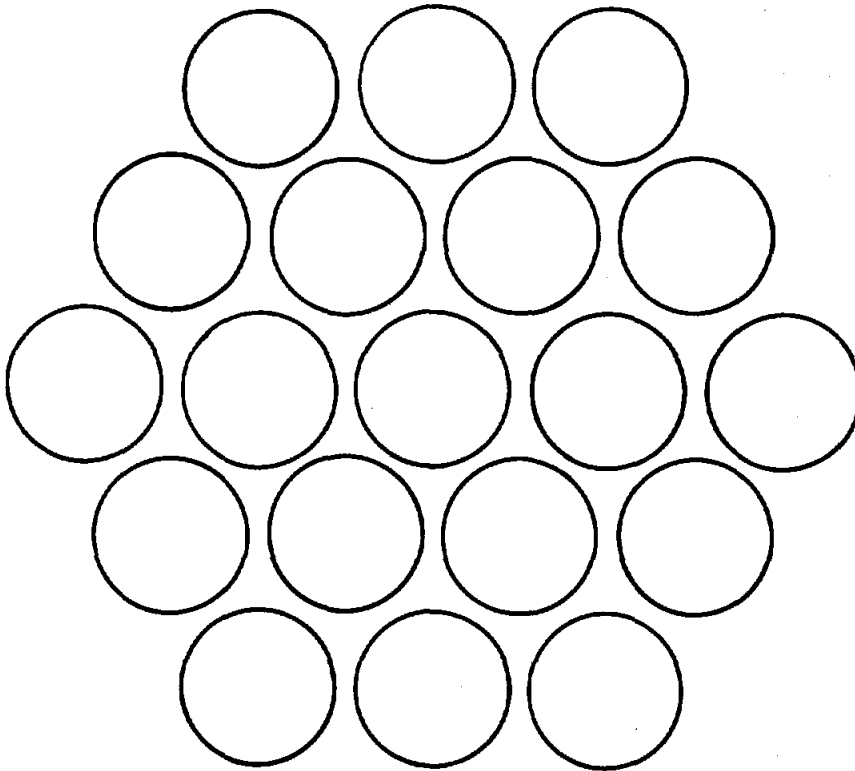


Figure 4-1. Simulated Heliostat Array Locations for Face-up Stowage Safety Analysis

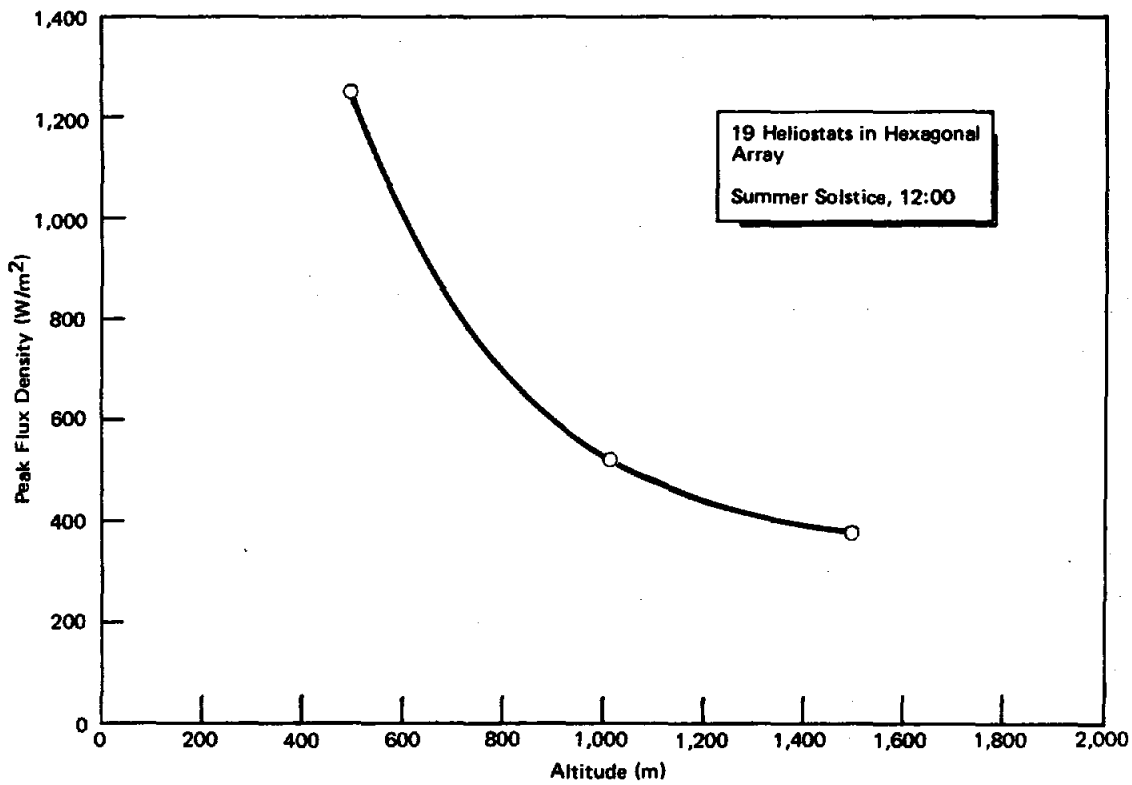


Figure 4-2. Peak Flux Density vs Altitude for Face-up Stowage

assumed for these cases. To investigate the possible effects of beam cross-over on the predicted peak irradiation, runs were made including random pointing errors from zero to 4 mr for each component (5.7 mr, rss). The variation in peak irradiation at 1000m altitude with pointing error is shown in Figure 4-3. To check the consistency of results with the random Monte Carlo processing used, four similar runs were made for the 1000m altitude 2 mr pointing error conditions. A standard deviation of the mean of 8.5% was shown.

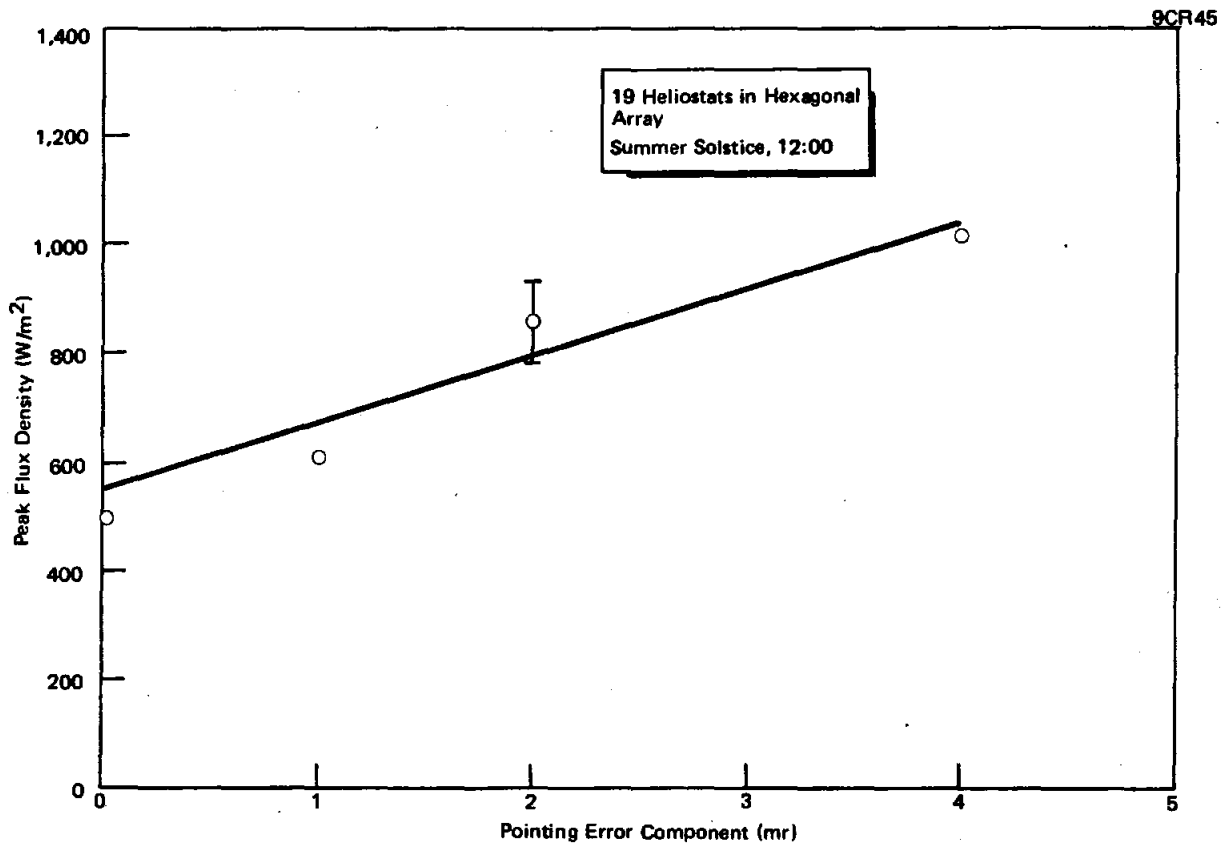


Figure 4-3. Peak Flux Density vs Pointing Error for Face-up Stowage

The second approach to simulating the irradiation from a field of face-up heliostats uses the CONCENC code, which describes the irradiation distribution from a commercial-size plant collector array. With this method the receiver configuration is a cylinder which is nominally irradiated on its outer surface. Program changes were made such that the irradiation on the inside surface of a cylinder concentric with the receiver can be computed. The height of the cylindrical surface can be made sufficient to include the peak irradiation at a given radius from the receiver. The nominal collector field is used, with the typical heliostat locations and surface configurations.

For the face-up condition, it is assumed that the azimuth settings of each heliostat are the same as if the collector were focused at a standby point above the receiver, and the elevation angles of the heliostat normals are all  $90^\circ$ . Nominal pointing errors are also assumed. For irradiation at summer solstice, 1400 hours, at a ground range of 500m from the receiver tower the peak irradiation occurs on a vertical cylindrical surface at an altitude of 1200m above ground, in a direction opposite to that of the sun from the receiver. A contour diagram of the irradiation distribution over the cylindrical surface is shown in Figure 4-4. The numbers shown in the diagram lie on contours of value equal to the indicated numbers of tenths of the peak irradiance level (shown as "P" in the diagram). The abscissa is the angular position about the receiver ( $0^\circ$  at south,  $90^\circ$  at east). The peak irradiation level is found to be  $4.9 \text{ KW/m}^2$ . The sharpness of the peak at the 1200 m altitude point is probably related to the combination of the single general direction of the reflected beams, the incident angle on the cylinder, and beam overlap due to pointing and surface errors.

#### 4.2.1.2 Focus Condition

Using the same computational approach as for the face-up heliostat condition, the irradiation on the inner surface of a cylindrical surface surrounding the receiver in a commercial-size system with all heliostats nominally focused at or near the receiver was simulated. By changing the input value of the cylindrical surface radius, the distribution of flux density as a function of distance beyond the receiver was obtained. The magnitude and altitude location of the peak irradiance values for focus conditions at the nominal receiver location, 250 m above the ground, and at a standby point 50 m above the receiver center are shown in Figures 4-5 and 4-6. A contour diagram of the irradiance distribution is given in Figure 4-7 for 500 m range beyond the receiver. Due to the rapid divergence of the focused beam beyond the focal point, the peak irradiation level decreases from about  $50 \text{ KW/m}^2$  at 100 m beyond the receiver to about  $1 \text{ KW/m}^2$  at 1000 m range, for typical operation on June 21 at 1400 hours. The altitude of the peak steadily increases from the focus altitude at zero range to 200 m above the receiver for focus at the receiver, or 250 m above the receiver for focus at the standby point.

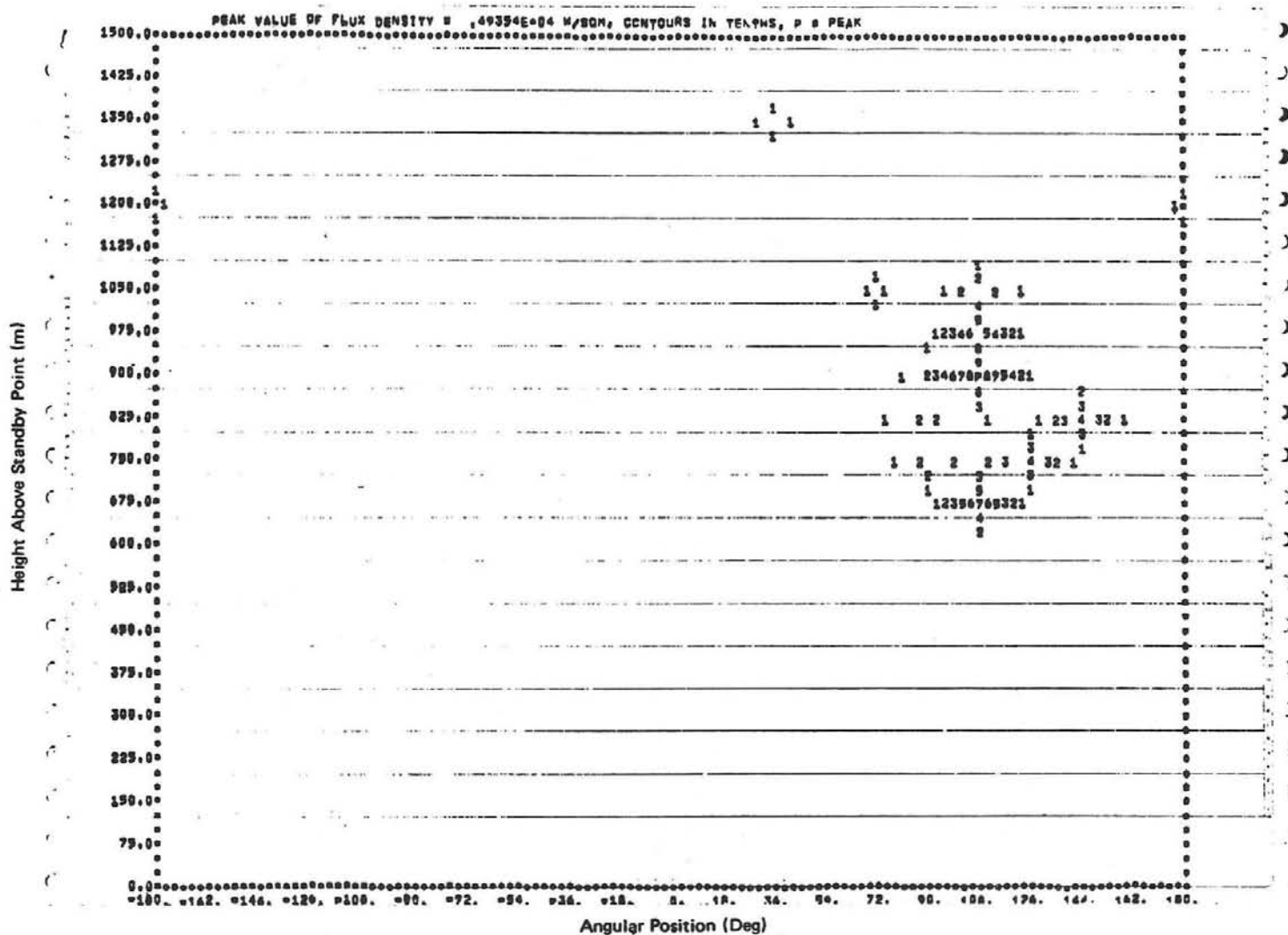


Figure 4-4. Irradiation Contour Diagram, Face-Up Stow Condition, Cylindrical Surface, Radius = 500m, Summer Solstice, 1400 hr

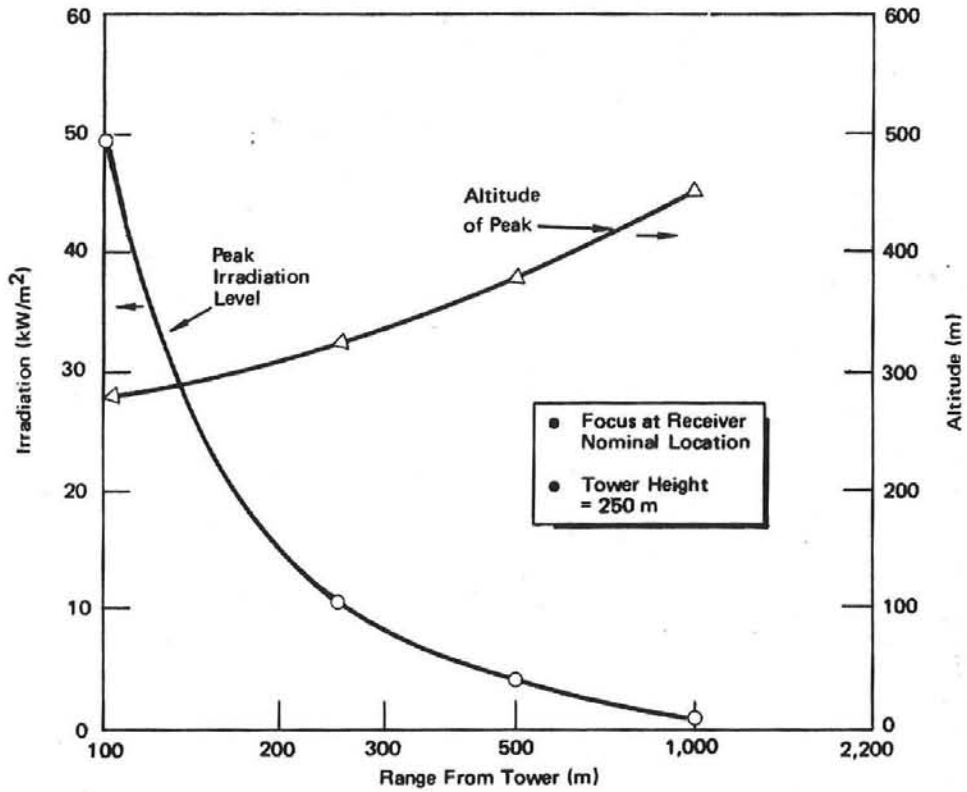


Figure 4-5. Peak Irradiation Beyond Receiver, Commercial Collector Field, 17,702 Heliostats, 7.4 m by 7.4 m, Summer Solstice, 1400 hr

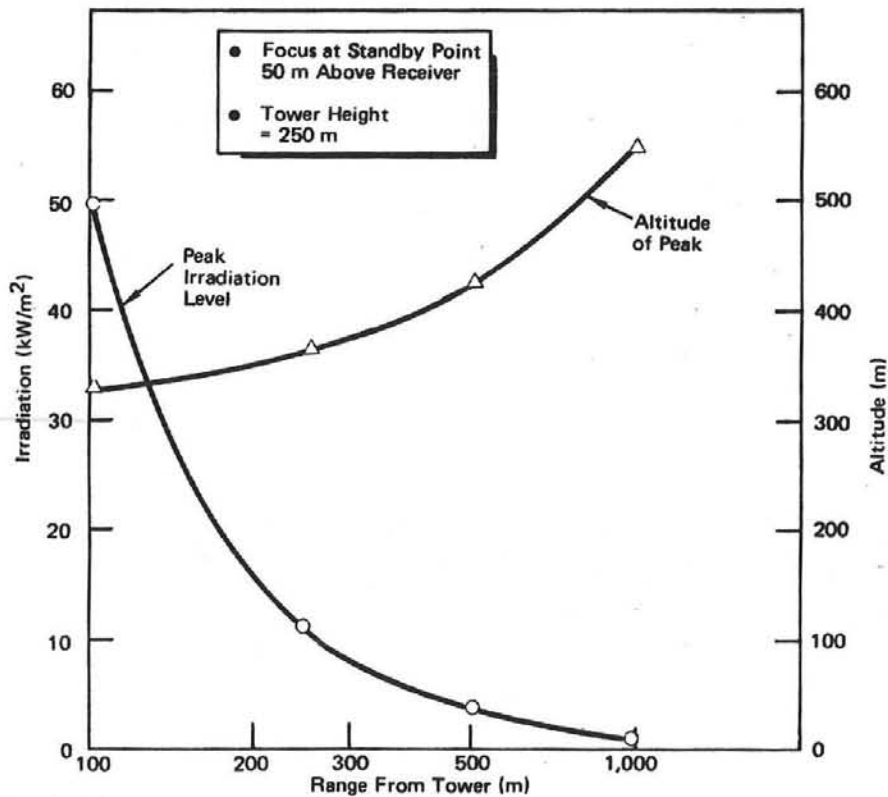


Figure 4-6. Peak Irradiation Beyond Receiver, Commercial Collector Field, 17,702 Heliostats, 7.4 m by 7.4 m, Summer Solstice, 1400 hr



#### 4.2.1.3 During Slew from Focus to Face-up Stow

The transient irradiation level to be expected in the airspace around the receiver was investigated to a limited extent by means of a variation of the cylindrical surface irradiation method. For this example it is assumed that the collector field is at nominal focus condition at a standby point 50 m above the receiver. At  $t = 0$  a command is given to slew all heliostats from their present elevation axis setting to face-up elevation ( $90^\circ$  elevation) at a rate of  $15^\circ/\text{min}$ . At the time each heliostat's elevation reaches  $90^\circ$  its slew drive is stopped. The peak irradiation to be observed on the inside of a cylinder of 500m radius around the receiver is shown in Figure 4-8, plotted as a function of slew time. The altitude variation of the peak location is also shown in this figure. At 160 seconds all heliostats have reached the face-up orientation. The dashed line indicates that no change in the irradiation pattern is expected beyond that time.

#### 4.2.1.4 Safety Implications for Fly-Over Personnel

The irradiation distribution patterns on the reference cylindrical surfaces characteristically show broad diffuse variations, with a small number of

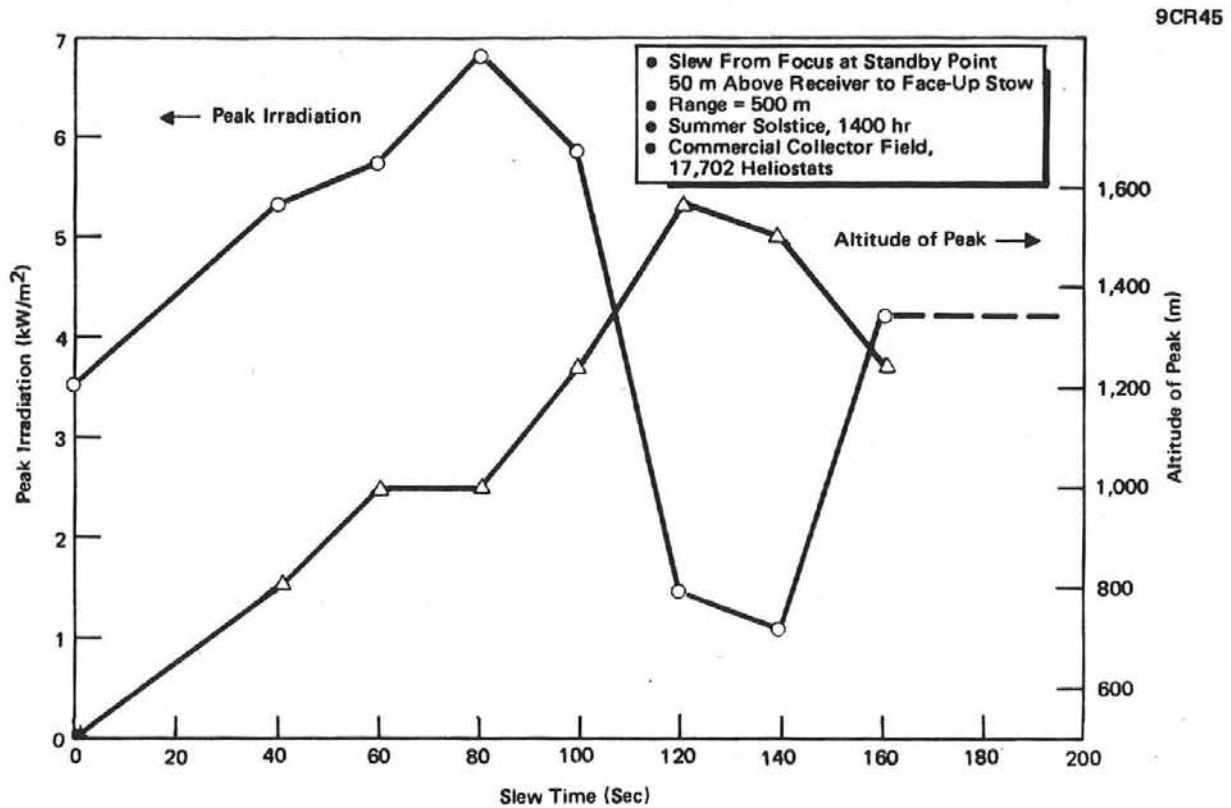


Figure 4-8. Irradiation Beyond Receiver During Slew

peaks, except for the face-up condition, where the irradiation field is generally confined around the direction away from the sun. Personnel flying in the region near the collector field during focus operation would have a low but finite probability of encountering a peak irradiation location. In any event passage through the peak location would be rapid, further reducing the hazard from excessive retinal exposure when looking down. In order to avoid any occurrence of irradiation levels higher than 1 sun ( $\sim 1 \text{ KW/m}^2$ ), it will be necessary to establish an exclusion volume 2000m diameter and 550m high around the central receiver of a commercial-size collector field. From the preliminary results of the face-up and slew conditions it appears that a much higher altitude for the exclusion volume would be required ( $>1600\text{m}$ ), with the 2000m diameter also, to completely avoid the encounter of regions of high irradiation.

#### 4.2.2 Ground-Level Irradiation

Since the heliostats are designed to provide focussing of the reflected radiation of the receiver it is apparent that, should the focused beam extend along ground level in areas where personnel could be located, a significant hazard would exist. Such a situation could arise when noninverting or inverting heliostats are moving to or from vertical stow positions to receiver focus or standby focus conditions, or when inverting heliostats are deployed to an inverted stow condition. In contrast to the greater frequency of occurrence of air space irradiation from noninverting heliostats, inverting stow heliostats present a greater frequency of occurrence of the ground level irradiation condition, due to the normal requirement to stow face-down whenever wind gusts exceed prescribed limits. Although the horizontal beam direction would be only a transient condition, enough time would be available to inflict appreciable damage on personnel or even equipment.

The degree of hazard is related to the focal length of the heliostat mirror, as explained by Brumleve. The shorter the focal length the greater the concentration and the greater the irradiation level at the focus. MDAC heliostats are focused principally by canting and curving the individual mirror panels. For installations where individual heliostat focus is employed the mirrors closest to the receiver have the shortest focal length and constitute the greatest safety hazard in the collector field.

#### 4.2.2.1 Single Heliostat Irradiation

In order to investigate quantitatively the irradiation level for horizontally-directed beams from representative MDAC heliostats, computer runs were made using the CONCENS code, designed for simulation of single heliostat performance, for typical operating conditions. Figures 4-9 and 4-10 show the peak irradiance occurring for inner and outer row heliostats, when the reflected beam is horizontal near ground level, as related to range from the heliostat. For the commercial collector field (Figure 4-9) the inner row heliostats, focused at 301m show a peak irradiance level of  $5.5 \text{ Kw/m}^2$  ( $\sim 5.5$  suns) at a range of about 250m. The outer row heliostats produce a broad peak of about  $1.5 \text{ Kw/m}^2$  at about the same range. The occurrence of the peak irradiance at ranges shorter than the focal distance is due to the broadening of the solar image proportional to range.

#### 4.2.2.2 Safety Implications for Ground-Level Personnel

According to Brumleve's analysis (Ref. 4-1), the safe retinal irradiance value ( $4.59 \text{ W/cm}^2$ ) would be exceeded by an ideal circular heliostat of

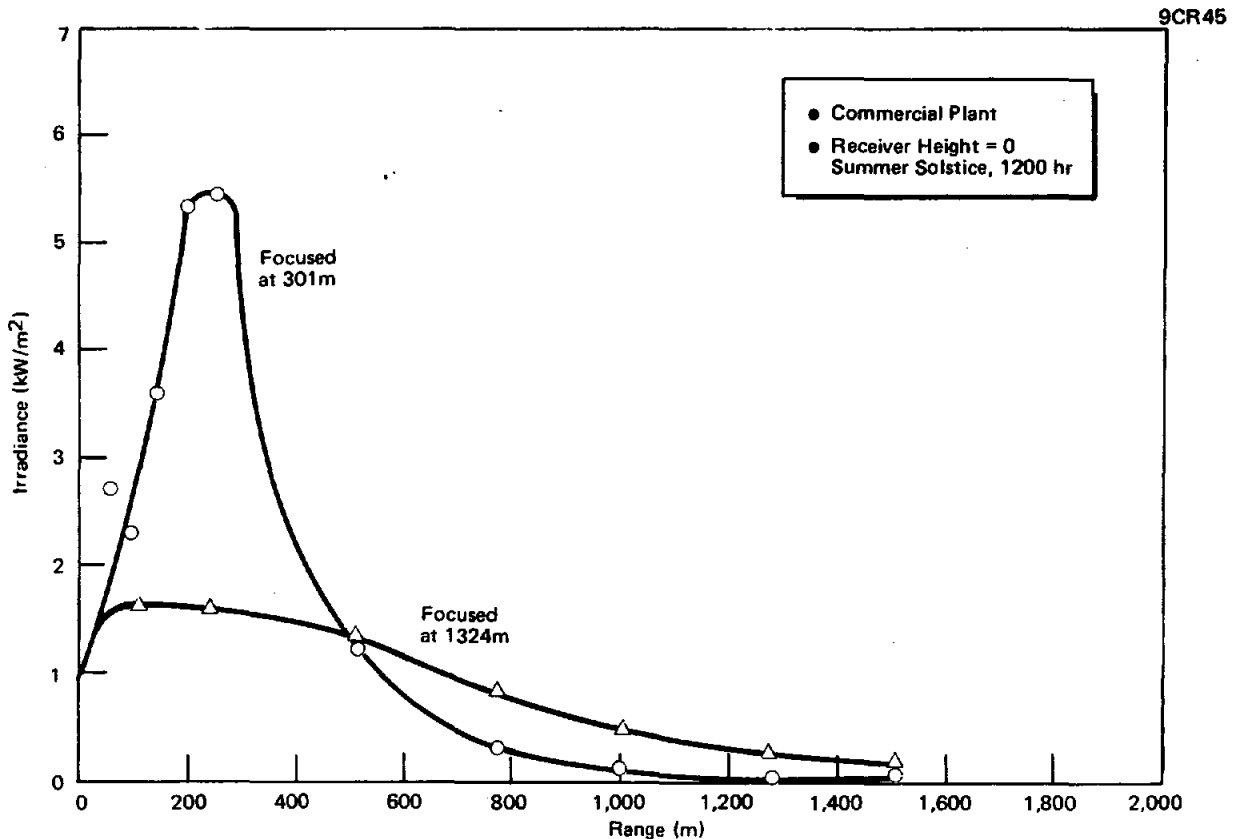
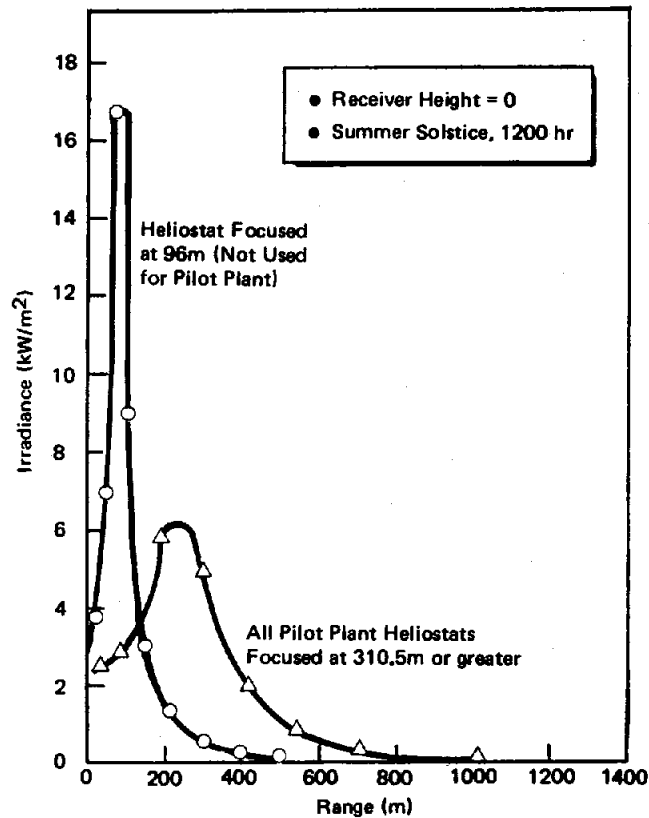


Figure 4-9. Peak Irradiance From Single Heliostat



**Figure 4-10. Peak Irradiance From Single Heliostat (Pilot Plant)**

focal length less than  $39D$ , where  $D$  is the mirror diameter. With an equivalent diameter of 7.6m for the MDAC heliostat, the safe retinal irradiance value is exceeded by heliostats of focal length less than about 300m. If, however, two or more beams from closely-spaced heliostats overlap where personnel are located, the size of the retinal image may cause the maximum permissible exposure level to be exceeded. From Figure 4-9, it can be seen that, for the commercial plant, the safe retinal irradiance is not exceeded anywhere in the collector area. Care must be taken, however, to prevent the overlap of two or more beams from the inner rows in the vicinity of 300m from the heliostats, to prevent the maximum permissible exposure level from being exceeded due to the enlarged retinal image size.

For the 10 MWe Pilot Plant, all heliostats are focused at the same range (310 to 400m) which is close to the safe value of 300m, as is seen from Figure 4-10. Thus, a single heliostat could produce retinal irradiance levels approaching or possibly greater than the maximum safe value in the vicinity of its focal distance. Particular concern must be shown to avoid the condition of horizontal beam direction anywhere that personnel may be located. The region around

the base of the receiver tower is particularly vulnerable to unsafe conditions, as the focal point of the inner row of heliostats, when extended along the ground, could occur at locations where personnel are working. It may, therefore, be advisable to surround the base of the tower with perimeter fences designed to block light from entering the tower and control facility zone, or provide fencing along roadways and work areas, in addition to protective eye-ware and operational precautions.

#### 4.2.3 Suggested Methods of Heliostat Redirection

During the period when the heliostats are being redirected to and from positions of stow and focus it is essential that adjacent beams not be allowed to overlap in groups greater than two or three at any time, in order to avoid regions of excessive irradiation in the airspace over the collector array. Orderly direction strategies should be employed which maintain the necessary angular spacing of adjacent beams. From the variation in peak irradiation during slew from focus to stow (Figure 4-8) it is seen that, for this range from the receiver (500m) at least, the peak irradiation stays below 7 KW/m<sup>2</sup>. For this example the elevation positions of all heliostats were driven at a constant rate from the focus condition to face-up for stow. Variations of this approach should be considered, to reduce the peak irradiation level further. A programmed slew of the elevation drive could be used in which neighboring heliostats are started at staggered times, with the avoidance of overlap of adjacent beams. Some version of the "wire-following" technique should also be considered for programmed staggered slew routines.

For ensuring that the ground-level irradiation is kept below the hazard point it is necessary to consider a special maneuver when taking the heliostats from a vertical stow condition to a focus condition or vice-versa. The reflected beams must pass through a horizontal ground-level direction at some time during the redirection process. By previously orienting the azimuth positions of each heliostat properly, the direction of each beam as it does through horizontal can be made to be toward the heliostat's nearest neighbor. Thus the beam will be blocked most effectively by the next heliostat and will not be allowed to reach its focus distance on the ground in areas where personnel may be located. Further redirection of the beams toward focus can be conducted according to a suitable strategy for airspace hazard reduction. Anticipatory redirection of the heliostats to one or more standby points before sunrise and to stow after sunset is also recommended for day-to-day operation.

#### 4.2.4 Further Investigations

Although several significant trends and limits of the irradiation levels under various conditions of transient and steady-state collector field operation have been found, it would be desirable to increase the coverage of the parametric analysis, particularly for the airspace irradiation hazard problem.

The lack of agreement between the two methods of simulation of the face-up heliostat array should be investigated by extending the coverage of both approaches to obtain more precise intercomparison of the analyses. The variation of peak irradiation with slew time for a full range of distances from the receiver should be explored in order to define the three-dimensional distribution of irradiation around the receiver. All of the conditions should be examined for other times of the day and days of the year.

From the three-dimensional distribution of irradiance at various times, it should be feasible to develop information on the probability of encountering hazardous conditions for locations in the vicinity of the collector field, both with and without use of personnel protection means, such as dark glasses. Although most of the heliostat redirection conditions can be confined to periods prior to dawn or after sunset. Since some of the hazardous conditions could occur during plant shutdown or start-up during daylight hours, thus, the projected frequency of these events should be included in the probability estimates.

#### 4.2.5 Conclusions

1. From the irradiation analyses made for air space and ground-level surrounding regions, there appears to be no compelling reason to require the use of invertible heliostats over noninvertible ones from the standpoint of safety. With reasonable control over the exclusion volume and heliostat orientation during transient conditions the expected hazard level for either type of heliostat should not be excessive for personnel in the vicinity of the collector field. Actual operating experience during two years for the Solar Thermal Test Facility and one year for research testing of heliostats at the Naval Weapons Center have shown an excellent safety record, with no personnel injuries experienced.

2. The preliminary data developed during this study should be extended in time and space to aid in developing an adequate statistical model for the hazard probability variations in the vicinity of the solar thermal power facility.

Section 5  
REFERENCES

- 2-1. C. R. Easton. Solar Central Receiver Prototype Heliostat, MDAC Final Technical Report, MDC G7399. August, 1978.
- 2-2. J. B. Blackmon. Interim Report. Non-Inverting Heliostat Study-Effects of Dust Buildup. MDAC Report MDC G7849. March, 1979. Prepared under Contract 18-7872.
- 2-3. J. B. Blackmon. Dust buildup Tests of Heliostat and Mirror Specimens, MDAC Report MDC G7543. September, 1978. Prepared under Contract EY-76-C-03-1108.
- 2-4. J. B. Blackmon and M. Curcija. Heliostat Reflectivity Variations Due to Dust Buildup Under Desert Conditions. Institute of Environmental Sciences Proceedings - Seminar on Testing Solar Energy Materials and Systems. May 22-24, 1978. Gaithersburg, Maryland.
- 2-5. J. M. Freese. Effects of Outdoor Exposure on the Solar Reflectance Properties of Silvered Glass Mirrors. Sept. 20, 1978. SAND 78-1649. DOE Contract AT (29-1)-789.
- 2-6. U.S. Naval Weapons Center Climatological Summaries for 1946 through 1976. January 1977. Available from Meteorology Section, Range Support Branch, Range Instrumentation Support Division, Range Department. Code 6234.
- 2-7. E. D. Eason. The Cost and Value of Washing Heliostats. Presented at ISES 1979 International Congress. May 28 and June 1, 1979. DOE Contract AT-(29-1)-789.
- 3-1. A. Changnon, Jr. The Scales of Hail. Journal of Applied Meteorology, 16, June 1977, pp 626-648.
- 3-2. G. E. Stout and S. A. Changnon. Climatography of Hail in the Central United States. CHIAA\* Res. Rep. 38 (1968).
- 3-3. A. E. Carte and G. Held. Variability of Hailstorms on the South African Plateau. Journal of Applied Meteorology, 17, March 1978, pp 365-373.
- 3-4. S. A. Changnon, Jr. Means for Estimating Area Hail - Day Frequencies. Journal of Weather Modification, 3. 1971. pp 154-159.

---

\*CHIAA: Crop Hail Insurance Actuarial Association, Chicago.

- 3-5. W. F. Hitschfeld. Hail Research at McGill 1956-1971. Stormy Weather Research Group. McGill University, Montreal. Sci. Report MW-68. May 1971.
- 3-6. S. A. Changnon, Jr., and G. M. Morgan, Jr. Design of an Experiment to Suppress Hail in Illinois. Illinois State Water Survey Bulletin 61, 1976.
- 3-7. C. Gonzalez. Environmental Hail Model for Assessing Risk to Solar Collectors. JPL Report 5101-45. December 1977.
- 3-8. J. E. Dye, A. J. Heymsfield, I. Paluch and D. W. Breed. Final Report - National Hail Research Experiment (NHRE) Randomized Seeding Experiment 1972-1974, Vol. II: Precipitation Measurements. NCAR, Boulder, Colorado, December 1976.
- 3-9. R. H. Douglas. Size Distribution of Alberta Hail Samples. Stormy Weather Research Group. McGill University, Montreal. Sci. Rpt. MW-36. 1963.
- 3-10. R. H. Douglas. Recent Hail Research: A Review. Meteor. Monographs, 5, 1963.
- 3-11. D. Atlas and F. Ludlum. Multi-Wavelength Radar Reflectivity of Hailstorms. Tech. Report No. 4. Contract AF61(052)254, Dept. of Meteorology. Imperial College of Science and Technology. London. 1960. Quoted in Reference 12, below.
- 3-12. C. W. Ulbrich, D. Atlas and R. E. Rinehart. Hail Parameter Diagram. NHRE Symposium/Workshop on Hail, Vol. I. Estes Park, Colorado. September 1975.
- 3-13. R. E. Rinehart. Private communication. 1975. Quoted in Reference 12, above.
- 3-14. B. Federer and A. Waldvogel. Hail and Raindrop Size Distributions From a Swiss Multicell Storm. Journal of Applied Meteorology, 14. 1975. pp 91-97.
- 3-15. J. F. Spahn and P. L. Smith, Jr. Some Characteristics of Hailstone Size Distributions Inside Hailstorms. Preprint, 17th Weather Radar Conference. Seattle, Washington. MAS, Boston. 1976. pp 187-191.
- 3-16. E. L. Crow, P. W. Summers, A. B. Long, C. A. Knight, G. B. Foote, and J. E. Dye. Final Report - NHRE Randomized Seeding Experiment 1972-1974. Vol. I: Experimental Results and Overall Summary. NCAR. Boulder, Colorado. December 1976.
- 3-17. J. S. Marshall and W. M. Palmer. The Distribution of Raindrops with Size. Journal of Meteor., 5. 1948. p 165.
- 3-18. D. Ludlum (Ed.). The "New Champ" Hailstone. Weatherwise, 24. p. 151. 1971.

- 3-19. R. E. Rinehart, Private Communication. 1978.
- 3-20. M. L. Smith. Hail Testing of Solar Reflector Panels. Presented at the Solar Reflector Materials Technology Workshop. Denver, Colorado. March 1978.
- 3-21. D. Moore and A. Wilson. Photovoltaic Solar Panel Resistance to Simulated Hail. JPL Report 5101-62. October 1978.
- 3-22. G. M. Morgan, Jr., and P. W. Summers. Private Communication. 1979.
- 3-23. E. G. Bilham and E. F. Relf. The Dynamics of Large Hailstones. Quarterly Journal Royal Meteor. Soc., 63, 1937. pp 149-162.
- 3-24. N. R. Gokhale. Hailstorms and Hailstone Growth. State University of New York Press. 1975.
- 3-25. W. C. Macklin and F. H. Ludlum. The Fallspeeds of Hailstones. Quarterly Journal Royal Meteor. Soc., 87. 1961. pp 72-81.
- 3-26. I. F. Gringorten. Hailstone Extremes for Design. AFCRL-72-0081. December 1971.
- 3-27. G. M. Morgan, Jr., and N. G. Towery. On the Role of Strong Winds in Damage to Crops by Hail and Its Estimation with a Simple Instrument. Journal of Applied Meteor., 15. August 1976. pp 891-898.
- 3-28. D. Vente and G. M. Morgan, Jr. Statistical Evaluation of Energy Imparted to Hail by Wind in Europe and the United States. Presented at the Second WMO Scientific Conference on Weather Modification. WMD No. 433. Geneva. 1976. pp 281-285.
- 3-29. G. M. Morgan, Jr. Private Communication. 1978.
- 3-30. D. G. Friedman and P. A. Shortell. Prospective Weather Hazard Rating in the Midwest with Special Reference to Kansas and Missouri. The Travelers Insurance Companies. Hartford, Connecticut. August 1967. Provided by D. G. Friedman. Private Communication. 1978.
- 3-31. G. M. Morgan, Jr. Results of Fine-Scale Studies of Surface Hailfall with Some Remarks on the Calibration of Hailpads: Recommendations for Further Research. Atmosphere/Ocean, 16. 1978. pp 49-60.
- 3-32. D. G. Friedman. Texas Hailstorms. The Travelers Insurance Companies. Hartford, Connecticut. May 1965. Provided by D. G. Friedman. Private Communication. 1978.
- 3-33. G. F. Collins and G. M. Howe. Weather and Extended Coverage. Final Report. TRC Service Corporation. Hartford. December 1964.
- 3-34. S. A. Changnon, Jr., et al [13 authors]. Hail Suppression Impacts and Issues. Final Report, Technology Assessment for the Suppression of Hail ("TASH Report"). ERP75-09980, RANN, NSF. April 1977.

- 3-35. T. T. Lingham. Insuring Solar Energy Systems. Best's Revie (date and volume unknown). Bulletin, Solar Energy Risks, R&F-PIC Bulletin #78-4. NAII\*. August 1978. Private Communication by C. R. Hall, NAII. 1979.
- 3-36. M. L. Smith, "Hail Testing of Solar Reflector Panels Presented at Solar Reflector Materials Technology Workshop, Denver, Colorado. March 28-30, 1978.
- 3-37. Raymond J. Roark. "Formulas for Stress and Strain." Second Edition. McGraw-Hill Book Company, Inc. 1943.
- 3-38. Central Receiver Solar Thermal Power System, Phase 1, Vol. III, Book 2. October 1977. McDonnell Douglas Astronautics Report MDC G6776. DOE Contract EY-76-C-03-1108.
- 4-1. T. D. Brumleve, "Eye Hazard and Glint Evaluation for the 5-MWt Solar Thermal Test Facility," Sandia Laboratoreis Energy Report, SAND 76-8022, May 1977.
- 4-2. R. H. McFee, "Power Collection Reduction by Mirror Surface Non-Flatness and Tracking Error for a Central Receiver Solar Power System," Applied Optics, 14, 1493 (1975).
- 4-3. R. H. McFee, "Computer Program CONCEN for Calculation of Irradiation of Solar Power Central Receiver," Proceedings of the ERDA Solar Workshop on Methods for Optical Analysis of Central Receiver Systems, August 1977.

---

\*NAII: National Association of Independent Insurers, 2600 River Road, Des Plaines, IL 60018.

APPENDIX A  
HAIL IMPACT  
IMPULSE-MOMENTUM VULNERABILITY MODEL

Impact of a deformable hailstone striking a glass panel is assumed to be represented by an impact force,  $F$ , imparted to the glass due to the rate of change of momentum of the hailstone. The momentum immediately prior to impact is  $MV$  where  $M = \frac{4}{3} \pi r_0^3$  and  $V$  is velocity of the stone. From  $F = ma$ , the force,  $F$ , can be approximated if we assume the momentum,  $mv$ , is imparted to the glass uniformly over a time  $\Delta t$ ; that is, a uniform deceleration is assumed to occur over the distance  $2r_0$ . Then, with  $v^2 = 2as$  ( $s$  is the characteristic distance,  $2r_0$ ) we obtain

$$a = \frac{v^2}{4r_0} \quad \text{and} \quad (1)$$

$$F = \frac{Mv^2}{4r_0} \quad (2)$$

Expressing mass in terms of the radius, and using equation (2)

$$F = \frac{\frac{4}{3} \pi r_0^3 v^2}{4r_0} = \frac{\pi r_0^2 v^2}{3} \quad (3)$$

Next assume that this force is uniformly exerted over an area of  $\pi r_0^2$ . Intuition dictates that the maximum actual force could be exerted over a somewhat smaller area, say  $\frac{\pi r_0^2}{2}$ , and deceleration could occur over a distance less than  $2r_0$ , but these effects will be ignored.

From Roark, (3-37) the maximum radial and tangential stresses at the center of a uniform load,  $W = w\pi r_0^2$ , on a circular edge supported disc of radius  $a_p$  and thickness  $t_p$  is

$$s_r = s_t = \frac{-3W}{2\pi m t_p^2} \left[ m + (m + 1) \log \frac{a_p}{r_0} - (m - 1) \frac{r_0^2}{4a^2} \right] \quad (4)$$

where  $m = \frac{1}{\nu} = 4$  and  $W = F = \frac{\pi \rho r_0^2 v^2}{3}$

Thus, the thickness of glass plate which will withstand a hailstone is given by:

$$\frac{t_p}{r_0} = \nu \left\{ \frac{\rho}{2ms r} \left[ m + (m + 1) \log_e \frac{a_p}{r_0} - (m - 1) \frac{r_0^2}{4a^2} \right] \right\}^{1/2} \quad (5)$$

It should be noted that this model implies that the thickness required to prevent breakage increases as  $\rho^{1/2}$ ,  $\nu$ , and  $(1/S)^{1/2}$ . The dependence on  $r_0$  is more complex because of the ratio  $a_p/r_0$  in the log term. Further use of stringers, effects of edge impact, etc., are not included in this equation, and other, more suitable equations may be more usefully employed. However, the above equation is used to compare predicted glass breakage conditions with the available data, and is shown to be in reasonable agreement.

UNLIMITED RELEASE

INITIAL DISTRIBUTION

T. B. Cook, 8000

L. Gutierrez, 8400

R. C. Wayne, 8450

S. Peglow, 8451 (3)

W. D. Wilson, 8451

Publications and Public Information Division, 8265, for TIC (27)

F. J. Cupps, 8265/Technical Library Processes Division, 3141

Technical Library Processes Division, 3141 (2)

Library and Security Classification Division, 8266-2 (3)